

AD-A034 948

AIR FORCE INST OF TECH WRIGHT-PATTERSON AFB OHIO SCH--ETC F/G 20/8
INTERACTION OF RELATIVISTIC PROTONS WITH MATTER.(U)
DEC 76 G P BENDER
GNE/PH/76D-1

UNCLASSIFIED

NL

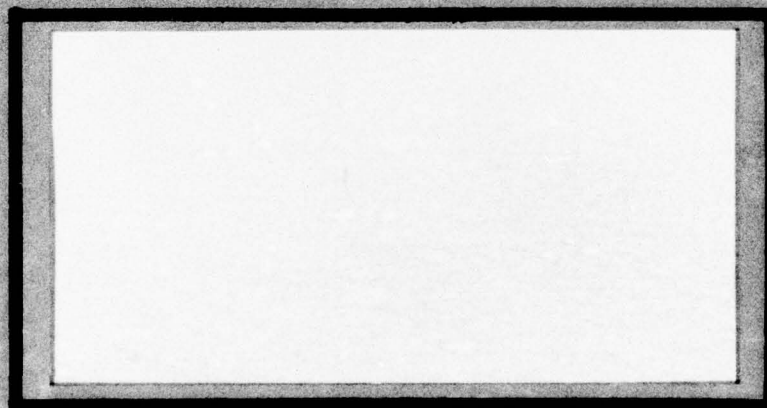
1 OF 2
ADA034948



ADA034948



COPY AVAILABLE TO DDC DOES NOT
PERMIT FULLY LEGIBLE PRODUCTION



DDC
JAN 28 1977
RECEIVED

UNITED STATES AIR FORCE
AIR UNIVERSITY
AIR FORCE INSTITUTE OF TECHNOLOGY
Wright-Patterson Air Force Base, Ohio

DISTRIBUTION STATEMENT A

Approved for public release;
Distribution Unlimited

GNE/PH/76D-1

INTERACTION OF RELATIVISTIC
PROTONS WITH MATTER

THESIS

GNE/PH/76D-1

Gene P. Bender
Lt USN



Approved for public release; distribution unlimited

(14) GNE/PH/76D-1

(6) INTERACTION OF RELATIVISTIC
PROTONS WITH MATTER.

(9) Master's THESIS

Presented to the Faculty of the School of Engineering
of the Air Force Institute of Technology
Air University
in Partial Fulfillment of the
Requirements for the Degree of
Master of Science

RECEIVED FOR	
NTIS	NTIS Section <input checked="" type="checkbox"/>
DDC	DDC Section <input type="checkbox"/>
UNCLASSIFIED	UNCLASSIFIED <input type="checkbox"/>
JUSTIFICATION	
BY	
DISTRIBUTION/AVAILABILITY CODES	
Dist.	Avail. and/or Special
A	

(12) 160p.

(10) by
Gene P. /Bender, B.S.
Lt USN

Graduate Engineering Physics

(11) December 1976

Approved for public release; distribution unlimited.

1473
012225
LB

Preface

In this thesis, an attempt was made to use a simple and direct approach to solve a complicated physical problem. As with most problems of this type, the analysis raised more questions than it answered. I feel that the problem of collisionless interactions deserves further detailed study, in order to truly establish the mechanism as an important contributor to energy deposition in a target.

I am deeply grateful to Capt. P. Nielsen and to Dr. D. Shankland for both their guidance and instruction during the course of this work and to those at home who are patient and expert typists.

Gene P. Bender

Contents

	Page
Preface	ii
List of Figures	v
List of Tables	vi
Abstract	vii
I. Introduction	1
History.	2
Analysis	3
Summary.	4
II. Collisional Interactions	6
Ionization Losses	7
Elastic Scattering	12
Nuclear Interactions	13
Bremsstrahlung	24
Summary of Collisional Interactions.	25
III. Collective Interactions	28
Two-stream Instability	29
Analytic I-D Model of Collective Interactions	32
IV. Method	51
The Plasma	53
The Solving Routine.	54
The Beam	55
The One-dimensional Model	57
The Initial Conditions	62
The Two-dimensional Model	62
V. Results and Conclusions.	72
Validity Runs	72
One- and Two-dimensional Runs with the Beam.	75
Things to be Done	79
Bibliography	81
Appendix A: Derivation of the Boltzmann-Vlasov Equation from Liouville's Equation	83

Appendix B:	The External Electric Field	95
Appendix C:	Derivation of Constants	101
Appendix D:	Moments for the One-Dimensional Model .	104
Appendix E:	Derivation of Moment Equations . . .	114
Appendix F:	The Computer Programs	135
Appendix G:	Derivation of Plasma Frequency From the Moments of the Vlasov Equation	145

List of Figures

<u>Figure</u>	<u>Page</u>
1 Range and Specific Ionization of Heavy Ions	7
2 Interaction Cross Sections of Elementary Particles14
3 Nuclear Cascade Diagram16
4 Average Number of Cascade Particles per Beam Proton Interaction (Low Energy)17
5 Average Number of Cascade Particles per Beam Proton Interaction (High Energy).17
6 Average Number of π^0 , π^+ , π^- for Various Elements	.22
7 Distribution of π^0 , π^+ , π^- , for Various Energies	.22
8 Solution to Two-stream Instability Model (Real Roots).31
9 Solution to Two-stream Instability Model (Imaginary Roots)31
10 Initial Distribution of Electrons63
11 Two-dimensional Nodal Grid65
12 Momentum Oscillations of Trial Runs76
13 Location of Residual Poles ($M < 1$).42
14 Solution to Residual Integral ($M < 1$).43
15 Phase Velocity as a Function of Normalized Frequency.45
16 Location of Residual Poles ($M > 1$)46
17 Solution to Residual Integral ($M > 1$)48
18 Force Due to Spherical Charge Distribution on a Point Charge38
19 Sketch of Distance Parameters for External Electric Field96

List of Tables

<u>Table</u>		<u>Page</u>
I	Quantitative Distribution of Cascade Particles for 5 GeV Beam	15
II	Quantitative Distribution of Cascade Particles for 10 GeV Beam	18
III	Summary of Energy Deposition in a Target by Various Mechanisms.	27
IV	Summary of Plasma Oscillations	73

Abstract

The mechanisms associated with the interaction of a relativistic proton beam with a target material are summarized, and a simple analytic calculation for each mechanism relates its importance in the deposition of energy. Because it was found that possible significant contributions could be related to collective effects, the first three moments of the Boltzmann-Vlasov equation and the equations necessary to describe the internal and external electromagnetic fields associated with the target are developed. These equations are then formulated into a computer program to describe the collective interaction process. Sample runs demonstrate the ability of the computer model to predict plasma oscillations at the proper frequency. Although an instability developed in the runs with the beam approaching the target, the preliminary analysis was accomplished, and the need for future detailed analysis of this process was established.

I. Introduction

In the past several years, there has been considerable interest in the interaction of relativistic electrons and ions with matter. This interest has been stirred in part by the prospect of major breakthroughs in the ability to accelerate charged particles to GeV energies with accelerators of reasonable size. Although most of the research being done today concerns construction of the accelerators or the propagation of the beam in the accelerator and through the atmosphere, some work is also being done on the mechanism of interaction of these beams with the target.

The known interaction mechanisms associated with the charged particle beam striking the target can be divided into the following two major categories:

1. Collisional interactions
2. Collective (sometimes termed collisionless) interactions

Collisional interactions include ionization losses due to inelalastic collisions with the atomic electrons, elastic interactions with the nucleus, Bremsstrahlung produced as the result of collisions, and inelastic nuclear interactions.

Collective interactions are those associated with the system as a group and not individual elements. External forces can induce oscillations within a plasma, and these oscillations may then be converted into random motion or heat through instabilities such as two-stream or return-current heating.

To date, considerable research has been done on the

collisional interactions of protons and electrons and collective effects of electron beams; however, very little has been done on the collective interactions of proton beams with matter. In this thesis, I propose, first, to survey the major interaction mechanisms associated with the proton beam; secondly, to develop the equations necessary to model the collective interaction mechanism; and thirdly, to use these equations to investigate the physical aspects of the relativistic proton beam passing through a target material.

History

In the early 1950's, the charged particle beam was investigated extensively as to the prospects of using the beam for research in nuclear structure by bombardment of nuclei with protons, investigation of high energy interaction mechanisms, transmission of high energy charged particles through waveguides, and also as a weapon system. After considerable time and effort, the state of the art limitations on accelerators and electronic components slowed the effort to a trickle. Today, with a new class of accelerators on the production horizon, the investigation of charged ion beams of relativistic energies has begun with renewed interest.

At present, numerous institutions are undertaking the development of collective ion accelerators which will be capable of producing the energies and quantities of protons or heavier ions necessary for propagation through the atmos-

phere.

Not only institutions within the United States, but the Soviet Union is also actively engaged in studying the interaction and propagation mechanisms of the charged particle beam. The topic of greatest concern in much of today's literature involves the choice of the electron or the proton for most desirable propagational and interaction properties. There are pros and cons on both sides of the question; however, the consensus is, if the proton beam can be produced, then it is the superior particle for interaction. Thus, at this point, the discussion will be limited to the proton beam except where noted.

Analysis

Assumption. The most basic assumption in this analysis is the beam itself. The assumption is that a proton accelerator capable of providing high enough energies and densities to propagate a beam over reasonable distance can be produced.

The second major assumption concerns the ability of numerical solutions to model accurately the real world processes involved in the interaction. Some assumptions will be stated later which have been chosen to permit a simplification of the model and equations used in the numerical calculations. These assumptions may produce slight deviations from the real world problem, but the overall trend and physics should still be preserved.

Facts. The premise used for the modeling of the collective and collisional interaction mechanisms has come from experimental studies done on very small scales. Although these small-scale experiments may not lead to a direct conversion to experiments on larger scales, the physics of the interactions should remain the same.

Electron beam propagation and interaction processes have been studied extensively over the past twenty years under various research topics. Even though single proton beam interactions are well categorized, limited amounts of research have been done with relativistic proton beams with large number densities in the beam. In the past fifteen years, the Soviet Union has devoted large amounts of time and effort in studying the relativistic proton beam interaction mechanism, and is today the probable leader in understanding the mechanisms of collisional processes.

Collective interactions have been used to explain such things as the effects on communication systems by solar flares for the past thirty years. The basic theory of collective interactions is well documented; however, application of this phenomenon as a proton beam interaction mechanism has not been attempted.

Summary

This thesis will summarize the various types of interactions associated with a proton beam and look in detail at the process of collective interactions. The results will tend to support the collective interaction mechanism as

an important part of the overall interaction process or
eliminate the mechanism as being a minor contributor to the
deposition of energy in a target material.

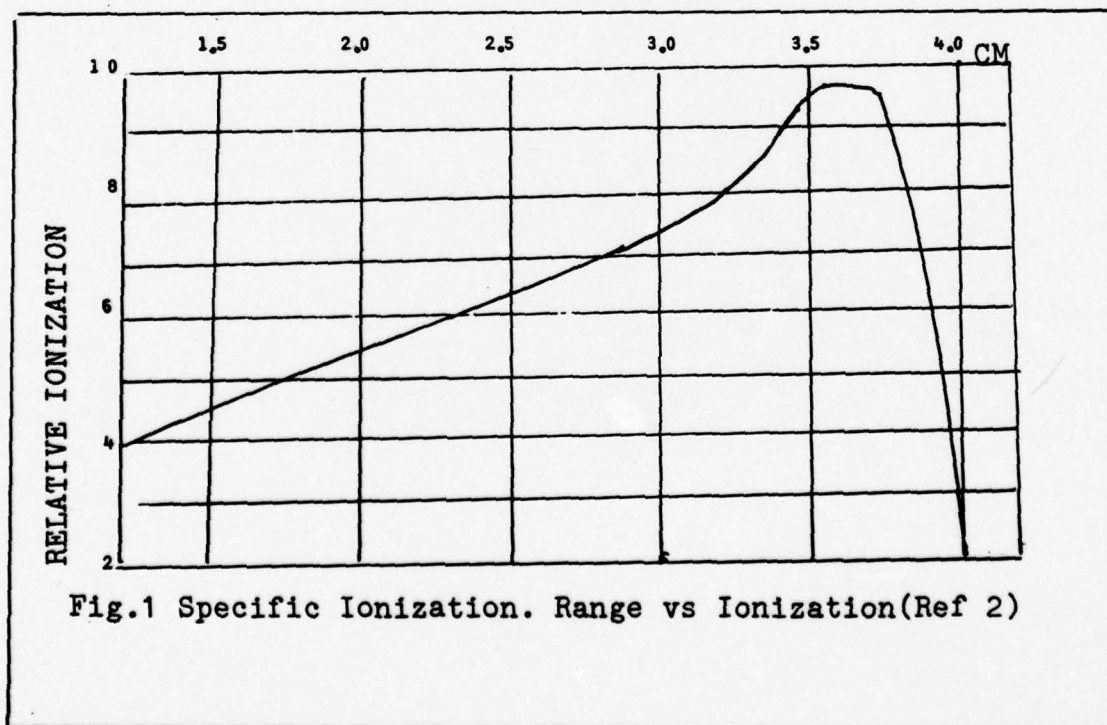
II. Collisional Interactions

A particle passing through matter makes collisions with both the atomic electrons and the nuclei of the target material. By collision, it is meant that the very strong short-range forces associated with interactions come into play. Short-range forces involve the interaction of either the nuclear forces or the coulombic fields associated with the charges of the two colliding particles. The range of these collisions is limited to several atomic radii. The proton, being some two thousand times heavier than the electron, will impart considerable energy to the electron, through the coulomb field collision, knocking it from orbit and leaving an ion behind. This process, known as ionization, is a major contributor to degradation of the beam energy. Collisions with the nucleus can take place via either elastic or inelastic mechanisms. In elastic collisions of a proton with a nucleus, the total kinetic energy of the system remains the same before and after the collision; thus, no energy is stored in the nucleus, and the collision is termed elastic. If the number of particles involved and their energy differ after collision or the total kinetic energy is not conserved, the collision is termed inelastic. Bremsstrahlung is produced as the result of acceleration or deceleration of charged particles as the result of collisions. This radiation will be stopped in the target material producing heat. The following discussion considers each of these mechan-

isms in more detail and tries to bring them into perspective as to importance in energy deposition in the target.

Ionization Losses

When heavy particles, such as protons with high energy, pass through matter, they do so in relatively straight lines dissipating a portion of their energy through a series of collision with the atomic electrons. This energy dissipation does not take place in a linear fashion, but as can be seen by Fig. 1, depends upon the velocity of the particle. This figure relates the number of ion pairs per millimeter of path length (specific ionization) formed as a result of collisions of the incident particle with the orbital electrons in the target material.



It can be seen that more ion pairs are formed and thus the largest energy losses occur at the end of the particle's range.

Another term frequently referred to in the literature when talking about ionization losses is "stopping power",

S , which is defined as the energy lost by a particle per unit length of travel in the stopping substance (Ref.

2)

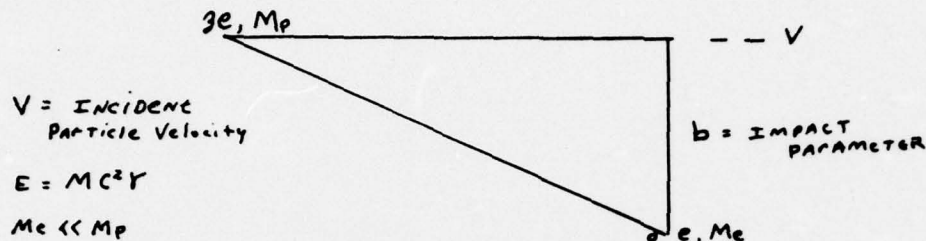
$$S(E) = - dE/dx \quad (1)$$

where E is the kinetic energy of the particle, and could be related to the slope of Fig 1. Stopping power, though usually thought of as a property of the medium, relates the energy transferred in a collision of a particle of charge (ze) and mass (M) with the orbital electrons of the stopping substance. Theoretically, no nuclear collisions are taken into account in this term.

If the velocity of the incident particle is large in comparison with the orbital velocity of the electrons, (electrons at room temperature have a velocity of $\approx 1 \times 10^5$ m/s) the electrons can be considered at rest (Ref. 3). If we assume that the momentum transfer, ΔP , is sufficiently small that the incident particle is not deflected from its straight-line path and that the recoiling electron does not move appreciably during the collision, then ΔP is a function of the electric field of the incident particle at the position of the electron.

$$\Delta P = \int_{-\infty}^{+\infty} e E(t) dt.$$

Magnetic effects are negligible if the electron is essentially at rest.



Only the transverse component of the electric field has a non-vanishing time integral in one dimension and is therefore given by:

$$E = \frac{\gamma g b}{(b^2 + \gamma^2 v^2 t^2)^{3/2}} \quad (2)$$

Where $g = ze$ and $\gamma = 1/(1 - v^2/c^2)^{1/2}$ (Ref 3).

Thus the momentum impulse, also only in the transverse direction, has magnitude

$$\Delta P = \int_{-\infty}^{+\infty} e E(t) dt = 2ze^2/bv. \quad (3)$$

The energy transferred to the electron is

$$T = \frac{(\Delta P)^2}{2M} = \frac{2z^2 e^4}{Me b^2 v^2}. \quad (4)$$

From Eq. (4) we see that the energy transferred, (T) depends upon the charge on the incident particle, z inversely as the square of the impact parameter, b , and is independent of the incident particle.

A very fast particle passing through matter "sees" electrons at various impact parameters. The number of possible collision sites (dN) , located at impact para-

meters between (b) and $(b + db)$, in a thickness dx of the material is

$$dN = N Z b \, db \, dx \quad (5)$$

where Z is the atomic number of the stopping material.

To find the energy lost per unit distance traveled by the incident particle, multiply Eq. (5) by the energy transferred $\Delta T(b)$ and integrate over the impact parameters.

$$dT = \frac{2 Z^2 e^4}{M_e V^2} N Z 2 \pi \int_{b_{min}}^{b_{max}} \frac{b}{b^2} dx \, db$$

$$\frac{dT}{dx} = \frac{4 \pi Z^2 e^4}{M_e V^2} N \int_{b_{min}}^{b_{max}} \frac{1}{b} db. \quad (6)$$

The correct choice of b_{min} and b_{max} must be based on quantum mechanical considerations as was done by Bethe (Ref. 20), but a rough indication of the result can be derived classically. The lower limit, b_{min} , insures from Eq. (4) and on noting that the maximum momentum transferred to an electron in a classical central collision is $2 M_e V$, that $b_{min} = \frac{Z e^2}{M V^2}$.

The upper limit, b_{max} , is determined by the finite binding energies of the electrons in an atom. A bound electron cannot accept arbitrarily small amounts of energy but must absorb sufficient energy to be raised to an unfilled energy state. We may introduce effective or average excitation energy, I , averaged over all the electrons in the atoms of the absorber and contend that there is no energy transferred unless $\Delta T \geq I$, i. e.;

$$\frac{2 Z^2 e^4}{M_e V^2 b^2} \geq I \quad (7)$$

therefore,

$$b \leq b_{max} = \frac{3e^2}{V} \left(\frac{2}{MeI} \right)^{1/2}. \quad (8)$$

Substitution of these limits into Eq (6) yields the approximate expression

$$-\frac{dT}{dX} = \frac{4\pi Z^2 e^4}{MeV^2} NZ \ln \left(\frac{2MeV^2}{I} \right)^{1/2} \quad (9)$$

which differs from the corresponding quantum mechanical expression only in the occurrence of the power $\frac{1}{2}$ in the logarithmic term. The quantum mechanical expression for stopping power is (Ref. 2)

$$-\frac{dT}{dX} = \frac{4\pi Z^2 e^4}{MeV^2} NZ \ln \left(\frac{2MeV^2}{I} \right). \quad (10)$$

Empirical values for I , the average excitation potential, are given by

$$I \approx 9.1Z (1 + 1.9Z^{-1/2}) \text{ ev.} \quad (11)$$

Sternheimer (Ref 6) corrected the Bethe equation [Eq. (10)] to include both relativistic particles and a better fit to experimental data at lower energies.

$$-\frac{dT}{dX} = \frac{4\pi Z^2 e^4}{Me c^2 \beta} NZ \left[\ln \frac{2MeV^2}{I(1-\beta)} - \beta^2 - \frac{5}{2} - \phi \right] \quad (12)$$

where $\beta = v/c$.

ϕ = a correction for non-participation of the K, L, ... shell electrons if the transferred energy of the incident particle is below that required to overcome the nuclear forces.

$\frac{5}{2}$ = a correction for polarization and conductivity in dense materials. This factor takes into account the reduction of ionization losses at high energies due to polarization of the medium by the effective field of the passing charged particles.

This effect becomes important above kinetic energies greater than 2 GeV. The value of ξ for specific materials and energies of incident particles is available for most materials (Ref 5 and 6).

Elastic Scattering

In the interaction process, elastic scattering is a minor contributor to the deposition of energy in the target material. However, the transverse spreading of the beam during propagation of the protons to the target is of significance, thus a brief summary of the process will be given.

Elastic scattering requires the total kinetic energy of the system, projectile and target, to be the same before the collision as after. Some kinetic energy is usually transferred from the incident particle to the target nucleus, but the latter is left in the same internal or nuclear state, as before the collision. A collision between two billiard balls, in which neither is damaged or changed otherwise, is an elastic collision.

In the propagation of the beam through a medium, the elastic collisions will impart transverse momentum to the scattered proton. This transverse momentum will tend to spread the beam in radius and therefore some particles will not strike the target. Once the beam has reached the target, the elastic collisions within the target will involve a spreading of the deposition energy. This spreading will

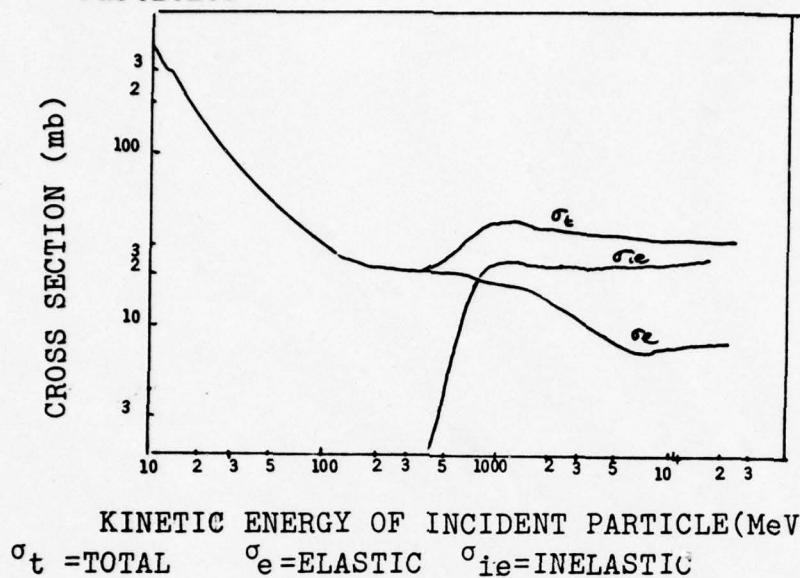
tend to decrease local heating at the beam center and thus reduce the damage caused by thermal heating. The cross sections for elastic interactions are slightly less than 300 millibarns (Ref. 7) for particles in the GeV energy range in aluminum. Thus, elastic collision will not result in significant beam spreading within the target material. The equations which describe this spread can be found in Refs. 3 and 7, but under the assumption that the beam has already reached the target, this phenomenon will be left to those studying propagational processes.

Nuclear Interactions

At proton energies of several hundred MeV and greater, the collision of protons with the nucleus involves a strong interaction of the incident particles with the nucleons. This interaction leads to the production of cascade particles, including pi-mesons. As the proton energy increases further (near 6 GeV), the production of antiparticles also becomes energetically possible. The cascade particles result from the primary collisions near the edge of the nucleus where the primary particles enter, and each secondary particle also has the capability of causing additional interactions of sufficient energy is present.

The cross sections for these inelastic collisions of relativistic protons are approximately constant in the 10 GeV range, as shown by Fig. 2.

Fig.2 Interaction Cross Sections for Elementary Particles



Steenberg (Ref 21) has developed an empirical formula for these high energy proton cross sections as a function of atomic number of the target materials.

$$\sigma_a(A) = \sigma_a(1) A^N$$

where $\frac{2}{3} < N < 1$, $\sigma_a = 38$ millibarns, and A is the atomic number of the target material. With such small cross sections, either the stopping material will have to be greater than normal density, or the number of protons in the beam will have to be exceedingly large in order to deposit an appreciable amount of energy within a reasonable range.

The interaction of high energy protons with the nucleons may produce a variety of particle species and reaction mechanisms as shown by Fig. 3. This figure pictorially describes the cascading process in which second-

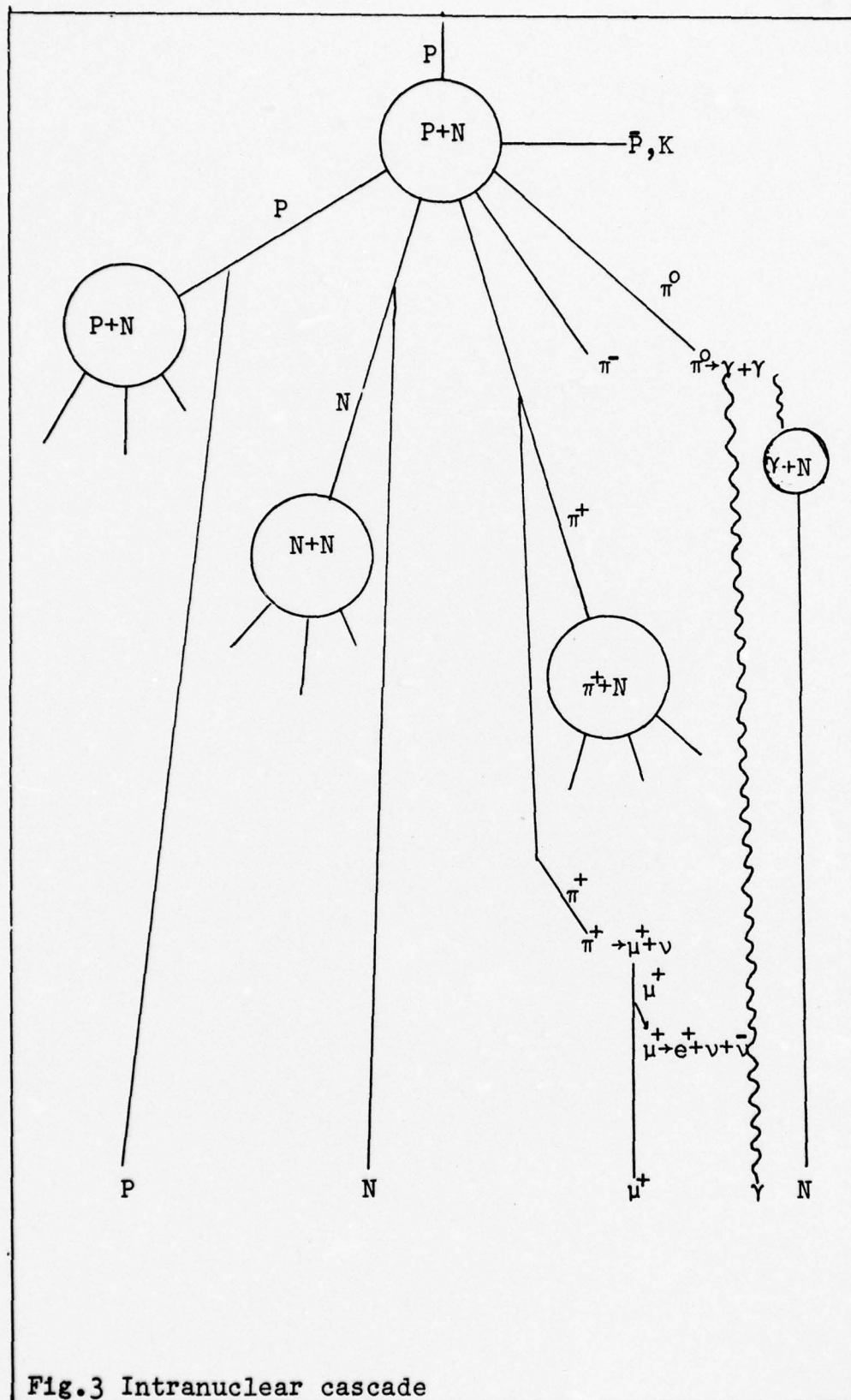
ary particles interact with surrounding nucleons and produce multiple interactions. The study of the nuclear cascade process is the subject of considerable amounts of present-day research in both the United States and the Soviet Union. The problems associated with the modeling of these cascades have produced extensive discussion as to the mechanism of the various interactions and the ability of suggested models to fit experimental data. Baronshkov has produced the most recent data on mechanism modeling (Ref 10). Fig. 4 shows a plot of the average number of cascade particles per beam proton interaction versus the energy of the incident proton.

For copper, there are approximately nine particles produced for each incident 5 GeV proton. The qualitative break-out of these nine particles is as follows:

TABLE I Distribution of cascade particles (5GeV Beam)

	Yield	(E) T/T0GeV	Y(T) GeV
Protons (S)	.7	.39	.27
Protons (C)	2.0	.015	.03
Neutrons (S)	.7	.39	.27
Neutrons (c)	2.0	.015	.03
π^+	1.3	.09	.12
π^-	1.3	.09	.12
π^0	<u>1.3</u>	<u>.09</u>	<u>.12</u>
	9.3		.96 GeV

The (S) above stands for shower particles and the (C)



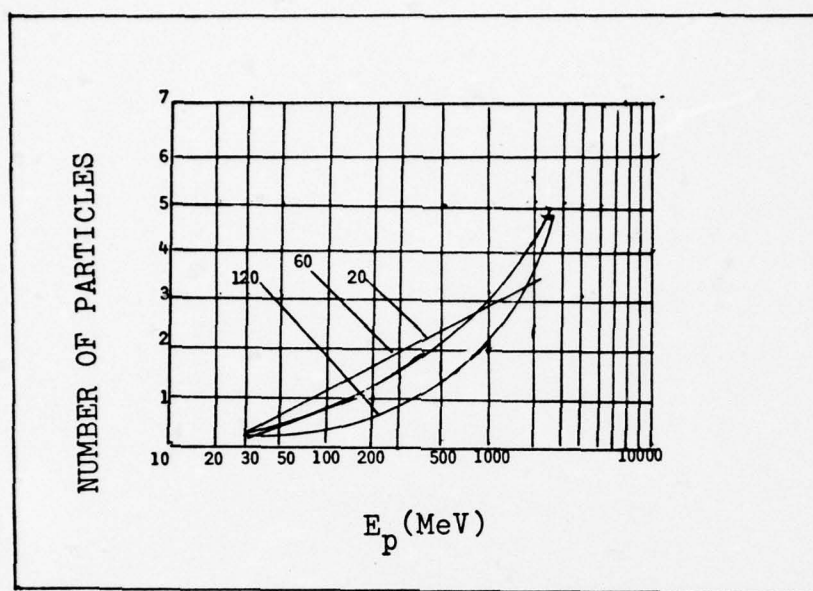


Fig.4 The number of cascade protons per incident primary proton as a function of atomic weight of target.

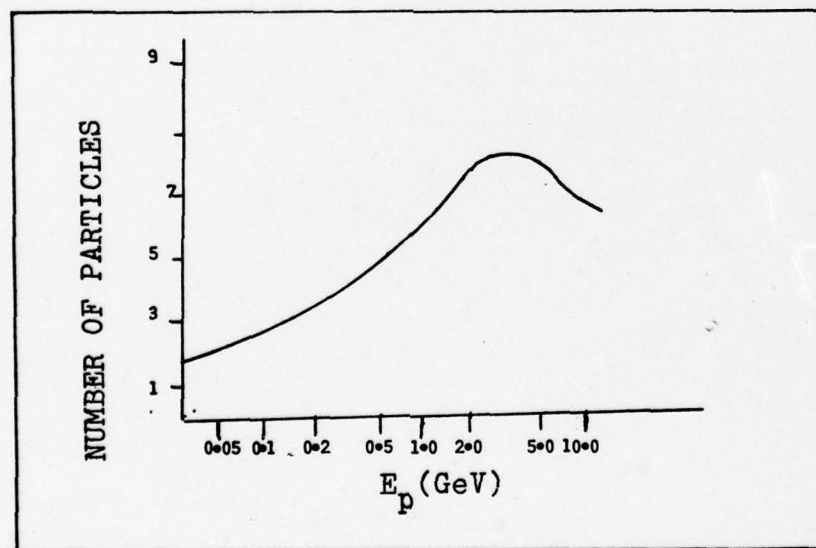


Fig.5 Average number of cascade particles per incident proton.

for cascade. In the cascading process, the initial 10 GeV proton may undergo a collision, producing a proton of energy only slightly less than the incident particle energy; these protons are still capable of proving further cascading and thus are termed cascade protons. If these cascade protons (C) interact, they produce secondary or tertiary protons with somewhat less energy (see Tables I and II), and these lower energy protons are called shower protons (S).

For energies on the order of 10 GeV the qualitative breakout is as follows:

<u>Table II Distribution of cascade particles (10 GeV Beam)</u>			
	(E) GeV	Relative #	Energy Fraction
Primary Protons (C)	8.5	2×10^{-3}	1.7×10^{-3}
Secondary Protons (S)	2.9	8.8×10^{-3}	2.6×10^{-3}
Tertiary Protons (S)	~ 1.0	1.1×10^{-3}	1.1×10^{-3}
Secondary Neutrons (S)	3.6	8.8×10^{-3}	3.2×10^{-3}
Tertiary Neutrons (S)	~ 1.2	1.1×10^{-2}	1.3×10^{-3}
π^+	.9	2×10^{-4}	1.8×10^{-5}
μ^+	.1	6×10^{-1}	6×10^{-3}

As can be seen, the mechanism for interactions in these high energy regions are continually changing, as are the products.

Fig. 5, a plot similar to Fig. 4, extends the energy of the incoming particle to show a maximum at approximately 5 to 10 GeV. This deviation from the expected (the higher the energy of the incident particle, the more cascade particles) is attributed to a change in the density of the nuclear nucleons during the course of development in the in-

ternuclear cascade (Ref 9). The large number of shower particles produced in the first inelastic N-N or N- π collisions inside the nucleus knock out the next nucleons along the path of cascade development, and because of the relativistic speeds under consideration, the nuclear density does not have time to become redistributed appreciably during the time of passage of the nuclear cascade, or simply the nucleus does not have time to redistribute its nucleons to a state which would allow further interactions. The cascade particles encounter smaller numbers of internuclear nucleons; thus, the excitation energy is accordingly smaller, and consequently, the number of evaporated particles (delayed emission) is lower. The energy at which this phenomenon occurs is termed "the saturation energy" and may present a limit on the energy of the protons.

Let us now look at some of the secondary particles produced in the cascade process in order to determine if reasonable amounts of energy may be deposited. The shower protons have somewhat less energy than the cascade protons, but their energies are still high enough that the cross sections are low, as can be seen by comparing Table II with Fig 2. The cascade particles have similar energies to the incident protons and thus also very low cross sections. Energy may be deposited due to multiple scatters of the above particles. With each scatter, the cross section for the next collision becomes larger until the particle dissipates large amounts of energy with each collision.

Neutrons, being similar to protons in mass and energy received during cascading, have very low cross sections for inelastic interactions. If fissionable material were present in the target, the increase in the fission barrier, due to deeper splitting at higher energies, could not be compensated for by an increase of excitation energy, and the fission cross section should decrease with increasing energy of the primary particle. In other words, if a nucleus is to fission, it must overcome a barrier caused by an increase in surface tension energy of the two new nuclei being formed. This increase forms an energy barrier which must be overcome by the energy of the incident particle. The lowest potential barrier occurs when nuclei of the same mass number are formed, but with higher energy incident particles, the new nuclei may not be symmetric and thus the fission barrier is much higher with this deeper splitting. This effect has been observed for plutonium and uranium nuclei. Neutrons, like protons, engage in nonfissionable nuclear interactions causing partial dissipation of their energy and thus continuing the cascade process.

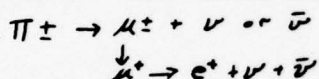
Large number of pions (π^{\pm}) are produced in the p-p and p-n reactions of the internuclear cascade. These particles have a mass of ~ 135 - 140 MeV and possess very short half-lives. The neutral pion, π^0 , has a half-life of 1.8×10^{-16} sec. decaying to two annihilation gamma rays. These gammas will be quickly stopped (a drop in intensity of $1/e$ in 2 cm Al) in most heavy materials due to the high

absorption coefficient. The mechanism for absorption will be almost totally pair production and show absorption coefficients near $.8\text{cm}^{-1}$ or a drop in intensity

$$I/I_0 = e^{-\mu x}$$

where I_0 - initial intensity of the radiation and I - the intensity after a distance x .

For a 70 MeV gamma I/I_0 would be 10^{-3} after traveling through one meter of aluminum. The π^\pm have considerably longer half-lives, $2.85 \cdot 10^{-8}$ sec., and since they are moving at the speed of light, may not deposit their energy in the target material. The π^+ may decay producing a muon and a neutrino. The muon may then interact and also decay.



where ν = neutrino and $\bar{\nu}$ = antineutrino.

The π^\pm may also undergo reaction with the nucleons and produce a multiple of subnuclear particles. Of the energy give to the π^\pm , fairly large amounts will be deposited in the target; thus, the number of pions produced becomes a major factor in determining the energy deposition in a target.

Fig. 6 shows the average number of pions emitted from the various elements when bombarded by protons of various energies. Fig. 7 shows the distribution of the pions between π^0 , π^+ , and π^- at various energies in copper. The π^0 becomes the dominant particle produced at high energies and, coupled with its short half-life, would indicate a slight increase in deposition energy from this process.

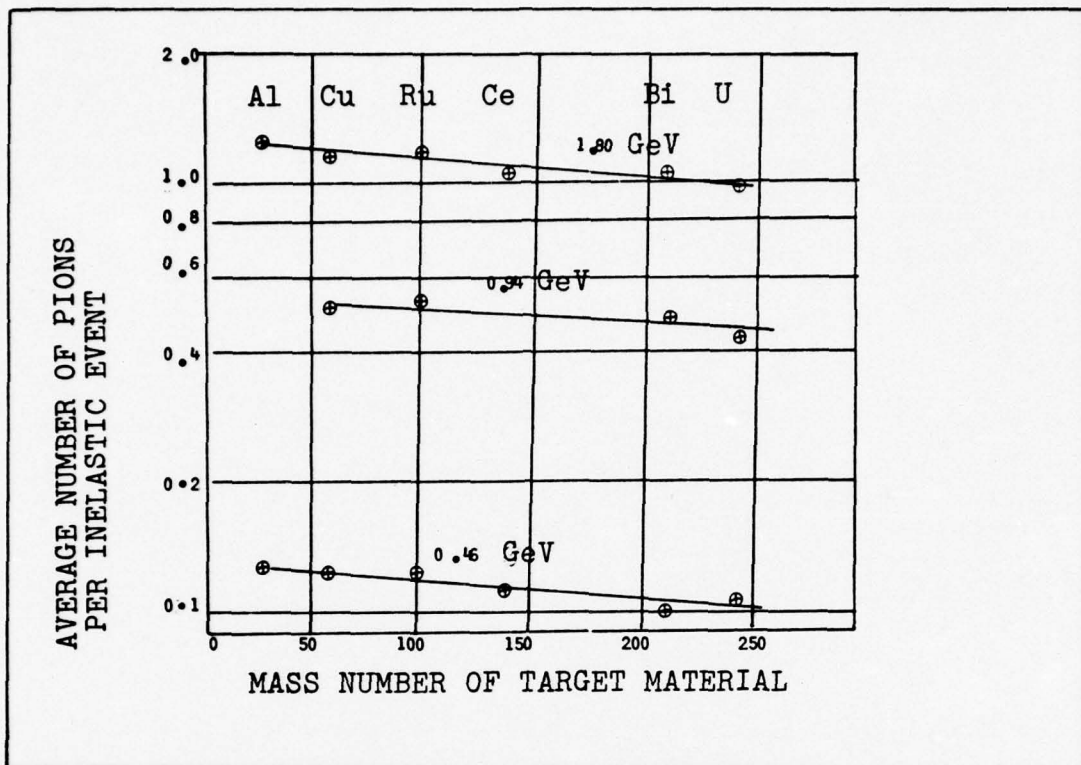


Fig. 6 Average number of pions emitted from various nuclei bombarded by protons of various energies.

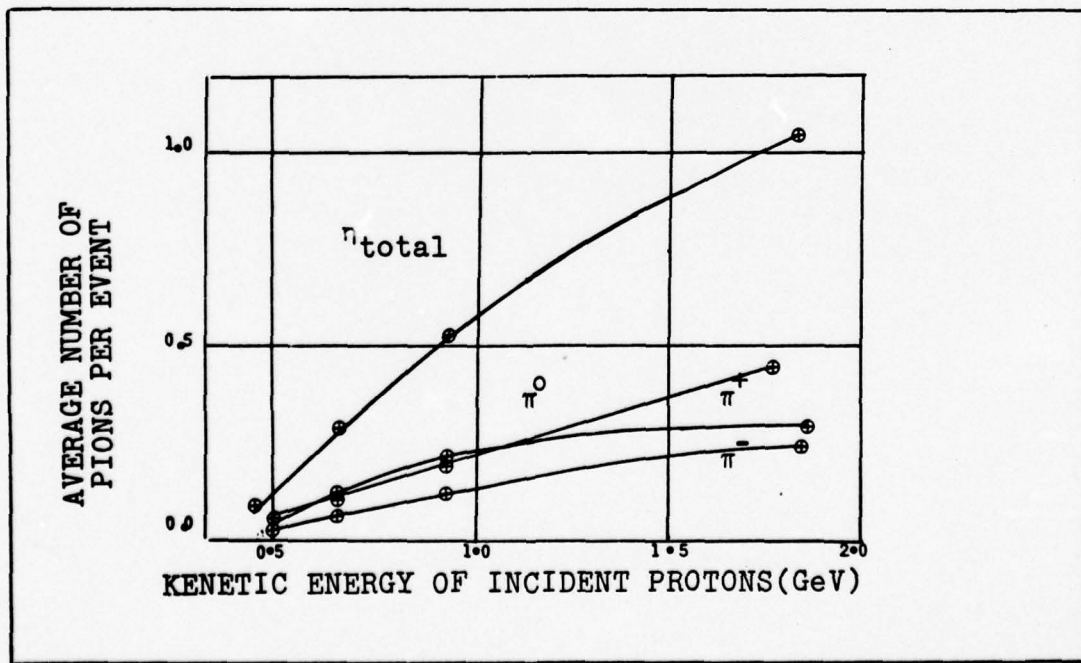


Fig. 7 Average number of π^+ , π^- , and π^0 emitted from a ^{64}Cu target bombarded by protons.

Nuclear interactions account for a major portion of the energy deposited in the target material. However, because of the complexity of the interaction mechanisms, large computer programs using Monte Carlo techniques are used at the present time. Computer codes such as HETC (High Energy Transport Code) (Ref 7) do not take into account secondary and tertiary particle interactions. Barenshkov has recently developed a code which does take into account the secondary interactions of the cascade and shows fair agreement with experimental results. Considerable modeling and experimental work must still be completed in this area before application of theory to experimental data involving nuclear cascading will be completely understood.

Bremsstrahlung

When a proton interacts with the coulomb field of the nucleus of the target material through inelastic collisions, the accompanying deceleration leads to the emission of electromagnetic radiation whose amplitude is proportional to the change in velocity or direction. Bremsstrahlung produced by collisions of fast particles with the atoms will make up a continuous spectrum of discrete photons whose wavelengths are related to the energy loss of the particle (Ref 3):

$$\frac{hc}{\lambda} = K - K'$$

where K and K' are the energies of the particle before and after interaction with the coulomb field, and h equals Planck's Constant, c equals the speed of light, and λ equals the wavelength of radiation emitted.

For a small deflection in a point coulomb field of charge, Ze , the momentum change on a particle of charge ze and mass (M) is transverse and is given, as was shown in the ionization case by:

$$\Delta P = Z \int_{-\infty}^{+\infty} e E(t) dt = \frac{2 Z z e^2}{b v} \quad (13)$$

where b is the impact parameter or distance of closest approach to the nucleus (Ref 3).

For a relativistic case, if we transfer reference frames from the laboratory frame where the particle moves to the K' frame where the particle is at rest, classical theory remains accurate with only a few minor changes in the impact parameter. Thus, from EQ (13) and $\Delta P = M \Delta V$

$$\Delta V = \frac{2Ze^2}{bVM} \quad (14)$$

The intensity of the radiation can be shown to be proportional to the square of the product of the amplitude and the charge Ze will vary as:

$$I \propto \frac{Z^2 Z^4 c^6}{M^2}$$

Thus, the total bremsstrahlung varies as the square of the atomic number of the stopping material and inversely with the square of the mass of the incident particle. Therefore, a proton will produce about one-millionth the bremsstrahlung of an electron of the same velocity. Because of this strong dependence on mass, bremsstrahlung is almost completely negligible for all fast particles other than electrons.

Summary of Collisional Interactions

In summary, let us look at examples of a few of the major types of interactions for specific cases and estimate the energy deposited in the target material. These calculations are only to the zero order and are intended to show trends and not meant to be exact.

As a trial case, let us use the following criteria:

The Beam

1. Energy of protons = 10 GeV
2. Current = 1×10^3 amps

3. Velocity of beam = $2.98 \times 10^8 \text{ m/s}$
4. Relativistic constant = .988
5. Radius of beam = .001 m
6. Flux of protons in beam = 1.99×10^{28}
protons/ $\text{M}^2 \text{ sec}$
7. Charge per nanosecond pulse = 1.0×10^{-6}
coul/pulse

The Target

1. Aluminum, $_{13}\text{Al}^{27}$
2. Mean excitation potential, $I = 166 \text{ eV}$
3. Density correction faction
$$S = 4.606X + C = 4.02$$
4. Cross section for interaction = 115
millibarns = $115 \times 10^{-27} \text{ m}^2$
5. Thickness = 1 m

The calculations will be done for each mechanism as follows:

1. Ionization losses will be calculated via Eq (12) where it has been assumed that the beam does not slow down with energy loss. If the target is thick with respect to the range of the proton, this is not a bad approximation. For this example, the range of a 10 GeV proton is on the order of a few meters; therefore, the amount calculated is somewhat below the actual value.

2. Nuclear interaction losses are calculated on the assumption that each interaction deposits its total energy locally. This is not the actual case, since we discussed

showering in a previous section. This approximation does not take into account the nuclear energy liberated in the interaction processes and will therefore be somewhat low.

3. Bremsstrahlung losses will be estimated from the equation

$$\frac{dE_{rad}}{dE_{coll}} = \frac{4}{3\pi} \beta^2 \frac{Z}{137} \frac{M_e}{M_{particle}} \left(\frac{V}{c}\right)^2 \frac{1}{\ln B}$$

which relates the energy loss due to radiation of bremsstrahlung to the energy loss due to collisions (Ref 2).

Table III clearly shows that the amount of energy deposited by the beam in a target is surprisingly small compared to the sublimation energy of aluminum (7.4×10^{16} MeV/gram); thus, there is some concern as to its usefulness. For the electron beam, we would expect the total energy of the beam to be deposited within a very short distance into the target by collisional interactions.

Table III
Summary of Energy Deposited by Various Interactions

Mechanism	Max Energy Deposited	% of Total
Ionization	3.5×10^5 MeV/sec	9
Nuclear Interactions	22.0×10^5 MeV/sec	91
Bremsstrahlung	0.6 MeV/sec	-

III. Collective Interactions

Because the plasma consists of extremely large numbers of particles, it becomes impossible to follow each individual particle and its interactions. A more practical approach is to represent the plasma components through a distribution function. If the kinetic equations are then applied to this function, instead of individual particles, a "mean" response will evolve. This mean response can be considered the response of the entire plasma, or a collective response, and is felt over large distances as compared to collisional effects.

Oscillations are probably the most basic collective response of a plasma. If a plasma is acted upon by an external force, it will tend to oscillate. These oscillations may be either stable or unstable in nature. If the oscillations are unstable, energy from the force will be continually pulled into the plasma to support this instability, and this energy will be converted into random motion or heat. This is the mechanism by which energy from the proton beam can be transferred into the plasma.

There are two major types of instabilities, velocity-space instabilities in which the plasma is unstable because of its particle distribution in phase space, and configuration-space instabilities in which the plasma is unstable because of its particle distribution in configuration (or real) space.

The two-stream instability is a well-known instability

associated with charge particle beams and will be discussed as an example of the method of deposition of energy in a plasma through unstable oscillations.

Two-stream Instability

Two-stream instability is an electrostatic phenomenon involving the coupling of oscillations within the electric field of the beam to oscillatory modes within the plasma. Because this coupling is an electrostatic phenomenon, and involves separation of charge, its magnitude is much larger than other electromagnetic effects. From the first two moments of the Vlasov equation for the beam and the target plasma, we obtain:

$$\frac{dN_a}{dt} = - \frac{d}{dx} (N_a u_a) \quad (15)$$

where $a = 1$ for the beam and $a = 2$ for the plasma and

$$\frac{d(N_a u_a)}{dt} = - \frac{d}{dx} (N_a u_a^2) + N_a a_a \quad (16)$$

where a = an acceleration term due to forces within the beam and plasma

N = number density

U = velocity of charges

$N_a u_a^2$ = energy term.

Coupling the above two equations and solving for a yields:

$$a = \frac{q \frac{dE}{dx}}{q \frac{\rho}{\epsilon_0}} = \frac{(q_1 N_1 + q_2 N_2)}{\epsilon_0} \quad (17)$$

By linearizing the above equations, they become;

$$\begin{aligned} N_a &= N_a^0 + N_a^1 && \text{(the 1 for superscript} \\ u_a &= u_a^0 + u_a^1 && \text{means a small pertur-} \\ &&& \text{bation term.)} \end{aligned}$$

thus Eq (15) becomes:

$$\frac{d(N_1^0 + N_1')}{dt} = -\frac{d}{dx}(N_1^0 + N_1')(u_1^0 + u_1') \quad (18)$$

and Eq (16) becomes:

$$\begin{aligned} \frac{d}{dt}(N_1^0 + N_1')(u_1^0 + u_1') = & -\frac{d}{dx}(N_1^0 + N_1')(u_1^0 + u_1')^2 + (N_1^0 + \\ & N_1')\left(\frac{d}{dx}(N_1^0 + N_1') + (N_2^0 + N_2')\right). \end{aligned} \quad (19)$$

Keeping only the first order terms, Eq (18) becomes:

$$\frac{dN_1'}{dt} = -\frac{d}{dx}(N_1^0 u_1' + N_1' u_1^0). \quad (20)$$

Eq (19) becomes:

$$\frac{d}{dt}(N_1^0 u_1' + N_1' u_1^0) - \frac{d}{dx}(2N_1^0 u_1^0 u_1' + N_1' u_1'^2) + N_1^0 \frac{e}{\epsilon_0} \frac{d}{dx}(N_1' - N_2') \quad (21)$$

where $q_1 = +e$ and $q_2 = -e$, and there is no zero order electric field

$$g_1 N_1^0 + g_2 N_2^0 = 0.$$

With the above equations, we have 4 equations and 4 unknowns, and the problem can be solved. If we wish to look at the normal modes of the two systems, assume:

$$N_1' = N_1' e^{-i(Kx - \omega t)}$$

$$u_1' = u_1' e^{-i(Kx - \omega t)}$$

where N_1^1 and u_1^1 are constants Eq (15) then becomes:

$$-i\omega N_1' = -iK(N_1^0 u_1' + N_1' u_1^0).$$

Eq (16) becomes: (after algebraic simplification):

$$-i\omega u_1' = -iK(u_1^0 u_1') + \frac{iKe}{\epsilon_0}(N_1' - N_2').$$

Solving the above four equations yields:

$$\left(1 - \frac{\omega_{p1}^2}{(\omega - Ku_1^0)^2} - \frac{\omega_{p2}^2}{(\omega - Ku_2^0)^2}\right) u_1' = 0 \quad \text{where } \omega_{p1}^2 = \frac{N_1^0 e^2}{m\epsilon_0}. \quad (22)$$

In order to have a nontrivial solution ($u \neq 0$), the quantity in the brackets must vanish. Therefore,

$$1 - \frac{\omega p_a^2}{(\omega - k u_a^0)^2} - \frac{\omega p_b^2}{(\omega - k u_b^0)^2} = 0$$

This equation will have four roots to its solution. For example:

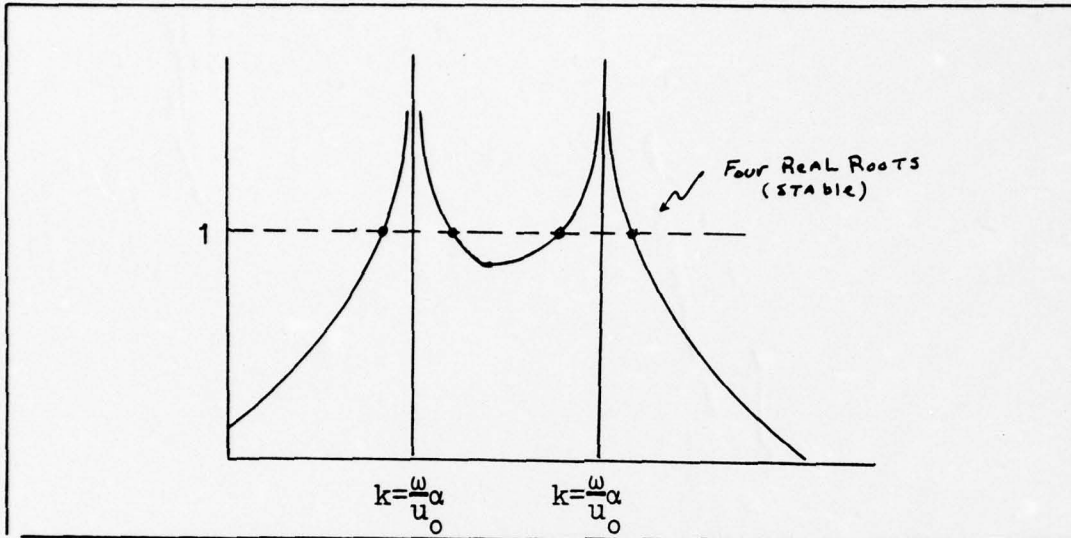


Fig.8 Solution to two-stream instability model(real roots). Sketch of as a function of wave number(k).

The circles represent four real solutions; however, as $\frac{\omega}{u_a^0}$ gets close to $\frac{\omega}{u_b^0}$, in other words, the oscillations of the beam and plasma couple, we get two real and two imaginary roots.

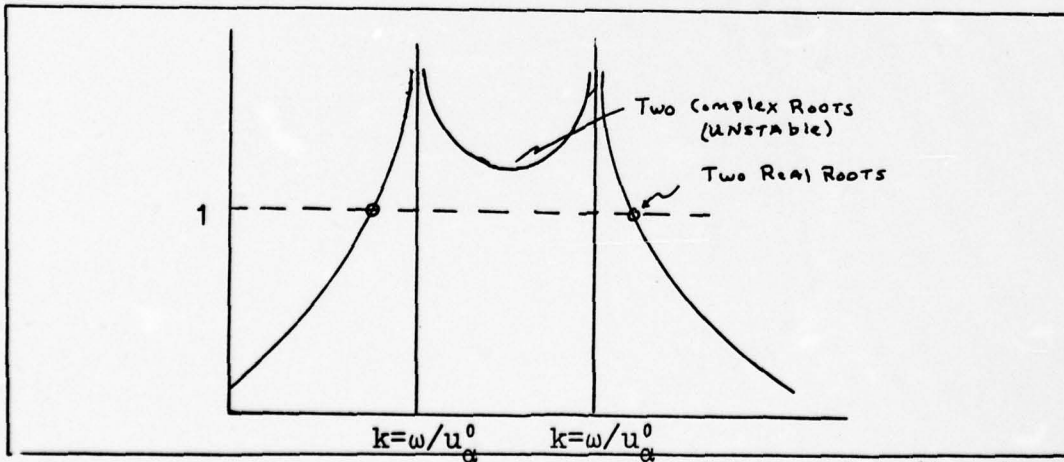


Fig. 9 Solutions to two-stream instability model (imaginary roots)

Analytic Estimate of Energy Deposited Through Collective Interaction in a 1-D Model

As can be seen from the conclusions in the section on interactions, collisional losses do not deposit large amounts of energy in the target material; therefore, the analysis of collisionless effects becomes important if it can be shown that reasonable energy can be deposited in the target by these effects. As a simple test of the procedure, the following first-order analytic solution was evaluated.

If we linearize the first two moments of the Vlasov equation in one dimension

$$\frac{d\rho}{dt} = - \frac{d(\rho u)}{dx}$$

and

$$\frac{d(\rho u)}{dt} = - \frac{d}{dx}(\rho u^2 + p) + \rho a$$

where ρ = particle density

u = velocity of particles

p = pressure term

a = force term = $\frac{q}{m} E$

and the adiabatic gas law which is a special case of the third moment,

$$p\rho^{-\gamma} = p_0\rho_0^{-\gamma}$$

where $\gamma = 1 + \frac{2}{f}$

f = the degrees of

freedom. By letting

$$\rho = \rho_0 + \rho_1$$

$$a = a_0 + a_1$$

$$u = u_0 + u_1$$

$$p = p_0 + p_1$$

where the zero order terms are constants and the first

order terms are small, the resulting equations are

$$\frac{d\rho_1}{dt} = -\rho_0 \frac{dU_1}{dx} \quad (23)$$

$$\rho_0 \frac{dU_1}{dt} = -\frac{dP_1}{dx} + \rho_0 a \quad (24)$$

$$P_1 = a^2 \rho_1 \quad (25)$$

where $a^2 = \frac{\gamma P_0}{\rho_0}$ = electron speed of sound, $U_0 = 0$, and all second order terms are neglected.

The result is Eqs (23), (24) and (25) are three equations in the three unknowns ρ , U , and P . Solving for U , take the second derivative of Eq (24) with respect to time

$$\rho_0 \frac{d^2 U}{dt^2} = -\frac{d^2 P_1}{dt dx} + \rho_0 \frac{da_1}{dt}$$

but $P_1 = a^2 \rho_1$ so that

$$\begin{aligned} \rho_0 \frac{d^2 U}{dt^2} &= -\frac{d}{dt} a^2 \frac{d\rho_1}{dx} + \rho_0 \frac{da_1}{dt} \\ &= -a^2 \frac{d^2 \rho_1}{dx dt} + \rho_0 \frac{da_1}{dt} \end{aligned}$$

Substituting in Eq (23)

$$\rho_0 \frac{d^2 U}{dt^2} = -a^2 \frac{d}{dx} \left(-\rho_0 \frac{dU_1}{dx} \right) + \rho_0 \frac{da_1}{dt}$$

and canceling the ρ_0 yields

$$\frac{d^2 U}{dt^2} = a^2 \frac{d^2 U_1}{dx^2} + \frac{da_1}{dt}, \quad (26)$$

since

$$a_1 = \frac{g}{M} E = \frac{g}{M} (E_1^{ext} - E_1^{int}) ,$$

where E^{ext} = the field due to the beam

and E^{int} = the field due to the plasma motion.

$$\frac{dQ_1}{dt} = \frac{g}{M} (E_1^{ext} - \frac{J}{\epsilon_0}) = \frac{g}{M} (E_1^{ext} - \frac{g u_1 \rho_0}{M \epsilon_0})$$

since $J = g \int u_1 \rho_0 = g u_1 \rho_0$ and E_1^{ext} will be a specified value obtained from outside methods. Thus,

$$\frac{dQ_1}{dt} = -\frac{g}{M^2} \frac{\rho_0}{\epsilon_0} u_1 + \frac{g}{M} \frac{dE_1^{ext}}{dt} . \quad (27)$$

Combining Eqs (26) and (27) yields

$$\frac{d^2 u_1}{dt^2} - a^2 \frac{d^2 u_1}{dx^2} + \frac{g \rho_0}{M^2 \epsilon_0} u_1 = \frac{g}{M} \frac{dE_1^{ext}}{dt} . \quad (28)$$

Let us call $\frac{g}{M} \frac{dE_1^{ext}}{dt} = F$, a forcing function, and note that

$$\frac{g \rho_0}{M^2 \epsilon_0} = \frac{g N_0 M}{M^2 \epsilon_0} = \frac{g N_0}{M \epsilon_0} = \omega_p^2$$

where ω_p is the plasma frequency. This frequency is the frequency at which a plasma oscillates. If an electron is displaced from the ion site, it will experience a force that seeks to return it to the original position. When it arrives at its equilibrium position, it will possess kinetic energy equal to the potential energy of the initial displacement and will go past the equilibrium position, thus setting up an oscillation of frequency ω_p . Equation (28) then becomes

$$\frac{d^2 u_1}{dt^2} - a^2 \frac{d^2 u_1}{dx^2} + \omega_p^2 u_1 = F . \quad (29)$$

Eq (29) is a linear differential equation in u_1 for which we would like to find a solution. Using Green's functions, if F has the form

$$F = \delta(x-x') \delta(t-t')$$

then the solution to the equation is Green's function, G

$$u_1 = G(x-x', t-t'). \quad (30)$$

Then, G must satisfy the equation

$$\frac{d^2 G}{dt^2} - a^2 \frac{d^2 G}{dx^2} + \omega_p^2 G = \delta(x-x') \delta(t-t'). \quad (31)$$

We must now find the functional form of G. u_1 for any F is

$$u_1 = \iint G(x-x', t-t') F(x', t') dx' dt'. \quad (32)$$

Multiplying Eq (32) by $(\frac{d^2}{dt^2} - a^2 \frac{d^2}{dx^2} + \omega_p^2)$ yields

$$(\frac{d^2}{dt^2} - a^2 \frac{d^2}{dx^2} + \omega_p^2) u_1 = \int (\frac{d^2}{dt^2} - a^2 \frac{d^2}{dx^2} + \omega_p^2) G(x-x', t-t')$$

but, from Eq (31)

$$F(x', t') dx' dt'$$

$$(\frac{d^2}{dt^2} - a^2 \frac{d^2}{dx^2} + \omega_p^2) u_1 = \int \delta(x-x') \delta(t-t') F(x', t') dx' dt'$$

then for any G which satisfied

$$G(x-x', t-t') = \delta(x-x') \delta(t-t')$$

then

$$u_1 = F(x, t)$$

Thus, we need to find a G for which this fact holds.

Let's take the fourier transform of $\delta(x-x') \delta(t-t')$

$$\delta(x-x') \delta(t-t') = \frac{1}{(2\pi)^2} \iint dk dw e^{ik(x-x')} e^{-i\omega(t-t')} \quad (33)$$

let

$$G(x-x', t-t') = \frac{1}{(2\pi)^2} \iint dk dw e^{ik(x-x')} e^{-i\omega(t-t')} g(k, \omega). \quad (34)$$

If we operate on Eq (34) with $(\frac{d^2}{dt^2} - a^2 \frac{d}{dx} + \omega_p^2)$ we obtain

$$(\frac{d^2}{dt^2} - a^2 \frac{d}{dx} + \omega_p^2)G = \frac{1}{(2\pi)^2} \iint dK d\omega g(K, \omega) (-\omega^2 + a^2 K^2 + \omega_p^2) e^{iK(x-x')} e^{-i\omega(t-t')} \quad (35)$$

We would like Eq (33) and (35) to be equivalent, thus

$$g(K, \omega) = \frac{1}{-\omega^2 + a^2 K^2 + \omega_p^2} \quad (36)$$

where $\omega^2 = \omega_p^2 + a^2 K^2$ is known as the Bohm-Gross dispersion relation and relates the frequency of the electrostatic wave to the vector.

A dispersion relation describes the ability of a specific pulse shape to pass through a plasma without being distorted. A pulse which is made up of several frequencies will be dispersed upon passing through a plasma since each frequency travels at a different speed. The extent of this dispersion is a function of the plasma and the number and range of frequencies in the pulse. Now that we know

$g(K, \omega)$, we can work back to find $G(x-x', t-t')$.

But an easier method may be to do the following: Let's look at the fourier transform of $u(x, t)$

$$u(x, t) = \frac{1}{(2\pi)^2} \iint dK d\omega u(K, \omega) e^{iKx} e^{-i\omega t}$$

The inverse transform is then

$$u(K, \omega) = \iint u(x, t) e^{-iKx} e^{i\omega t} dx dt \quad (37)$$

but $u(x, t)$ is given by Eq (32) thus

$$u(K, \omega) = \iiint G(x-x', t-t') F(x', t') e^{-iKx} e^{i\omega t} dx' dt' dx dt. \quad (38)$$

Transforming $F(x', t')$ and $G(x-x', t-t')$ yields

$$F(x', t') = \frac{1}{(2\pi)^2} \iint dk' d\omega' F(k', \omega') e^{i k' x'} e^{-i \omega' t'} \quad (39)$$

$$G(x - x', t - t') = \frac{1}{(2\pi)^2} \iint dk'' d\omega'' g(k'', \omega'') e^{i k'' (x - x')} e^{-i \omega'' (t - t')} \quad (40)$$

Substituting Eqs (40) and (39) into Eq (38) yields

$$u(k, \omega) = \iiint \frac{1}{(2\pi)^4} dx dt dx' dt' dk' d\omega' dk'' d\omega'' \\ F(k', \omega') G(k'', \omega'') e^{i x'(k - k'')} e^{i x(k'' - k')} \\ e^{-i t(\omega - \omega'')} e^{-i t'(\omega'' - \omega)}$$

But

$$\frac{1}{2\pi} \int dx e^{i x(k - k'')} = \delta(k - k'')$$

$$\frac{1}{2\pi} \int dt e^{i t(\omega - \omega'')} = \delta(\omega - \omega'')$$

etc. so that where

$$k' = k'', \quad k'' = k, \quad \omega = \omega'', \quad \omega' = \omega''$$

$$u(k, \omega) = F(k, \omega) g(k, \omega).$$

If we know what $F(k, \omega)$ is, then we can find $u(k, \omega)$ since we also know $G(k, \omega)$.

If we model the beam as a chopped system in which the pulses are so short (10^{-11} seconds) that the radius of the beam and its length are approximately equal, the pulse could be assumed to be a spherically symmetric charge distribution. For such a sphere of radius R , the electric field at a point r is given by (Ref. 3)

$$E = \frac{1}{4\pi\epsilon_0} \frac{qr}{R^3}$$

when r is less than or equal to R and very approximately equal to

$$E = \frac{1}{4\pi\epsilon_0} \frac{q}{r^2}$$

for $r > R$.

Fig. 18 is a plot of the expected force ($F = qE$) associated with the model of the pulse.

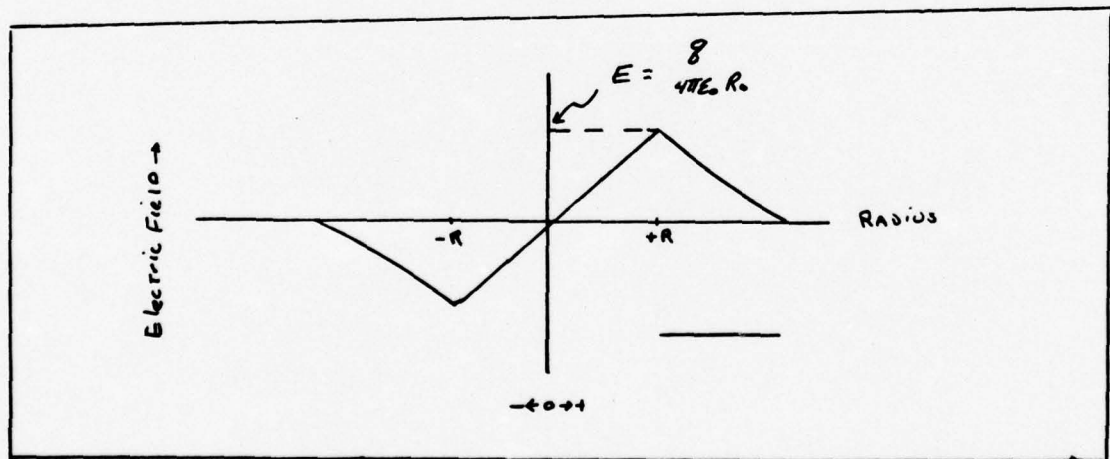


Fig. 18 Force due to spherical charge distribution on a point charge.

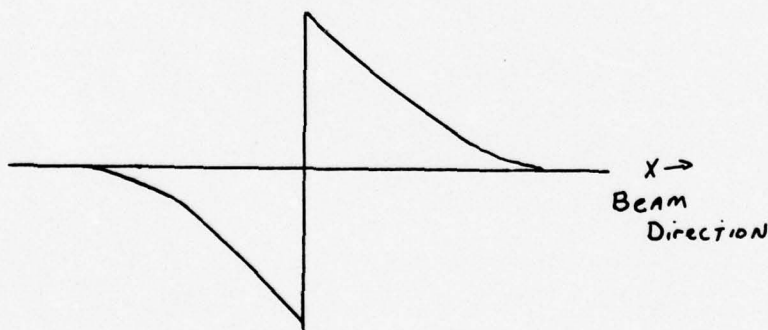
For relativistic proton pulses, the electrons first see the effects of the beam at fairly short ranges. These forces continue to grow until the beam just reaches the position of interest. As the beam passes the force decreases to zero at the center of the pulse. The force will then increase to a maximum at the opposite edge of the pulse and decay back to zero as the pulse moves rapidly away.

Figure 18 is somewhat similar to the plot of the derivative of the delta function. Thus, the force on the particle was taken to be proportioned to

$$F(x,t) = \frac{qc}{M_e} \frac{d\delta'(x-vt)}{dt} \quad (41)$$

where c is a constant of dimension $\frac{V}{M} (M^2)$.

A plot of $\delta'(x-vt)$ would look like



where first the electrons are pulled toward the beam and then pushed as the beam passes.

Transforming Eq (41) yields

$$F(k, \omega) = \frac{gC}{M_e} \int dx dt \frac{df'(x-vt)}{dt} e^{-ikx} e^{i\omega t}$$

which reduces to

$$\begin{aligned} F(k, \omega) &= \frac{gC\omega k}{M_e} \int e^{i(\omega - kv)t} dt \\ &= \frac{gC\omega k (2\pi)}{M_e} \delta(\omega - kv) \quad (42) \end{aligned}$$

after integrating with respect to t and then x . Thus,

$$\begin{aligned} U(k, \omega) &= F(k, \omega) g(k, \omega) \\ &= \frac{gC\omega k (2\pi)}{M_e(a^2 k^2 + \omega_p^2 - \omega^2)} \delta(\omega - kv) \quad (43) \end{aligned}$$

Taking the inverse transform yields

$$U(x, t) = \frac{1}{(2\pi)^2} \iint \frac{-gC\omega k (2\pi)}{M_e(a^2 k^2 + \omega_p^2 - \omega^2)} \delta(\omega - kv) e^{ikx} e^{-i\omega t} d\omega dk$$

integrating over ω

$$\begin{aligned} U(x, t) &= \frac{1}{2\pi} \int \frac{-gCk^2 v}{M_e(a^2 k^2 - \omega_p^2 - (kv)^2)} e^{ikx} e^{-ikvt} dk \\ &= \frac{-gC}{2\pi M_e} \int \frac{k^2 v e^{ik(x-vt)}}{k^2(a^2 - v^2) - \omega_p^2} dk \quad (44) \end{aligned}$$

Let us now define $M = (V/a)$. Where M is the Mach number of the beam in the electron gas. Then,

$$U(x,t) = -\frac{8C}{2\pi M_e} \int \frac{K^2 M e^{i(x - Mat)K}}{K^2(1-M^2) - \omega_p^2/a^2} dK. \quad (45)$$

The value of the integral in Eq (45) will depend upon the value of M , the Mach number of the beam in the plasma. Solutions to the integral can be found through the use of Cauchy's integral theorem, the theorem of residues. The theorem of residues states that the integral of $f(k)$ around a closed path enclosing a single pole of $f(k)$, a point where the function goes infinite, is given by $2\pi i$ times the residue at the pole.

$$\oint_C f(z) dz = 2\pi i (A_1 + B_1 + \dots)$$

where A_1 represents the residue of the pole at a_1 .

Thus, the value of the integral in Eq (45) is given by $2\pi i$ times the value of the residue at any pole lying within the area of integration. Let us divide the solution to $u(x,t)$ into two cases: Case 1 where $M < 1$ and the beam moves slower than the speed of sound in the plasma; and Case 2, where $M > 1$.

If $M < 1$, then the function will have poles on the imaginary axis and will be exponential in character. Looking at the denominator, we find that the value of the poles is given when

$$\frac{1}{K^2(1-M^2) + \omega_p^2/a^2}$$

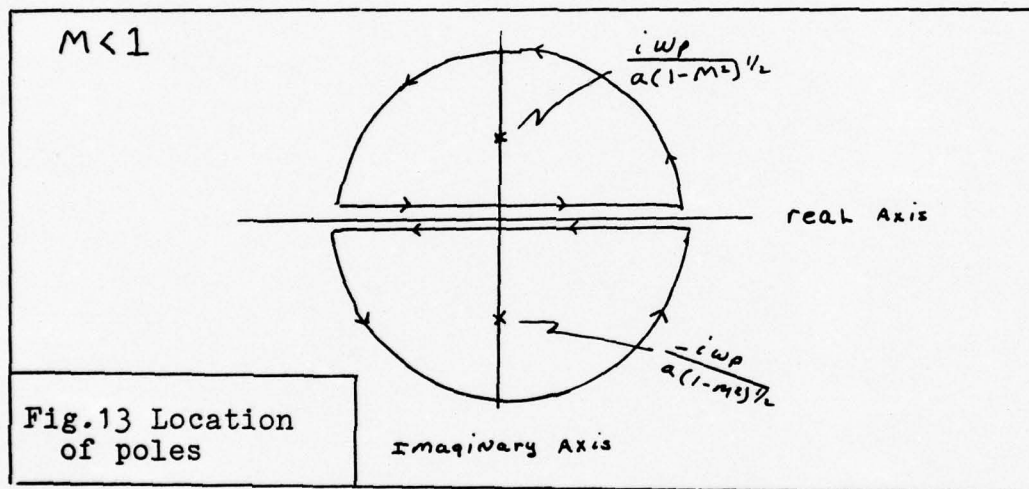
goes to infinity. Thus the pole can be found by

$$\frac{1}{K^2(1-M^2) + \omega_p^2/a^2} = \frac{1}{(1-M^2)\left(K^2 + \frac{\omega_p^2}{a^2(1-M^2)}\right)} = \frac{1}{(1-M^2)\left(K + \frac{i\omega_p}{a(1-M^2)^{1/2}}\right)\left(K - \frac{i\omega_p}{a(1-M^2)^{1/2}}\right)} \quad (46)$$

and the poles are located at

$$\pm \frac{i\omega_p}{a(1-M^2)^{1/2}}$$

on the imaginary axis.



a) If $(x - Mat)$, the beam has not yet reached the point of interest, and we have closed in the upper-half plane, and the residue there is equal to

$$\frac{i\omega_p}{a(1-M^2)^{1/2}}$$

thus

$$U(x,t) = \frac{8CM\omega_p}{2M_e a^2 (1-M^2)^{1/2}} e^{-(X-Mat)\frac{\omega_p}{a(1-M^2)^{1/2}}}$$

b) If $(X-Mat) < 0$, then the beam has hit and passed through the point of interest. This would close in the lower-half plane of Fig. 13. Thus, the only pole exists at the point

$$K = -\frac{i\omega_p}{a(1-M^2)^{1/2}}$$

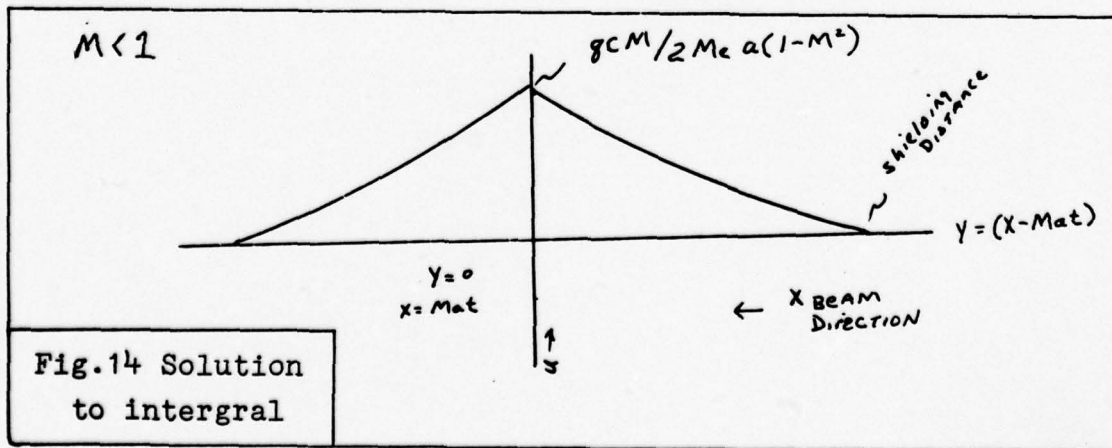
thus

$$U(x,t) = \frac{-i8CM}{2\pi M_e a} 2\pi i \left(\frac{\left(\frac{-i\omega_p}{a(1-M^2)^{1/2}}\right)^2 e^{+i(-Mat+X)\frac{-i\omega_p}{a(1-M^2)^{1/2}}}}{\frac{2(-i\omega_p)}{a(1-M^2)^{1/2}} (1-M^2)} \right)$$

$$U(x,t) = \frac{8CM}{M_e a} \frac{e^{(X-Mat)\frac{\omega_p}{a(1-M^2)^{1/2}}}}{2(1-M^2)} \quad (47)$$

where the limits of integration require us to add an additional minus sign when following the counterclockwise rules of residue integration.

If we now plot $u(x,t)$ for $M < 1$, we see



As can be seen from the equations and the Fig. 14, the amplitude of $u(x,t)$ depends upon the value of M . The region over which the beam is felt is also a function of M . For very small M , exponential fall off is quite slow, and the beam can be felt at long distances, which is as would be expected. As the beam increases its energy and the Mach number increases toward 1, the area affected by the beam becomes quite small. In other words, if M is close to 1, the point of interest does not feel the beam's approach until it is almost upon the point, and at that time, it produces a large shock-front type influence on the point. Once the beam passes, the beam effects decay rapidly. Thus, the delta function beam leads to a rapid acceleration of particles at the points close to beam passage.

In this case, $M < 1$, as y goes to $+$ or $-$ infinity, $u \rightarrow 0$ because of the shielding effects of the neutralizing background ions.

As a side note, if we let M go to zero, the shielding distance is a/ω_p where a can be written as $\left(\frac{KT}{M\epsilon}\right)^{1/2}$

and $\omega_p = \left(\frac{Ne^2}{M\epsilon\epsilon_0}\right)$

thus

$$\frac{a}{\omega_p} \propto \left(\frac{KT}{M} \frac{M\epsilon\epsilon_0}{Ne^2}\right)^{1/2} = \lambda_D$$

the Debye length. The Debye length is the length at which electric effects can be felt in a plasma.

Case II where $M > 1$

$$U(x,t) = \frac{igM}{2\pi M_e a} \int_{-\infty}^{\infty} \frac{k^2 e^{ik(x-Mat)}}{(M-1)^2 k^2 - \omega_p^2/a^2}$$

The poles will be on the real axis, and we should also note that since the beam is moving faster than the speed of sound in the plasma, no prior information can be passed ahead of the beam. Since we have ignored the magnetic field effects of the beam and the plasma, only the longitudinal wave will be present, and its velocity will approach the speed of sound in the plasma instead of the speed of light.

Fig. 15 shows the relation between the phase velocity of a wave with magnetic effects and plasma wave without magnetic effects.

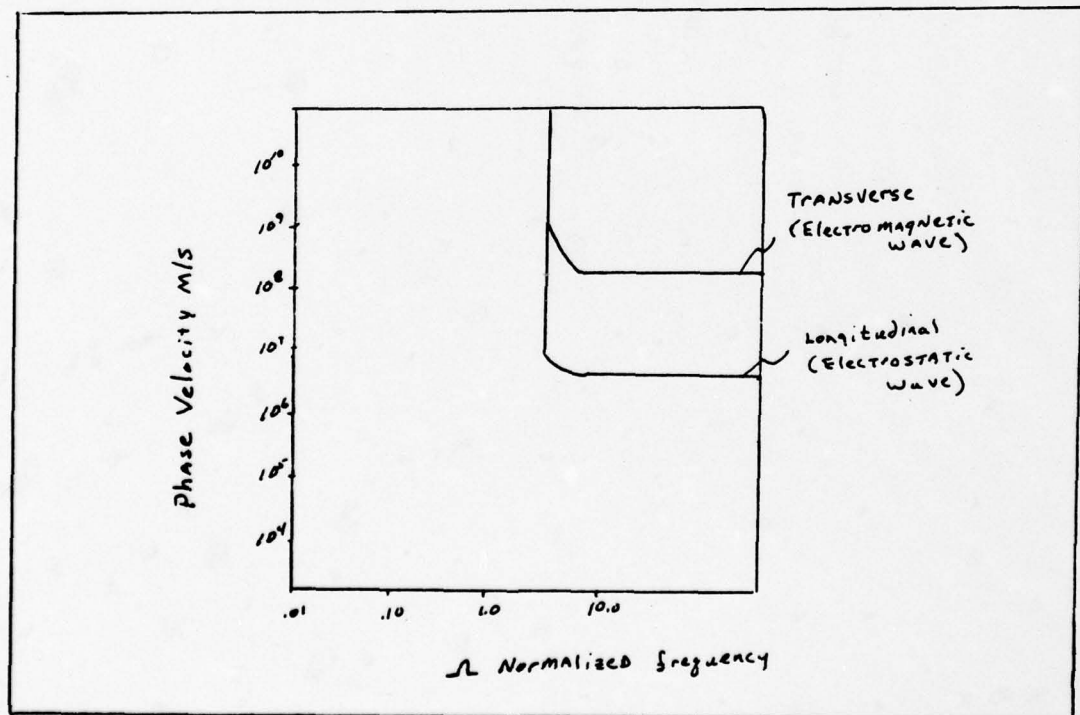


Fig. 15 Phase velocity as function of normalized frequency for transverse and longitudinal waves.

At low normalized frequencies, the phase velocities are

unbounded; however, as the frequencies increase, the phase velocity of the electron plasma is smaller than the velocity of the beam, and no electromagnetic effects will be seen before the wave strikes. This leads to the fact that until $t = 0$, $u(x,t)$ must integrate to zero, and therefore no poles can be located in the upper-half plane of the figure.

Thus, for Case II-a where $(x - Mat) > 0$

$$u(x,t) = 0.$$

The remaining case (II-b) in which $(x - amt) < 0$ would be described by the lower half-plane of Fig. 16

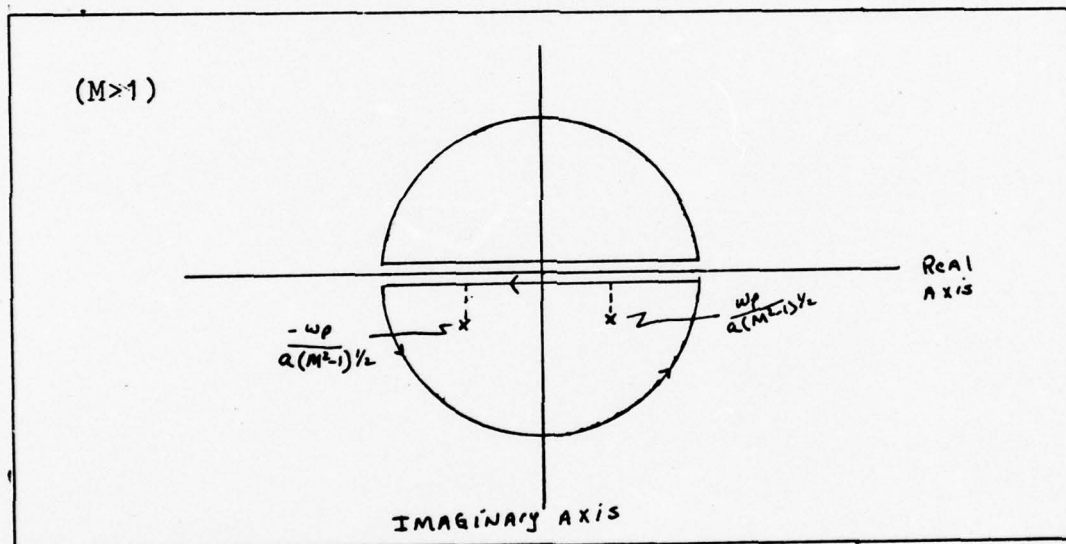


Fig. 16 Location of residual poles

where the poles have been displaced from the axis by $i\epsilon$, the denominator of Eq (46) then becomes

$$(M^2 - 1) \left(K - \frac{wp}{a(M^2-1)^{1/2}} + i\epsilon \right) \left(K + \frac{wp}{a(M^2-1)^{1/2}} + i\epsilon \right) \quad (48)$$

Thus, the poles are located

$$K = \left(\frac{\omega_p}{a(M^2-1)^{1/2}} - i\epsilon \right)$$

$$K = \left(\frac{-\omega_p}{a(M^2-1)^{1/2}} - i\epsilon \right)$$

taking the limit as $\epsilon \rightarrow 0$ yields $K = \pm \frac{\omega_p}{a(M^2-1)^{1/2}}$

Thus, from the residue theorem

$$U(x,t) = -\frac{gCM}{M_e a} [2\pi i] \left\{ \frac{\left(\frac{\omega_p}{a(M^2-1)^{1/2}} \right)^2 e^{\frac{i\omega_p}{a(M^2-1)^{1/2}} (x-Mat)}}{(M^2-1) \frac{2\omega_p}{a(M^2-1)^{1/2}}} + \frac{\left(\frac{-\omega_p}{a(M^2-1)^{1/2}} \right)^2 e^{-\frac{i\omega_p}{a(M^2-1)^{1/2}} (x-Mat)}}{(M^2-1) \left(\frac{-2\omega_p}{a(M^2-1)^{1/2}} \right)} \right\}.$$

$$U(x,t) = \frac{gCM \omega_p}{M_e a^2 (M^2-1)^{3/2}} \cos \left[\frac{\omega_p (x-Mat)}{a (M^2-1)^{1/2}} \right] \quad (49)$$

Fig. 17 shows a plot of Case II-b $M > 1$

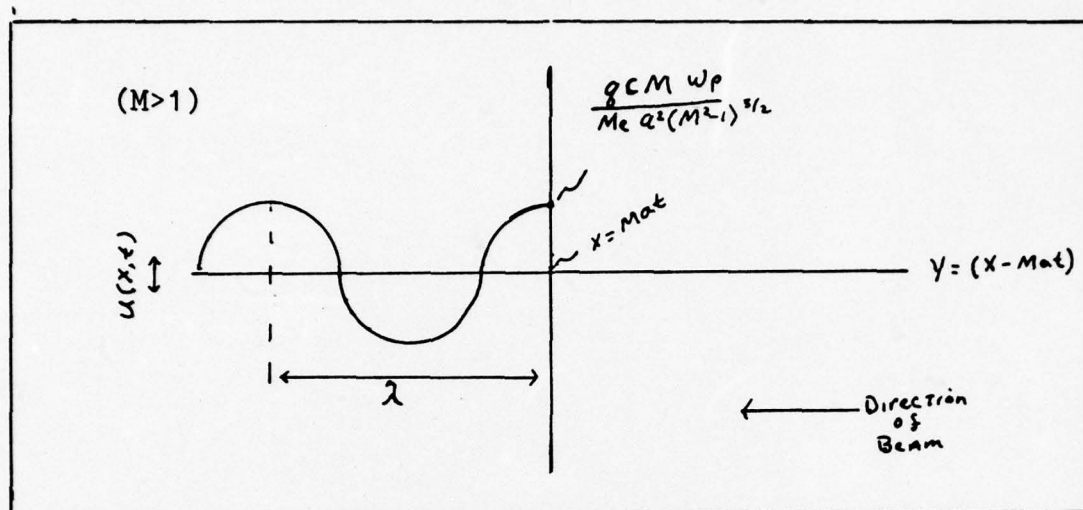


Fig. 17 Solution to residual integral ($M > 1$).

where

$$\lambda \propto \frac{a (M^2 - 1)^{1/2}}{\omega_p} = \lambda (M^2 - 1)^{1/2}. \quad (50)$$

At times, prior to the beam hitting the point of interest, nothing happens. After passage, we now have waves traveling at $V = Ma$ of the beam, without dispersion at a frequency

$$\left. \begin{aligned} \omega &= \frac{\omega_p M}{(M^2 - 1)^{1/2}} \\ K &= \frac{\omega_p}{a (M^2 - 1)^{1/2}} \end{aligned} \right\} \begin{aligned} \frac{\omega}{K} &= V_p, \text{ the phase velocity} \\ \frac{d\omega}{dK} &= V_g, \text{ the group velocity} \end{aligned}$$

From Fig. 17, we can also see that the amplitude of the wave is proportional to $1/M$; thus, for maximum interaction we would want $v \approx a$ or

$$v \simeq a = \left(\frac{kT}{M} \right)^{1/2} \simeq 4.4 \times 10^{13} \frac{\text{ergs}}{\text{gram}}$$

= 66×10^4 m/sec which is far below relativistic speeds. Also, as M becomes large $\omega \rightarrow \omega_p$, and as expected the plasma will not oscillate below the plasma frequency.

The maximum electric field associated with the pulse is given by

$$E_{\text{max}} = \frac{q}{4\pi\epsilon_0 R^2} = 9.0 \times 10^7 \text{ V/m}$$

where q = the total charge in the pulse, (1×10^{-8} coul); and R = the radius of the pulse (.001 meters).

From Fig. 17, the amplitude or maximum velocity of the electron was given by

$$A = \frac{8C M \omega_p}{M_e a^2 (M^2 - 1)^{3/2}}$$

where $M = v/a = 4515$

$$\omega_p = \frac{Ne^2}{M\epsilon_0} = 2.4 \times 10^{16} \text{ sec.}^{-1}$$

C = the forcing function constant

$$\frac{8C}{M} \frac{d\delta(X-vt)}{dt} = \frac{8}{M} \frac{dE^{\text{ext}}}{dt}$$

Therefore, $C\delta' = E$

$$C = Ex \text{ (a radius for the } \delta' \text{ function)}$$

$$C = E R^2 = 90 \frac{\text{V}}{\text{m}} \cdot \text{m}^2$$

thus, $A = 4.3 \times 10^{12}$ m/s which is faster than the speed of light and the model breaks down at this point. If we continue the analysis, we find the kinetic energy of each electron is given by

$$E = \frac{1}{2} M_e A^2 = 5.2 \times 10^6 \text{ MeV}$$

This amount of energy is, to say the least, not a small perturbation, and the linear analysis is clearly incorrect; however, it does indicate that energy of considerable amounts may be transferred by this process, and further investigations are warranted.

If we scale the charge in the pulse by a factor of 1000 down to 10^{-11} coulombs, the velocity of the plasma electrons is equal to 4.2×10^7 m/s and relates to an energy of approximately 5.2 KeV. At this level, the energy of the actual beam (10^{-8} coulombs) would be considerable if scaled up to the 10^{-8} coulomb value.

IV. Method

As was demonstrated in the previous section, there is a need for further understanding in the area of configuration-space instabilities. Configuration-space instabilities occur when the potential energy of a system is lowered through the redistribution of its spatial components. Thus, to reach this lower energy level, the members of the plasma must flow to a new spatial location. The movement of particles in a plasma is best described by the Boltzmann equation. It shows the change in the distribution of particles in a plasma subject to both internal and external electromagnetic fields and collisional interactions. For this thesis, we have assumed that the collective interactions take place on time scales much shorter than the binary collision times; thus, the collision effects on the particle distribution can be ignored. This approximation is commonly called the Vlasov approximation, and as expected, the one-particle Boltzmann equation becomes the Boltzmann-Vlasov equation

$$\frac{df}{dt} + \bar{v} \cdot \nabla_x f + q(\bar{E} + (\bar{v} \times \bar{B})) \cdot \nabla_p f = 0 \quad (51)$$

where

f = the one particle distribution function

t = time

\bar{v} = vector velocity of the particle

$q(\bar{E} + \bar{v} \times \bar{B})$ = the Lorentzian force acting on the particles.

The force is composed of the electric, $q\bar{E}$, and magnetic, $q(\bar{v} \times \bar{B})$ forces from both in-

ternal and external sources.

The development of the Vlasov equations from the basic equations associated with particle motion (Liouville's equation) involves many assumptions that are not readily apparent; thus, the development of this equation is done in Appendix A.

Exact solutions to the Boltzmann-Vlasov equations become very difficult, because the distribution functions are defined in phase space. Large amounts of computer storage would be necessary to describe any distribution in phase space and would become practically impossible to follow during interactions.

Thus, the moments of the Vlasov equations were taken, and the velocity space was integrated out, leaving the equation in real space and a more tractable problem.

Through the moments, the variation in density, average momentum of the particles, and average temperature or pressure can be readily computed. Other physical parameters of the plasma can be investigated by taking higher order moments; however, the complexity of the equations increases rapidly beyond the third moment.

The first three moments of the Vlasov equation are usually termed the hydro-equations, because they involve the flow or redistribution of the particles and the physical properties associated with that flow. Thus, we shall develop the first three moments of the Vlasov equation to examine the response produced by a charged particle beam

in a target plasma.

For our moment analysis, two models will be used: a one-dimensional model, and a three-dimensional model with two degrees of freedom, hereafter to be referred to as two-dimensional.

The one-dimensional model was used to establish the procedures for modeling the target and the beam, and served to iron out major problems which develop in computational and physical analysis. The beam target interaction area closely resembles a cylindrical volume; thus, the two-dimensional model will be structured in cylindrical coordinates with angular symmetry. As the beam strikes the target, it is expected that there will be variations in density, momentum and temperature in the axial and radial directions, but none in the angular direction. Thus, the assumption of angular symmetry reduces the number of degrees of freedom to two. Other specific assumptions will be made and discussed with each model, but the properties of the beam, plasma structure and solving routine will be common to both models and discussed before the specific models are introduced.

The Plasma

The target material is assumed to be an aluminum slab of approximately one meter in thickness. The outer shell electrons in aluminum ($3S^2, 3P^1$) are free to move in the conduction bands of the ionic lattice. The assumption is made that Fermi-Dirac statistics hold for these electrons

or that they are indistinguishable and cannot be located simultaneously in the same state. As the beam deposits energy in the plasma, the temperature and density will change. In the limit as the temperature increases and the density decreases, Fermi-Dirac statistics become Maxwell-Boltzmann statistics, and since our simple analytic example indicates considerable heating, the assumption was made that the plasma could be represented by a Maxwellian distribution.

The electromagnetic forces which act upon the metallic structure will tend to displace both the electrons and the residual ions, but because of the large mass difference between the electrons and ions, the electrons will move much farther in a given time and with much greater velocity. Compared to the electrons, the ions appear stationary over short time scales.

It will be convenient to represent the target as an electron gas with a Maxwellian distribution. The ions, although they do not move, serve as neutralization sites and function as stationary positive charge sites for the restoring electric field developed, if the electrons should be displaced. Thus, the target may be categorized as a single species, Maxwellian distributed, charge neutralized, electron gas.

The Solving Routine

The solving routine used in this thesis was an eight-point ordinary differential equation-solving routine which used the Newton-Raphson method of solution. The routine

solves a system of first order ordinary differential equations at a point B, given initial conditions at point A, and a subroutine for determining the values of the partial derivatives.

Because the equation-solving routine can be extremely complex or extremely simple, depending upon availability to the user, no specific emphasis will be placed on the solving routine in this report.

The Beam

The proton beam is assumed to be a 10^3 amp. beam of 10 GeV protons chopped into pulses at nanosecond intervals. Because of the poor propagational properties of charged particle beams in the atmosphere, considerable amounts of energy per particle and fairly high density will be required to propagate the beam over any reasonable distance. Accelerators capable of producing such high energies and densities are not yet available; thus, these figures should be considered only as representative of actual values. With such high energies, the properties of the beam will clearly have to be treated in a relativistic manner, and the range of these particles in solids will be on the order of a few meters. As was discussed in the collisional interaction section, the energy lost by the beam will take place over the entire range of its interaction, with ionization losses becoming important only near the end of the particle's range.

We have assumed the target to be one meter thick; thus, let us also assume the energy lost by the beam in passing through the target is small and that the beam does not slow down. Since we are more concerned with the effects on the plasma caused by the fields of the beam, this assumption should not induce any major errors.

The chopping of the beam into pulses was assumed because of the hose-instability phenomenon which occurs in beam propagation. The instability so-called because the beam will tend to act like a high-pressure fire hose if not restrained. By pulsing the beam, a major portion of this instability can be eliminated. If the pulses are short enough and we assume the radius of the beam to be small in relation to the target, one could consider the beam to be a series of point charges pulsed at nanosecond intervals. This has been the assumption made, and the electric field associated with the model is calculated in Appendix B. The magnetic field of the beam has been ignored in both models. In the one-dimensional model, the field is not defined since the dimension of choice is that along the direction of travel of the beam. In the two-dimensional model, the magnetic field will produce an outward radial force on the plasma; however, for the initial look into collective interactions, only the electric field will be considered. Additional future work will have to include the magnetic forces of the beam.

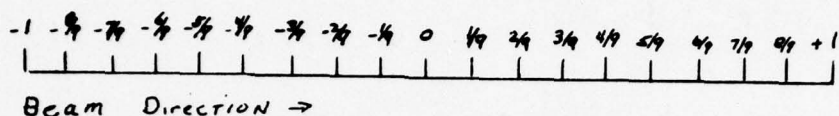
The One-dimensional Model

In the development of the models, the space under consideration will first be discussed. Because of the large areas under consideration and the small areas of interaction, scaling parameters will be applied to the various parameters. The development of the moments will then be undertaken. The internal and external electric and magnetic fields will be coupled to the moments and initial conditions specified.

One-dimensional space. The one-dimensional model assumes variation only in the direction of motion of the beam, and since the solving routine uses an eight-point fitting routine, the number of nodal points (points of solution) will be multiples of eight, plus an additional node to account for the infinity of space outside the target material even though no solution will be obtained at this node. The beam will initially be at $X = -\infty$ at time $t = -\infty$ and will move toward $+\infty$ as time increases. Since the target is finite in dimensions, most of the time the beam will be too far away to be of any consequence and of little interest. To eliminate this problem of extremely large axial distances, a scale transformation was chosen to allow movement from $x = -$ to $+$ infinity over the scaled range of $u = +1$ to -1 . By picking the proper function, the region of interest can comprise the greatest amount of scaled space, and the areas further away can be drastically condensed.

The function $Z = Z_0 \frac{u}{\sqrt{1-u^2}}$ serves such a purpose.

The constant Z_0 can be adjusted to concentrate on areas of interest. If we let $\Delta u = 1/9$ and run u between -1 and $+1$, we obtain 18 intervals.



If we let zero equal the center of the target and the points $\pm 8/9$ equal the end of the target, we will concentrate the area of little interest in the last cell on either end. These cells will not be analyzed since we have the 17 inner points for the solving routine. This method also may prevent problems with fitting the large jump in the density, momentum and temperature between the target and no-target regions.

In a similar manner, the time and the momentum of the electrons were scaled to concentrate on areas of interest. We wish to examine the plasma at the time of impact of the beam without doing much computation in the areas of little interest. The scaling function

$$T = T_0 \sinh(s) \quad (52)$$

was selected. This function takes very small steps at times near zero (when beam reaches center of slab) and large steps with increasing values of (s) . By adjusting T_0 , the specific times of interest can be used.

The momentum is likewise a candidate for scaling with

$$P = P_0 \sinh(v) \quad (53)$$

Thus, the region of concentration is the region of small momentum. If large amounts of energy are deposited by the beam, P_0 can be adjusted as necessary.

The Moment and Force Equations. In one dimension, the Vlasov equation reduces to

$$\frac{df}{dt}(x, v) + v \frac{df}{dx} + F_x \frac{df}{dp_x} = 0. \quad (54)$$

The force term, $F = g(E + (v \times B))$, also reduces since the magnetic field associated with the beam, and any internal magnetic field caused by charge motions, will be undefined in one dimension. Thus, the Vlasov equation takes on the form

$$\frac{df}{dt}(x, p) + \frac{p}{M_0} \frac{df}{dx} + g(E_{int} + E_{ext}) \frac{df}{dp} = 0 \quad (55)$$

where $p = mv$, and it is assumed that the motion of the electrons is non-relativistic. If considerable energy is dumped into the system by the beam, this equation will require the momentum to take on the form $p = \gamma M_0 v$, and a fully relativistic model will have to be examined.

The external electric field, E_{ext} is developed in Appendix B, and estimates of the electric field due to the beam at specific points are given by the function

$$E(x) = \frac{\frac{Q}{4\pi\epsilon_0} \left(\frac{2\beta}{1-\beta^2} \right) - \frac{vt}{\sqrt{R^2(1-\beta^2) + (vt-x)^2}}}{\left[\left(\frac{2\beta}{1-\beta^2} \right) (vt-x) - \sqrt{R^2(1-\beta^2) + (vt-x)^2} \right]}. \quad (56)$$

Where Q = the total charge per pulse in the beam (See Appendix C)

β = the relativistic constant

v = the velocity of the beam

t = the time, where the beam is at the center of the target at $t = 0$

R = radius of interaction - in 1-D chosen as an arbitrary constant

X = the position under consideration.

The internal electric field is obtained from the solution to Maxwell's equation:

$$\frac{(\nabla \times B)}{\mu_0} = \epsilon_0 \frac{dE}{dt} + J \quad (57)$$

where J is the current density.

Since $B=0$ from symmetry and the current density is given by

$$J = \frac{g}{M} \int p f(p) dp.$$

Eq (57) simplified to

$$\frac{dE}{dt} = \frac{g}{\epsilon_0 M} \int p f(p) dp.$$

In Appendix D, the first three moments to the one-dimensional Vlasov equation and the equations necessary to solve the time derivative of the internal electric field are developed.

The analysis in Appendix D resulted in four equations for the time derivatives of the density, momentum, temperature and the internal electric field.

The first moment, continuity equation

$$\frac{d \ln N}{dt} = -\frac{1}{M} \left[N \frac{d\bar{p}}{dx} + \bar{p} \frac{d \ln N}{dx} \right] \quad (58)$$

The second moment

$$\frac{d\bar{p}}{dt} = F - \frac{1}{M} \left[\tilde{p}^2 \frac{d \ln N}{dx} + \frac{d\tilde{p}^2}{dx} + \bar{p} \frac{d\bar{p}}{dx} \right] \quad (59)$$

The third moment

$$\frac{d\tilde{p}^2}{dt} = -\frac{1}{M} \left[2\tilde{p}^2 \frac{d\bar{p}}{dx} + \bar{p} \frac{d\tilde{p}^2}{dx} \right] \quad (60)$$

where N = the particle density

\bar{p} = the average momentum of an electron

\tilde{p}^2 = a modified pressure term since

$$\frac{N(\tilde{p}^2)}{M} = \text{pressure}.$$

If the scale factors and constants are now applied to these equations, they reduce to:

The first moment

$$\frac{dY_1}{ds} = R \left[Y_2 \frac{dY_1}{du} + \frac{dY_2}{du} \right] \quad (61)$$

The second moment

$$\frac{dY_2}{ds} = R \left[Y_3 \frac{dY_1}{du} + \frac{dY_3}{du} + Y_2 \frac{dY_2}{du} \right] - \frac{(E_{int} + E_{ext}) \cosh(s)}{E_0} \quad (62)$$

The third moment

$$\frac{dY_3}{ds} = R \left[2 Y_3 \frac{dY_2}{du} + Y_2 \frac{dY_3}{du} \right] \quad (63)$$

where $Y_1 = \ell_m N$ the scaled density parameter

Y_2 = the scaled momentum parameter

Y_3 = the scaled pressure parameter

R = a series of condensed constants

E_0 = an electric field scale factor

s = time (scaled)

u = distance (scaled) .

The internal electric field is given by

$$\frac{dE_{int}}{ds} = -2 E_0 \cosh(s) Y_2 \exp(Y_1) . \quad (64)$$

Equipped with Eqs (61), (62), (63), and (64), and the differential solving routine described earlier, the value can

be stepped forward in time once given a set of initial conditions.

The Initial Conditions. The initial conditions for the one-dimensional model are as follows:

- 1) The plasma is initially cold. Thus at

$$t = -\infty$$

$$y_2 = 0, \text{ the momentum equals zero}$$

$$y_3 = 0, \text{ the temperature is zero}$$

- 2) y_1 , the initial density distribution is given by a slightly smoothed-out step function. Fig (10) shows the initial distribution of particles normalized to let 1 = the density of the plasma electrons.

This initial distribution was obtained by use of the following exponential

$$f(u) = \exp(-32 u^3 + 12 u^2 - 1.125 u + .015625) \quad (65)$$

- 3) At time $t = -\infty$ the external electric field should be zero, and the position of the beam pulse should be $x = -\infty$.

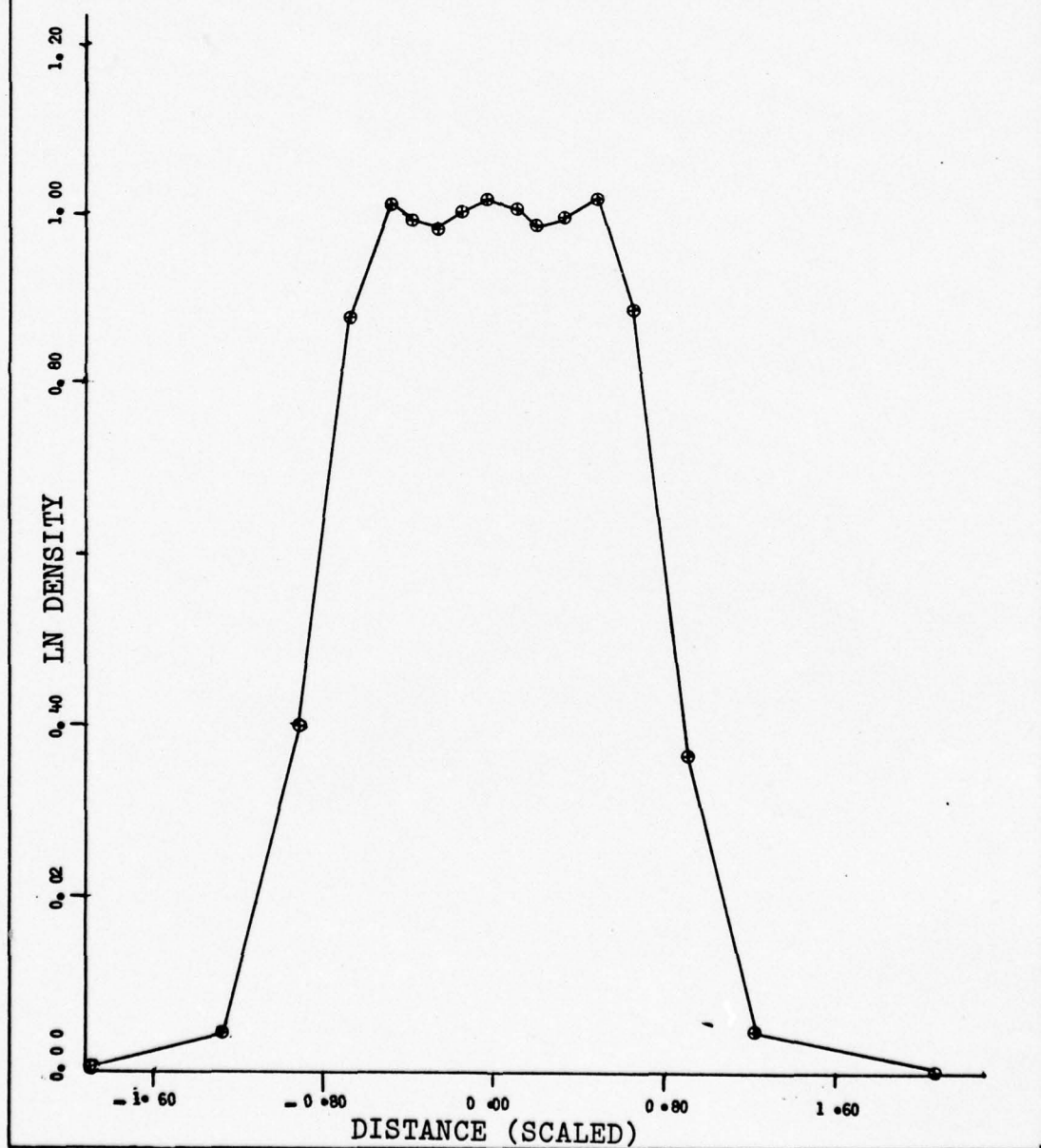
The parameters of the one-dimensional model are now specified. The one-dimensional computer program can be found in Appendix F.

The Two-dimensional Model

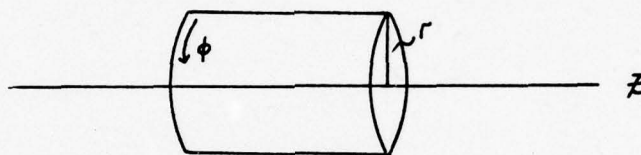
The two-dimensional model has many of the same features as the one-dimensional model, and where similar, the detailed analysis will not be given.

Two-dimensional Space. The one-dimensional model was

Fig. 10
INITIAL DISTRIBUTION
OF ELECTRONS



a rough approximation to the real physical setup of the problem. The two-dimensional model is, however, a more realistic model of the problem. The beam, considered as a point charge, will interact symmetrically in the angular direction of the cylindrical coordinate system. In the axial direction this will not be the case unless the charge pulse is exactly at $z=0$, the center of the target. For this reason, the target is considered a cylinder of finite radius and length, being struck along the axial line of symmetry by the point charge.



The symmetry associated with motion of the plasma in the angular direction leads to the assumption that there are no variations in density and momentum in this deviation; thus, in the analysis, these terms will be set to zero.

As was done in the one-dimensional model, the distance, momentum and time parameters were scaled in order to concentrate the analysis in areas of greatest interest. The same scale factors will be used in the two-dimensional model with the addition of a scale factor in the radial direction,

$$R = R_0 \frac{\omega}{1-\omega} . \quad (66)$$

In a similar manner as was done in the axial direction

of the 1-D problem, w can range from 0 to 1 in scaled values corresponding to 0 and infinity in real space. The interval Δw will also be $1/9$, thus by a proper choice of R_0 the last cell, although ignored, contains all of the space outside of the cylinder in the radial direction. The model space therefore looks like a planar grid with 17 divisions in the axial direction and 9 spaces in the radial direction.

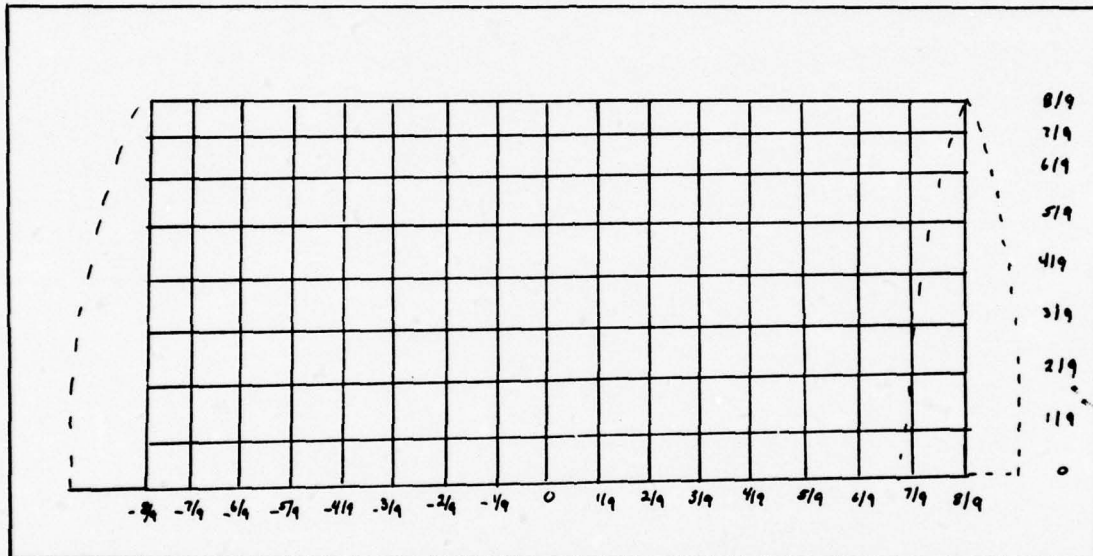


Fig.11 Two dimensional nodal grid

The Moment and Force Equations. The Boltzmann-Vlasov equation in tensor notation is given by

$$\frac{df}{dt} + p^\alpha \frac{df}{dX^\alpha} + f^\alpha \frac{df}{dp^\alpha} = 0 \quad (67)$$

where α equals the summation over 1, 2 and 3 and corresponds to the coordinates r, ϕ, z

f = the particle distribution

p^α = the momentum in the α direction

\mathcal{F}^{α} = the force, for our purpose the Lorentzian force

$\mathcal{F}^{\alpha} = g(E^{\alpha} + (V \times B)^{\alpha})$, in the α direction.

The first three moments of Eq (67) were taken to yield.

(See Appendix E):

The first moment

$$\frac{d}{dt} \rho_0(x) = -\frac{1}{M} [\rho_0(x) \rho_1^{\alpha}],_{\alpha} \quad (68)$$

The second moment

$$\begin{aligned} \frac{d}{dt} \rho_1^{\alpha}(x) \rho_0(x) = & -\frac{1}{M} [\rho_0(x) \rho_2^{\alpha\beta}(x) + \rho_0(x) \rho_1^{\alpha}(x) \rho_1^{\beta}(x)],_{\alpha} \quad (69) \\ & + \mathcal{F}^{\alpha} \int d\rho^{\alpha} S_2^{\alpha} f \end{aligned}$$

The third moment

$$\begin{aligned} \frac{d}{dt} [\rho_0(\rho_2^{\alpha\beta} + \rho_1^{\alpha} \rho_1^{\beta})] = & -\frac{1}{M} [\rho_0(\rho_3^{\alpha\beta\gamma} + \rho_1^{\alpha} \rho_2^{\beta\gamma} + \rho_1^{\beta} \rho_2^{\alpha\gamma} + \rho_2^{\alpha\beta} \rho_1^{\gamma} \\ & + 4 \rho_1^{\alpha} \rho_1^{\beta} \rho_1^{\gamma}),_{\alpha} + \mathcal{F}^{\alpha} [\rho_0 \rho_1^{\alpha}] + \mathcal{F}^{\beta} [\rho_0 \rho_1^{\beta}] \quad (70) \end{aligned}$$

where ρ_0 = Number density of electrons or number of electrons per cubic meter per unit momentum

ρ_1^i = The momentum in the i direction where $i = 1, 3$
or $i = r, z$, respectively

ρ_2^{ij} = The temperature term in the i direction where ij can form any combination 1, 2 or 3 corresponding to r, ϕ, z . ($rz = zr$ etc. in Eulerian theory)

\mathcal{F}^i = the force on the electrons in the i direction.

And the subscript $(, \alpha)$ means derivative over all components

$$X_{, \alpha} = \frac{dX}{dr} + \frac{dX}{d\phi} + \frac{dX}{dz} .$$

$\rho^{ijk} = A$ heat flux term, which will be set to zero in order to close the set of equations; ijk can be any combination of r , ϕ and z .

After adding the scaling factors and making the simplification ($\rho^{\alpha\beta\gamma} = 0$), the three moments reduce to:

The first moment

$$\frac{d\rho}{dt} = -\frac{1}{M} \left[\frac{d\rho}{dr} \rho^r + \frac{d\rho}{dz} \rho^z + \rho \left[\frac{d\rho^r}{dr} + \frac{d\rho^z}{dz} + \frac{1}{r} \rho^r \right] \right] \quad (71)$$

The second moment

$$\begin{aligned} \frac{d\rho^r}{dt} = & \mathcal{F}^r - \frac{1}{M} \left[\rho_z^{rr} \frac{d \ln \rho}{dr} + \rho_z^{zz} \frac{d \ln \rho}{dz} + \frac{d\rho_z^{rr}}{dr} + \frac{d\rho_z^{zz}}{dz} \right. \\ & \left. + \frac{1}{r} \rho_z^{rr} - r \rho_z^{\phi\phi} + \rho_r^r \frac{d\rho^r}{dr} + \rho^z \frac{d\rho^r}{dz} \right] \quad (72) \end{aligned}$$

$$\begin{aligned} \frac{d\rho^z}{dt} = & \mathcal{F}^z - \frac{1}{M} \left[\rho_z^{rz} \frac{d \ln \rho}{dr} + \rho_z^{zz} \frac{d \ln \rho}{dz} + \frac{d\rho_z^{rz}}{dr} \right. \\ & \left. + \frac{d\rho_z^{zz}}{dz} + \rho_r^r \frac{d\rho^z}{dr} + \rho^z \frac{d\rho^z}{dz} \right] \quad (73) \end{aligned}$$

The third moment

$$\begin{aligned} \frac{d\rho_z^{rr}}{dt} = & -\frac{1}{M} \left[\frac{d \ln \rho}{dr} (\rho_r^r)^3 + \frac{d \ln \rho}{dz} (\rho^z (\rho_r^r)^2) + (\rho_r^r)^2 \left[\frac{d\rho_r^r}{dr} \right. \right. \\ & \left. \left. + \frac{d\rho^z}{dz} \right] + 2(\rho_z^{rr} \rho_r^r + \rho_z^{zz} (\rho_r^r)^2 + \rho^z \rho_r^r) \left[\frac{d\rho_r^r}{dr} + \frac{d\rho^z}{dz} \right] \right. \\ & \left. + \rho_r^r \left(\frac{d\rho_z^{rr}}{dr} \right) + \rho^z \left(\frac{d\rho_z^{rr}}{dz} \right) \right] \quad (74) \end{aligned}$$

$$\frac{d\rho_2^{\theta\theta}}{dt} = -\frac{1}{M} \left[\rho_2^{\theta\theta} \left(\frac{1}{r} \rho_1^r \right) + 4 \rho_2^{\theta\theta} \frac{\rho_1^r}{r} + \rho_1^z \frac{d\rho_2^{\theta\theta}}{dz} \right] \quad (75)$$

$$\begin{aligned} \frac{d\rho_2^{zz}}{dt} = & -\frac{1}{M} \left[\frac{d \ln \rho_0}{dr} \rho_0 (\rho_1^r (\rho_2^z)^2) + \frac{d \ln \rho_0}{dz} (\rho_1^z)^3 + (\rho_1^z)^2 \right. \\ & \left. \left(\frac{d\rho_1^r}{dr} + \frac{d\rho_1^z}{dz} + \frac{1}{r} \rho_1^r \right) + 2 \left[\rho_2^{rz} + \rho_2^{zz} + \rho_1^r \rho_1^z + \right. \right. \\ & \left. \left. (\rho_1^z)^2 \right] \left(\frac{d\rho_1^z}{dr} + \frac{d\rho_1^z}{dz} \right) + \rho_1^r \left(\frac{d\rho_2^{zz}}{dr} \right) + \rho_1^z \left(\frac{d\rho_2^{zz}}{dz} \right) \right] \quad (76) \end{aligned}$$

$$\begin{aligned} \frac{d\rho_2^{rz}}{dt} = & -\frac{1}{M} \left[\frac{d \ln \rho_0}{dr} \rho_0 (\rho_1^r)^2 (\rho_1^z) + \frac{d \ln \rho_0}{dz} (\rho_1^z)^2 \rho_1^r \right. \\ & + \rho_1^z \rho_1^r \left(\frac{d\rho_1^r}{dr} + \frac{d\rho_1^z}{dz} + \frac{1}{r} \rho_1^r \right) + (\rho_2^{rz} + \rho_2^{zz} + \rho_1^r \rho_1^z \\ & + (\rho_1^z)^2) \left[\frac{d\rho_1^r}{dr} + \frac{d\rho_1^r}{dz} \right] + (\rho_2^{rr} + \rho_2^{zz} + (\rho_1^r)^2 + \rho_1^z \rho_1^r) \\ & \left. \left[\frac{d\rho_1^z}{dr} + \frac{d\rho_1^z}{dz} \right] + \rho_1^r \left[\frac{d\rho_2^{rz}}{dr} \right] + \rho_1^z \left[\frac{d\rho_2^{rz}}{dz} \right] \right] \quad (77) \end{aligned}$$

where the off-diagonal components of the pressure in the ϕ direction have been set to zero because of symmetry. The momentum component in the ϕ direction is by the same argument zero.

The only term yet unspecified is the force term. The Lorentzian force, as in the one-dimensional model, is composed of the forces due to both external and internal fields. The external fields have been limited to only the electric field from the beam. In the two-dimensional case, however, there is both an axial and a radial component to the field. Appendix C derives the equations used to evaluate these components. The axial component is given by the same equation as in the one-dimensional model.

$$E(x) = \frac{\frac{Q}{4\pi\epsilon_0} \left(\frac{2\beta}{1-\beta^2} \right) - \frac{Vt}{\sqrt{R^2(1-\beta^2) + (Vt-x)^2}}}{\left[\left(\frac{2\beta}{1-\beta^2} \right) (Vt-x) - \sqrt{R^2(1-\beta^2) + (Vt-x)^2} \right]} \quad (78)$$

where Q = the total charge in the point beam

β = the relativistic constant

V = the velocity of the beam

t = the time

R = the radial position of the point of interest

x = the axial position of the point of interest

except that the value of R will not be a constant but will vary with the position of the point of interest.

The radial component of the electric field is given by

$$E(R) = \frac{Q}{4\pi\epsilon_0} \frac{R(1-\beta^2)}{\left[\left(\frac{2\beta}{1-\beta^2} \right) (vt-X) - \sqrt{R^2(1-\beta^2) + (vt-X)^2} \right]^2 \sqrt{R^2(1-\beta^2) + (vt-X)^2}} \quad (79)$$

The internal fields consist of both electric and magnetic components and are described by Maxwell's equations

$$\frac{d\vec{B}}{dt} = -\vec{\nabla} \times \vec{E}$$

and

$$\frac{d\vec{E}}{dt} = \frac{1}{\mu_0\epsilon_0} \vec{\nabla} \times \vec{B} - \frac{\vec{J}}{\epsilon_0}$$

In Appendix E, these two equations are expanded in cylindrical coordinates and scaled to the parameters used in the model. The time derivatives of these two fields then become:

$$\frac{dE^r}{dt} = \frac{e}{\epsilon_0 M} (\rho^0 \rho^r) - c^2 \frac{dB^\phi}{dz} \quad (80)$$

$$\frac{dE^z}{dt} = \frac{e}{\epsilon_0 M} (\rho^z \rho^0) + c^2 \left(\frac{dB^\phi}{dr} + \frac{B^\phi}{r} \right) \quad (81)$$

$$\frac{dB^\phi}{dt} = - \left(\frac{dE}{dz} - \frac{dE}{dr} \right) \quad (82)$$

The force in the radial direction is then given by

$$f_r = -e [E^r - \rho_m^z B^\phi] \quad (83)$$

and in the z direction by

$$f^z = -e [E^z + \rho_m^r B^\phi] \quad (84)$$

Equipped with Eqs (71), (72), (73), (74), (75), (76), (77), (80), (81), and (82) and the solving routine described in an earlier section, the values of the density, momentum and temperature can be stepped in time from a set of initial conditions.

Initial Conditions. The initial conditions for the two-dimensional model are as follows:

1. The plasma is initially cold. Thus, at

$$\rho_i^i = 0 \text{ for } i = r, z$$

$$\rho_z^{ij} = 0 \text{ for } ij = rr, rz, \phi\phi, zz$$

2. All other parameters remain the same as the one-dimensional model.

V. Results and Conclusions

In this section, the sample runs which would establish credibility to the model and methods used will be discussed first, followed by an analysis of data received from both the one- and two-dimensional models. A short conclusion section and a few words about "what should be done next" will follow.

Validity Runs

The most basic configuration-space property of a plasma is a simple oscillation. The plasma system, as described by the first three moments, resembles a simple harmonic oscillator. When the particles are initially given a small amount of momentum in one direction, the internal electric restoring force, which develops because of this displacement, will accelerate the particle in the opposite direction of the displacement. As the particle returns to the neutral position, it possesses some kinetic energy and continues, thus the process can be represented as the perfect spring model for simple harmonic motion. Appendix G is a short derivation of the frequency of this harmonic motion and shows the frequency to be

$$\omega_p^2 = \frac{Ne^2}{Me\epsilon_0}$$

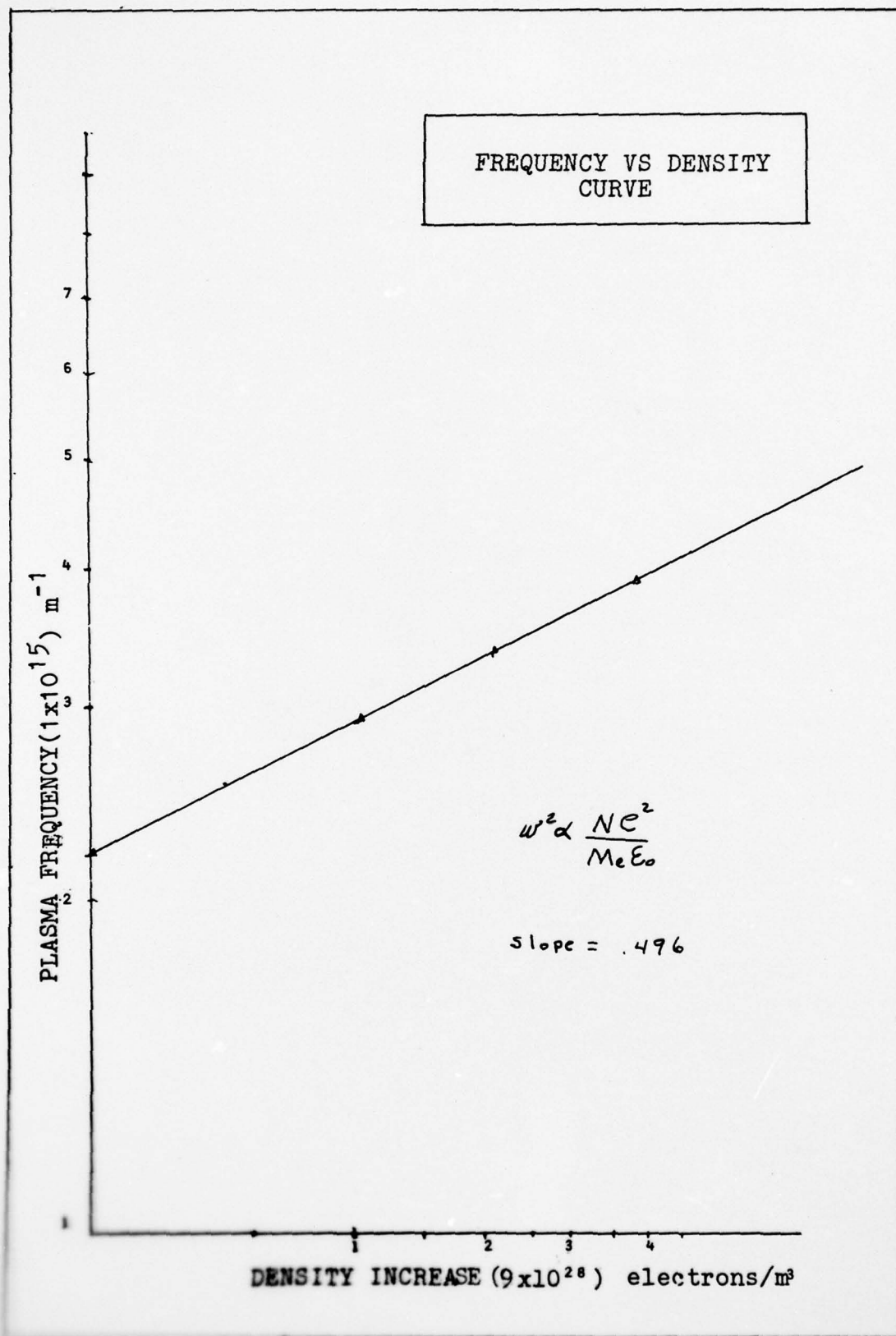
where ω_p = the plasma frequency
 N = the number of electrons per cubic meter
 m_e = the mass of the electron
 ϵ_0 = the permittivity of free-space

If our model could demonstrate these oscillations at the proper frequency, then some credibility must be given to the equations and techniques used. Table IV summarizes the results of the introduction of a small amount of momentum into both models.

Table IV Summary of plasma oscillations.

Model	ω_p (sec ⁻¹)
Calculated (Infinite)	$2.4 \times 10^{+16}$
1-D	$3.12 \times 10^{+15}$
2-D axial	$3.8 \times 10^{+15}$
2-D radial	$3.8 \times 10^{+15}$

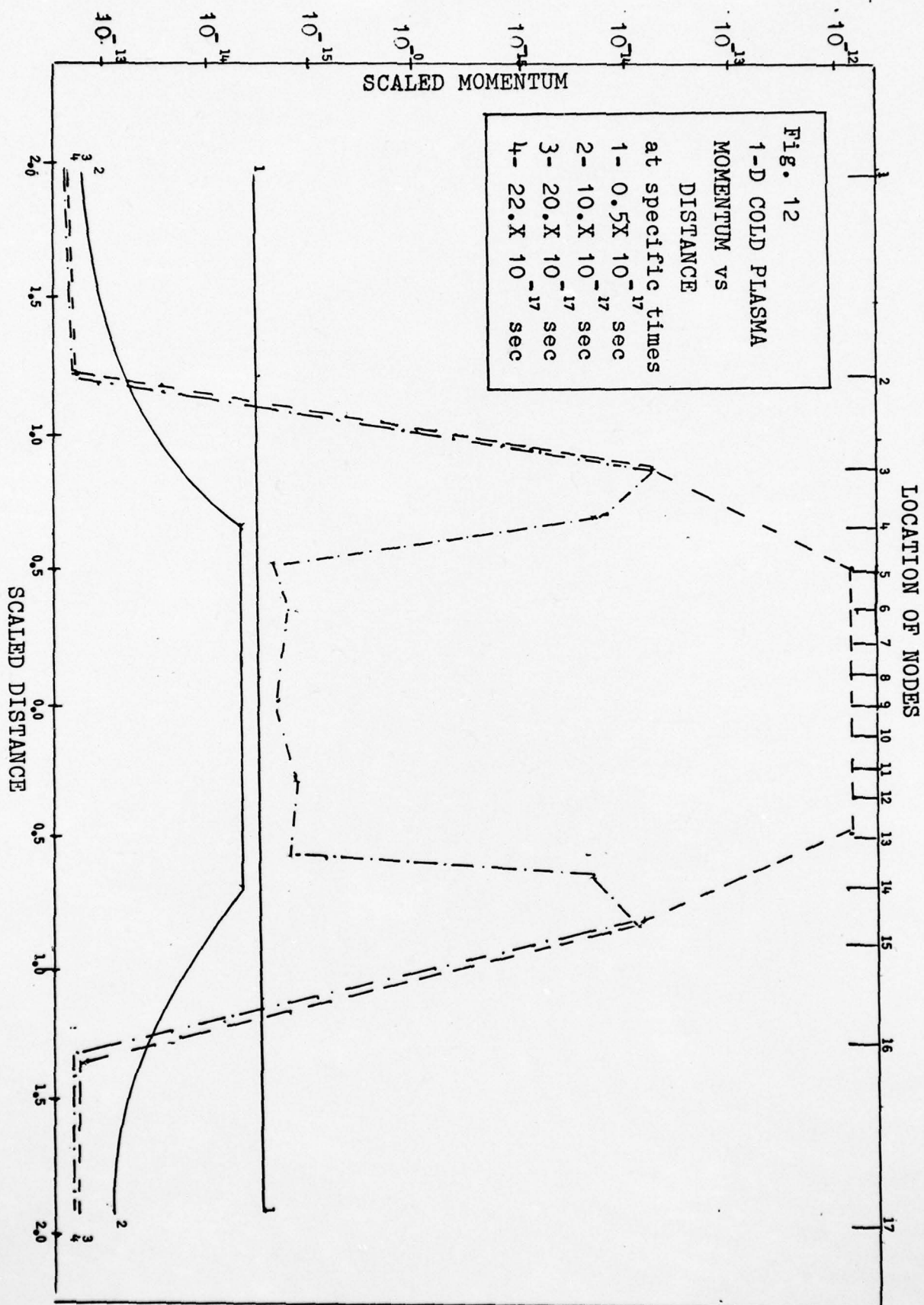
Although the calculated frequencies listed are not as close to the calculated values as one might like, it should be noted that the calculated value is for an infinite model and our model is finite. This fact should decrease the value of ω_p as will be shown in Appendix G and thus make our calculated values much closer. Additional runs were made to verify the analysis by varying both the density of the plasma and the amplitude of the initial momentum induced. We would expect the frequency of the plasma to vary as the square root of the particle density. From the following figure in which N was varied, this variance is established.



One- and Two-Dimensional Runs with the Beam

An initial time was calculated in order to place the position of the beam just in front of the left edge of the material, and the program was started. There should be a small initial displacement of the electrons toward the beam, and then as the beam passed, a rapid acceleration in the beam direction. These directional displacements would be detected first by an increase in the momentum in the negative direction (beam sucking electrons toward itself) and then small changes in the density distribution. The internal electric field should increase in the restoring direction as the momentum starts to change. These three factors should allow us to analyze the movement and forces which act upon the electrons. The magnitude of the electric field at the various positions should also correspond to the change in momentum as a function of position. Since the beam is initially at the left ($-\infty$), the external electric field should be directed to the right or positive. The motion of the electrons should be initially toward the beam (-) as should the momentum. The internal electric field caused by this change in momentum should be a restoring field to the left (-).

All of these projections are seen in the initial few time steps of the calculations; however, after a short period, depending upon the interval of the step, the momentum starts to oscillate as described in Fig. 12. The



momentum is initially a function of the distance away from the beam, but an unstable oscillation soon develops over time periods in which the external electric field does not appreciably change. It would appear that if a small amount of momentum is continually supplied to the system of electrons, an unstable oscillation would develop. This phenomenon could not be explained, and a method for damping the oscillation was sought.

It was felt that the energy induced by the external field was not being transferred properly into heat or pressure without a small collisional term; therefore, the pressure term (\tilde{p}^2) was analyzed. It was felt that if the stress tensor was added to this noncollisional form of the pressure

$$\text{Pressure} = p - \sigma'$$

where $p = \frac{N\tilde{p}^2}{M}$ as described in earlier sections

$\sigma' =$ the stress tensor

stability might be achieved.

This stress tensor involves a viscosity constant times the derivative of the momentum with respect to position

$$\sigma' = \nu \frac{d\bar{p}}{dx}.$$

Thus, the second moment becomes (1-D)

$$\frac{d}{dt} [\bar{p}N] = - \frac{1}{M} \frac{d}{dx} [N\tilde{p}^2 + N\bar{p}^2 + M\sigma'] + FN$$

and the third moment becomes

$$\frac{d}{dt} [\tilde{P}^* N + \bar{P}^* N] = - \frac{1}{M} \frac{d}{dx} [N \bar{P}^* + N \tilde{P}^* \bar{P} + N \tilde{P}^3 + 2N \bar{P} \tilde{P}^2 + 2M \delta'].$$

It was hoped that a value for the viscosity term could be picked which would stabilize these oscillations and allow the hopefully larger effects to be seen as the beam came closer to the target.

Various ranges of ν were tried without success. The divergence of the oscillation could be slowed but never stopped.

Another possible problem was encountered with the solving routine. The ability of the routine to establish the proper 8-point fit to the distribution and momentum curves was occasionally in doubt. For example, in one run to establish plasma oscillations, the program diverged in a manner similar to previous difficulties with the stability in the momentum. A second run was made over the same time region at a finer time step, and the program was stable as predicted. Thus, one would say it could be possible to stabilize the momentum in a run with the beam present by shortening the initial time step, even though the solving routine chose its own working time step. For several runs, the time step was reduced to 10^{-8} of a scaled unit. The program would run, but this narrow time step would not be feasible for any computer routine.

At this point, it was apparent that this simple moment approach to the analysis of the beam-target inter-

action needed to be expanded to include either collisional terms or higher moments which would bring in stability terms to help dampen the divergence. Artificial viscosity has been used by several hydro-code programs and may also be a candidate for this problem; however, a shortage of time has prevented further analysis.

Things to be Done

The attempt to describe a complex mechanism by a simple analytic tool did not work; thus, the following two approaches could be followed: One, patch up the existing program to include terms which will eliminate the instability; or two, start from the beginning with a more detailed analysis, including higher order moments or even solutions to the Vlasov equations for several particles. It is felt that a patch of this method would not be advisable at this point. The linear approach as was done in the collective example should be expanded to its maximum and also possibly include a quasi-linear approach in which the second order perturbations are kept and the higher orders discarded. This approach should provide insight into not only the moments but to the physics of the plasma. The plasma frequency, dispersion relations and damping terms should be evaluated as to their importance before starting a program design.

The other approach would be to examine solutions of the Boltzmann-Vlasov equations for particles. This approach

would probably not be appropriate to a master's thesis because of the time and details involved in its solution. However, it might be the only way to accurately model the problem.

Bibliography

1. Holloway, M.G. and M.S. Livingston. "Range and Specific Ionization of α Particles." Physical Review, 54: 18, (1938).
2. Kaplan, I. Nuclear Physics. Reading, Massachusetts: Addison-Wesley, 1964.
3. Jackson, J. Classical Electrodynamics. New York: Wiley, 1967.
4. Sternheimer, R.M. "Range Energy Relations for Protons." Physical Review, 115: 138, (1959).
5. Sternheimer, R. M. "Range Energy Relations for Protons." Physical Review, 88: 851 (1952).
6. Sternheimer, R.M. "Range Energy Relations for Protons." Physical Review, 103: 511 (1956).
7. ORNL, Monte Carlo High Energy Nucleon-meson Transport Code CCC-178 Jan (1972)
8. Barashenkov, V.S. "Interaction Cross Sections of Elementary Particles." Israel Program for Scientific Translation, Jerusalem, 1968.
9. Barashenkov, V.S., et al. "Change of Mechanism of Inelastic Interactions Between Particles and Nuclei in Energy Regions $T \sim 5$ GeV." Soviet Journal of Nuclear Physics, 10 #4: 435, (1970).
10. FTD. Interaction of High Energy Particles and Anti-particles with Nuclei. Report No. FTD HC-23-2670-2674. Wright-Patterson Air Force Base, Ohio, 1974.
11. Segre, E. Nuclei and Particles (Second Printing) New York: Benjamin Inc., 1965.
12. Evans, R.D. The Atomic Nucleus (Eleventh Printing) New York: McGraw-Hill, 1967.
13. Seshadri, S.R. Fundamentals of Plasma Physics. New York: American Elsevier Publishing Co., 1973.
14. Gartenhaus, S. Elements of Plasma Physics. New York: Holt, Rinehart, Wilson, 1964.

15. Krall, N.A. and A.W. Trivelpiece. Principles of Plasma Physics. New York: McGraw-Hill, 1973.
16. Harlow, F. and A. Amesden. Fluid Dynamics. Los Alamos, California: United States Atomic Energy Commission, 1971.
17. Hawkins, G. A. Multilinear Analysis for Students in Engineering and Science. New York: Wiley, 1963.
18. Sokolnikoff, I.S. Tensor Analysis. New York: Wiley, 1951.
19. Milne, W. Numerical Calculus. Princeton, New Jersey: Princeton University Press, 1949.
20. Bethe, H.A. and J. Ashkin in E. Segre' (ed.) "Experimental Nuclear Physics", Vol. 1, New York, John Wiley.
21. Steenberg, N.R. "Nuclear Cross Sections At High Energies," Nuclear Physics, 35 (1962) 455-471
22. S. Hayakawa Cosmic Ray Physics, Vol XXII, Pg. 169 New York, Wiley, 1969

Appendix A

Derivation of the Boltzmann-Vlasov Equation From Liouville's Equation

The equation of motion of a charged particle which is acted upon by an electromagnetic field is given by Newton's equation of motion (Ref 15)

$$M_p \frac{d\bar{V}}{dt} = \gamma \left(1 - \frac{v^2}{c^2}\right)^{1/2} \left(\bar{E} + (\bar{V} \times \bar{B}) - \frac{V}{c^2} \bar{V} \cdot \bar{E} \right).$$

Eq (1) is a means of calculating the unique trajectory of the particles in terms of their initial or present position and velocity. Liouville's equation

$$\frac{df}{dt} + \bar{H}_p \cdot \frac{df}{d\bar{r}} - \bar{H}_r \cdot \frac{df}{d\bar{p}} = 0,$$

where $\bar{H}_p = \frac{dH}{d\bar{p}}$, $\bar{H}_r = \frac{dH}{d\bar{r}}$,

is a similar formulation for the dynamics of a single particle in terms of the Hamiltonian operator, H. The advantage of Hamiltonian mechanics over the statistical nature of Newtonian mechanics is that it can more readily be adapted to a many-particle system. Except for very trivial systems (few particles), Newton's laws of motion cannot be explicitly solved, and thus in order to proceed further, it becomes necessary to make some mathematical approximations that will produce a more manageable equation out of Liouville's equation.

If the range of forces within a plasma is fairly long, an appreciable force will develop on a single particle if all of the other particles in the plasma.

move in some collective way. These so-called collective forces can be expected to be much more smoothly behaved functions of both space and time than the forces produced by rare mutliparticle collisions. When this theory is carried to extremes, the argument leads us to suspect that in the lower-order we could replace all of the inter-particle forces by certain macroscopically-smoothed electromagnetic fields. According to this point of view, every particle moves completely independently of all other particles but follows its predictable trajectory in these smoother fields. Physically, it is evident that the choice of the fields must consist of those fields that are produced by all of the particles in the plasma, and these fields are referred to as self-consistent. These fields are obtained by solving Maxwell's equations. In this section, we will develop the collisionless Boltzmann equation (Boltzmann-Vlasov) from the many particle Liouville equation with the aid of this independent trajectory assumption and the fields developed from Maxwell's equations.

For reasons of simplicity, let us consider a gas of identical particles and assume that each particle follows an independent trajectory, or equivalently, the N particle distribution function, $F^{(N)}(t)$, may be expressed in the form

$$F^{(N)}(t) = \prod_{i=1}^N f(r_i, p_i, t)$$

where f is the single-particle distribution function.
 Liouville's equation for the dynamics of a many-particle
 system is

$$\frac{d F^N(t)}{dt} + \sum_{j=1}^N H_{r_j} \cdot \frac{d F^N(t)}{d r_j} - \sum_{j=1}^N H_{p_j} \cdot \frac{d F^N(t)}{d p_j} = 0 \quad (A-1)$$

where H = the Hamiltonian operator and the J refers to the
 J th particle

$$H_{r_j} = \frac{d H}{d r_j}, \quad H_{p_j} = \frac{d H}{d p_j}.$$

For most physical situations of interest, one expects
 only a very small number of inter-particle correlations to
 play an important role. Thus, it is convenient and pract-
 ically mandatory that $F^N(t)$ be reduced to distribution
 functions involving only small numbers of particles by
 averaging out the coordinates and momenta of the remaining
 large collection of particles.

Since we have restricted $F^N(t)$ to only one species,
 $F^N(t)$ will be symmetrical with respect to exchange of the
 coordinates and momenta of any two particles. The s -part-
 icle distribution function $F^s(t)$ ($s \ll N$) is obtained by
 averaging over the coordinates and momenta of the remaining
 $N-s$ particles, thus

$$F^s(t) = \int F^N(t) \prod_{j=s+1}^N (d r_j d p_j) \quad (A-2)$$

where $F^s(t) \prod_{i=1}^s (d r_i d p_i)$ is the joint

probability at time (t) of finding a particular collection of s particles located at $r_1, r_2, r_3 \dots r_s$ in the range $dr_1, dr_2 \dots dr_s$ respectively, and with momentum $p_1, p_2 \dots p_s$ in the respective ranges $dp_1, dp_2 \dots dp_s$ regardless of the states of motion of the remaining n-s particles.

The Hamiltonian operator is given by the equation (Ref 15)

$$H = \frac{1}{2M} \sum_{i=1}^N (\vec{P}_i - \frac{e}{c} \vec{A}(\vec{r}_i, t))^2 + e \sum_{i=1}^N \phi(\vec{r}_i, t) + \frac{e^2}{2} \sum_{\substack{i,j=1 \\ i \neq j}}^N \frac{1}{r_{ij}} - \frac{e}{4Mc^2} \sum_{\substack{i,j=1 \\ i \neq j}}^N \left(\frac{\vec{P}_i \cdot \vec{P}_j}{r_{ij}} + \frac{\vec{P}_i \cdot \vec{r}_{ij} \vec{P}_j \cdot \vec{r}_{ij}}{r_{ij}^3} \right) \quad (A-3)$$

where A and ϕ are the potentials associated with the external E and B fields.

It will become more convenient to write the Hamiltonian in terms of two components. The first component h^1 depends only upon the coordinates and momenta of the single-particle distribution, $F^{(1)}$, and the second component, h^2 , depends upon the two-particle distribution, $F^{(2)}$. Extracting these components from Eq (3) yields

$$h^1 = \frac{1}{2M} \left\{ \vec{P}_i - \frac{e}{c} \vec{A}(\vec{r}_i, t) \right\}^2 + e \phi(\vec{r}_i, t) \quad (A-4)$$

$$h^{(1,2)} = \frac{e^2}{r_{ij}} - \frac{e^2}{2Mc^2} \left(\frac{\vec{P}_i \cdot \vec{P}_j}{r_{ij}} + \frac{\vec{P}_i \cdot \vec{r}_{ij} \vec{P}_j \cdot \vec{r}_{ij}}{r_{ij}^3} \right) \quad (A-5)$$

From Eqs (4) and (5), we can write

$$H = \sum_{i=1}^N h'_i(p_i, r_i) + \frac{1}{2} \sum_{i \neq j}^N h^2_{ij}(p_i, p_j, r_i, r_j)$$

then

$$H_{p_j} = \frac{dH}{dp_j} = \frac{dh'_j}{dp_j} + \frac{1}{2} \sum_{j \neq k}^N \frac{dh^2_{jk}}{dp_j} + \sum_{j \neq k}^N \frac{dh^2_{kj}}{dp_j}$$

but, since the particles are indistinguishable

$$\frac{dH}{dp_j} = \frac{dh'_j}{dp_j} + \sum_{j \neq k}^N \frac{dh^2_{jk}}{dp_j}. \quad (A-6)$$

Also, note from our definition of $F^N(t)$ and the chain rule that

$$\frac{dF^N(t)}{dr_j} = \frac{df_j}{dr_j} \prod_{i \neq j}^N f_i. \quad (A-7)$$

Combining Eqs (6) and (7) yields

$$\frac{dH}{dp_j} \frac{dF^N(t)}{dr_j} = \left(\frac{dh'_j}{dp_j} + \sum_{k \neq j}^N \frac{dh^2_{jk}}{dp_j} \right) \left(\frac{df_j}{dr_j} \prod_{i \neq j}^N f_i \right). \quad (A-8)$$

By similar techniques, it can be shown that

$$\frac{dH}{dr_j} \frac{dF^N(t)}{dp_j} = \left(\frac{dh'_j}{dr_j} + \sum_{k \neq j}^N \frac{dh^2_{jk}}{dr_j} \right) \left(\frac{df_j}{dp_j} \prod_{i \neq j}^N f_i \right). \quad (A-9)$$

Substituting Eqs (8), (9) and

$$\frac{dF^N(t)}{dt} = \sum_{i=1}^N \frac{df_i}{dt} \prod_{\substack{j=1 \\ j \neq i}}^N f_j$$

AD-A034 948 AIR FORCE INST OF TECH WRIGHT-PATTERSON AFB OHIO SCH--ETC F/G 20/8
INTERACTION OF RELATIVISTIC PROTONS WITH MATTER.(U)
DEC 76 G P BENDER

AIR FORCE INST OF TECH WRIGHT-PATTERSON AFB OHIO SCH--ETC F/G 20/8
INTERACTION OF RELATIVISTIC PROTONS WITH MATTER.(U)
DEC 76 G P BENDER

GNE/PH/76D-1

NL

2 of 2
ADA034948

END

DATE
FILMED
3 - 77

into Liouville's equation results in

$$0 = \sum_{j=1}^N \left[\frac{df_j}{dt} \prod_{i \neq j}^N f_i + \left(\frac{dh'_j}{dr_j} + \sum_{k \neq j}^N \frac{dh_{j,k}^2}{dr_j} \right) \frac{df_j}{dr_j} \prod_{i \neq j}^N f_i - \left(\frac{dh'_j}{dr_j} + \sum_{k \neq j}^N \frac{dh_{j,k}^2}{dr_j} \right) \frac{df_j}{dr_j} \prod_{i \neq j}^N f_j \right]. \quad (A-10)$$

Let us now look at each term of Eq (10) and integrate out the one body term f^1 . Later we will examine the two body terms.

Integrating the first term of Eq (10)

$$\int dr_2 \rightarrow dr_N, \quad dp_2 \rightarrow dp_N \left(\sum_{j=2}^N \frac{df_j}{dt} \prod_{i \neq j}^N f_i + \frac{df_1}{dt} \prod_{i \neq 1}^N f_i \right). \quad (A-11)$$

The integral reduces if we bring out the summation. For each term then we have

$$\left(\sum_{j=2}^N \int dp_j dr_j \frac{df_j}{dt} \right) f_i \quad \text{or} \quad f_i \sum_{j=2}^N \frac{df_j}{dt} \int dp_j dr_j f_j$$

but $\int dp_j dr_j f = 1$ for each term of the sum and

$$\frac{d}{dt} (1) = 0.$$

Thus, the only remaining term from Eq (11) is

$$\int dp dr \frac{df'_1}{dt} \prod_{i \neq 1}^N f_i = \frac{df_1}{dt} \quad (A-12)$$

since each of the product terms equals 1, the total product = 1.

The second term of Eq (10)

$$\sum_{j=1}^N \frac{dh'_j}{dr_j} \frac{df_j}{dr_j} \prod_{i \neq j}^N f_i$$

after integrating out the $J \neq 1$ terms yields

$$\int \frac{dh'}{dr_1} \frac{df_1}{dp_1} \prod_{i \neq 1}^N f_i \, dr_i \, dp_i = \frac{dh'}{dr_1} \frac{df_1}{dp_1} \quad (A-13)$$

plus

$$\sum_{j=2}^N \int dr_j \, dp_j \prod_{k \neq j}^N \frac{dh'_j}{dr_j} \frac{df_j}{dp_j} \left(\prod_{i \neq j}^N f_i \right) f_i$$

$$\sum_{j=2}^N \int dr \, dp \frac{dh'_j}{dr_j} \frac{df_j}{dp_j} f_i.$$

Since the integral over each $f_i = 1$ the summation is written

$$(N-1) \int dr \, dp \frac{dh'_j}{dr_j} \frac{df_j}{dp_j} \quad \text{or} \quad (N-1) \int \frac{df_j}{dp_j} h'_j \, dp_j.$$

Integrating by parts leaves

$$- (N-1) f_1 \int dr_2 \, dp_2 f_2 \frac{d^2 h_2}{dp_2 dr_2} \quad (A-14)$$

where $j = 2$ is an arbitrary substitution for any one of a set of $(N-1)$ values.

Doing the same for the third term of Eq (10)

$$\sum_{j=1}^N \left(\frac{dh'_j}{dr_j} \frac{df_j}{dp_j} \right) \prod_{i \neq j}^N f_i$$

yields

$$\frac{dh'}{dr_1} \frac{df_1}{dp_1} + (N-1) f_1 \int dr_2 \, dp_2 f_2 \frac{d^2 h_2}{dp_2 dr_2}. \quad (A-15)$$

Combining Eqs (13), (14) and (15) yields

$$\frac{df_i}{dt} = \frac{dh_i}{dr_i} \frac{df_i}{dP_i} - \frac{dh_i}{dP_i} \frac{df_i}{dr_i} + \text{The Two Body terms.} \quad (A-16)$$

Returning to Eq (10) and looking at the two body terms

$$\sum_{j=1}^N \sum_{k \neq j}^N \left(\frac{dh_{j,k}^2}{dr_j} \frac{df_j}{dP_j} \right) \prod_{i \neq j}^N f_i - \sum_{j=1}^N \sum_{k \neq j}^N \left(\frac{dh_{j,k}^2}{dP_j} \frac{df_j}{dr_j} \right) \prod_{i \neq j}^N f_i$$

rewriting the $\prod_{i \neq j}^N f_i$ as $f_k * \prod_{i \neq j \neq k}^N f_i$

and factoring out the $J = 1$ term

$$\sum_{j=2}^N \left(\sum_{k \neq j}^N \left[\frac{dh_{j,k}^2}{dr_j}, \frac{df_j}{dP_j} \right] \left[\prod_{i \neq j \neq k}^N f_i \right] + \sum_{k \neq j}^N \left[\frac{dh_{j,k}^2}{dP_j}, \frac{df_j}{dr_j} \right] \left[\prod_{i \neq j \neq k}^N f_i \right] * f_k \right) \quad (A-17)$$

where $\left[\frac{dh_{j,k}^2}{dr_j} \frac{df_j}{dP_j} - \frac{dh_{j,k}^2}{dP_j} \frac{df_j}{dr_j} \right]$ combine to form a Poisson bracket.

Integrating Eq (17) over all space and momenta except 1,

$$\sum_{j=2}^N \sum_{k \neq j}^N \int dP_j dr_j dP_k dr_k \left\{ \frac{dh_{j,k}^2}{dr_j}, \frac{df_j}{dP_j} \right\} * f_k +$$

$$\sum_{k=2}^N \int dP_k dr_k \left\{ \frac{dh_{1,k}^2}{dr_1}, \frac{df_1}{dP_1} \right\} f_k$$

all of the other terms, $\int dr_i dP_i f_i = 1 \quad i \neq k \neq j$.

Looking at the first term of Eq (18)

$$\sum_{j=2}^N \sum_{k \neq j}^N \int dP_j dr_j dP_k dr_k \left\{ \frac{dh_{j,k}^2}{dr_j} \frac{df_j}{dP_j} - \frac{dh_{j,k}^2}{dP_j} \frac{df_j}{dr_j} \right\} f_k.$$

Integration by parts with respect to dp in the first term and dr in the second yields, i.e. the first term

$$\int \left[\frac{d^2 h_{JK}}{dr^2} \frac{df}{dp} dp \right] f_K \quad \text{let } du = \frac{df}{dp} dp$$

$$v = \frac{d^2 h_{JK}}{dr^2} \quad (A-18)$$

then the integral equals

$$\left[\frac{d h_{JK}}{dr} f \right]_{-\infty}^{\infty} - \frac{d^2 h_{JK}}{dp dr} f_K;$$

the second term yields

$$+ \frac{d^2 h_{JK}}{dp dr}$$

so the first term of Eq (18) disappears and Eq (12) reduces to

$$\sum_{K=2}^N \int dp_K dr_K \left\{ \frac{d h_{1K}}{dr_1} , \frac{df_1}{dp_1} \right\} f_K. \quad (A-19)$$

Since h^2 is a function of (p^1, p^2, r^1, r^2) all terms of the sum will be the same. Therefore, Eq (19) reduces to

$$(N-1) \int dp_2' dr_2' \left[\frac{d h_{12}}{dr_1} \frac{df_1}{dp_1} - \frac{d h_{12}}{dp_1} \frac{df_1}{dr_1} \right] f_2$$

where $K = 2$ is a dummy selection or rewriting

$$\frac{d}{dr_1} \left[(N-1) \int dp_2 dr_2 h_{12} f_2 \right] \frac{df_1}{dp_1} - \frac{d}{dp_1} \left[(N-1) \int dp_2 dr_2 h_{12} f_2 \right] \frac{df_1}{dr_1}$$

where $(N-1) \int dp_2 dr_2 h_{12} f_2$ is the potential due to all other $(n-1)$ charges on particle 1. Therefore,

$$V^2(r, p) = (N-1) \int dr_2 dp_2 h_{12}^2 f_2. \quad (A-20)$$

Combining all the terms, Liouville's equation becomes

$$\frac{df_1}{dt} = \frac{dh'}{dr_1} \frac{df_1}{dp_1} - \frac{dh'}{dp_1} \frac{df_1}{dr_1} + \frac{dV^2}{dr_1} \frac{df_1}{dp_1} - \frac{dV^2}{dp_1} \frac{df_1}{dr_1}.$$

If we let

$$h^{\text{eff}} = h' + V^2$$

then

$$\begin{aligned} h^{\text{eff}} &= h'(r, p) + \int dr' dp' f(r, p) * h^2(r r' / p p') \\ &= h^1(r, p) + V(r). \end{aligned}$$

Excluding magnetic effects,

$$h^{\text{eff}}(r, p) = \frac{p^2}{2M} + \phi(r)$$

where ϕ is an external potential so that

$$\frac{dh^{\text{eff}}}{dp} = \frac{p}{M}$$

$$\frac{dh^{\text{eff}}}{dr} = \frac{d\phi}{dr} + \frac{dV}{dr}$$

and

$$\frac{df}{dt} = \{h^{\text{eff}}, f\} = \left\{ \frac{dh^{\text{eff}}}{dr} \frac{df}{dp} - \frac{dh^{\text{eff}}}{dp} \frac{df}{dr} \right\}$$

but

$$\frac{dh^{eff}}{dr} = \frac{d\phi}{dr} + \frac{dV}{dr}$$

then

$$\frac{df}{dt} = \left(\frac{d\phi}{dr} + \frac{dV}{dr} \right) \frac{df}{dp} - \frac{p}{m} \frac{df}{dr}$$

but

$$-\frac{p}{m} \frac{df}{dr} = -\bar{v} \cdot \bar{\nabla} f$$

and

$$\left\{ \frac{d\phi}{dr} + \frac{dV}{dr} \right\} \frac{df}{dp} = (-\text{Force}(\text{Ext}) - \text{Force}(\text{Int})) \frac{df}{dt}$$

therefore,

$$\frac{df}{dt} + \bar{v} \cdot \bar{\nabla} f + \text{Force} \cdot \bar{\nabla}_p f = 0.$$

The internal force

$$F_{\text{Int}} = -\nabla \int dr' dp' f(r', p') * \frac{e^2}{4\pi\epsilon_0 |r-r'|}$$

letting

$$\rho = \int dp f(r, p)$$

$$F_{\text{Int}} = -\nabla \int \frac{dr' \rho(r') e^2}{4\pi\epsilon_0 |r-r'|} = eE.$$

Therefore, Liouville's equation becomes

$$\frac{df}{dt} + \bar{v} \cdot \bar{\nabla} f + eE \cdot \bar{\nabla}_p f = 0.$$

If magnetic effects are included, h^{eff} becomes

$$h^{eff} = \frac{1}{2m} (p - \frac{e}{c} A)^2 + \phi$$

where A is the magnetic potential and $B = (\nabla \times A)$.

Through a similar process of taking the derivation of h^{eff} with respect to ρ and r and substituting into Eq (21) Liouville's equation becomes

$$\frac{df}{dt} + \bar{V} \cdot \nabla f + e [\bar{E} + (\bar{V} \times \bar{B})] \cdot \frac{df}{dP} = 0$$

the Boltzmann-Vlasov equation, where the symbol ∇ takes on the form $\nabla = \frac{1}{M} (P - eA)$ instead of $\nabla = \frac{P}{M}$.

Appendix B

The External Electric Field

The external electric field, due to the presence of a 1K amp beam of 10 GeV protons chopped into pulses of 10^{-9} seconds, has been modeled as a point charge of 10^{-6} coulombs moving at a velocity of 2.98×10^8 m/s. The assumed radius of interaction has been selected as .001 m or in other words, the radius of the beam is assumed to be on the order of .001 m, but since we are modeling it as a point charge, the area of greatest concern will be the cylindrical area .001 m from the axis of motion of the point charge. In this section, we will develop the equations for the axial and radial components of the relativistic point charge. These equations will be used in the calculation of the Lorentzian force felt by the electrons in the plasma.

The electric potential, ϕ , due to a point charge at a distance $|r-R|$, is given by

$$\phi(R,t) = \frac{1}{4\pi\epsilon_0} \int \frac{dr \rho(r, t - \frac{|r-R|}{c})}{|r-R|} \quad (B-1)$$

where ρ is a retarded charge density of a point charge given by

$$\rho(r,t) = Q \delta(z-vt) \delta(r)$$

where the point charge is represented by the delta function in radial and axial dimensions, V = the velocity of the beam and t = time.

c = the speed of light

$|\vec{r}-\vec{R}|$ = the distance from the point of interest to the beam as shown in Fig. 19.

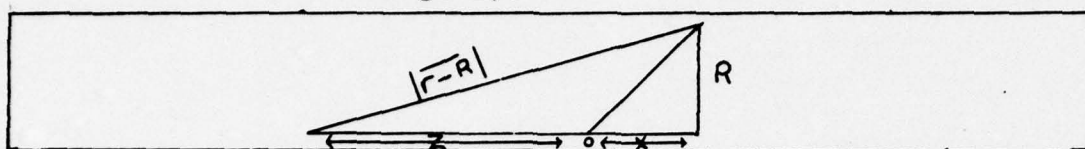


Fig.19 Sketch of distance parameters for E_{ext} calculation.

Then

$$\phi(R,t) = \frac{1}{4\pi\epsilon_0} \int \frac{dr dx \delta(r) \delta(z - v(t - \frac{|\vec{r}-\vec{R}|}{c})}{|\vec{r}-\vec{R}|}$$

and $|\vec{r}-\vec{R}| = R^2 + (X-z)^2$. (B-2)

Let us define

$$F(z) = z - vt - \beta \sqrt{R^2 + (x-z)^2}$$

then

$$\delta(F(z)) = \sum_N \frac{1}{|F'(z_N)|} \delta(x - x'_N)$$

for

$$F(z) = 0 = F(z_0)$$

$$F'(z_N) = 0$$

thus,

$$\frac{dF(z_0)}{dz} = 1 + \frac{\beta(z-x)}{\sqrt{R^2 + (x-z)^2}} \quad (B-3)$$

$$z_0^2 - 2z_0 vt + v^2 t^2 = \beta^2 R^2 + \beta^2 x^2 - 2\beta^2 x z_0$$

Rearranging with powers of z_0 yields

$$z_0^2 (1 - \beta^2) - z_0 (2vt - 2\beta^2 x) + (v^2 t^2 - \beta^2 R^2 - \beta^2 x^2) = 0.$$

If we now let

$$a = (1 - \beta^2), \quad b = (2vt - 2\beta^2 x), \quad c = (v^2 t^2 - \beta^2 R^2 - \beta^2 x^2)$$

and use the quadratic equation to find the roots

$$\begin{aligned} z_0 &= \frac{2(vt - \beta^2 x) \pm \sqrt{(2vt - \beta^2 x)^2 - 4(1 - \beta^2)(v^2 t^2 - \beta^2 R^2 - \beta^2 x^2)}}{2(1 - \beta^2)} \\ &= \frac{vt - \beta^2 x \pm \beta \sqrt{R^2(1 - \beta^2) + (x - vt)^2}}{(1 - \beta^2)}. \end{aligned} \quad (B-4)$$

In order to determine which sign should go with the square root term, let us add

$$(-vt + \beta \sqrt{R^2(1 - \beta^2) + (x - vt)^2})$$

to both sides

$$z_0 - vt + \beta \sqrt{\quad} = 0 = \frac{vt - \beta^2 x \pm \beta \sqrt{\quad} - vt(1 - \beta^2) + \beta \sqrt{(1 - \beta^2)}}{(1 - \beta^2)} \quad (B-5)$$

In the line as $(vt - x)$ goes to zero, the right-hand side goes to

$$0 = \pm R \sqrt{1 - \beta^2} + R \sqrt{(1 - \beta^2) + \beta^2(1 - \beta^2)} \quad (B-6)$$

therefore, it is clear that the sign must be negative. Then

$$z_0 = \frac{vt - \beta^2 x - \beta \sqrt{R^2(1-\beta^2) + (vt-x)^2}}{1-\beta^2} \quad (B-7)$$

From Eq (3)

$$\frac{dF(z_0)}{dz} = \frac{\sqrt{R^2 + (x-z_0)^2} + \beta(z_0-x)}{\sqrt{R^2 + (x-z_0)^2}} \quad (B-8)$$

But, Eq (5) says

$$\sqrt{R^2 + (x-z_0)^2} = \frac{z_0 - vt}{\beta}$$

thus,

$$\frac{dF(z_0)}{dz} = \frac{\frac{z_0 - vt}{\beta} + \beta(z-x)}{\frac{z_0 - vt}{\beta}} = \frac{z_0 - vt + \beta^2(z-x)}{(z_0 - vt)} \quad (B-9)$$

Returning to Eq (7) and subtracting (vt) from both sides

$$(z_0 - vt) = \frac{\beta^2(vt-x) - \beta \sqrt{R^2(1-\beta^2) + (vt-x)^2}}{1-\beta^2} \quad (B-10)$$

and subtracting (x) from both sides of Eq (7)

$$(z_0 - x) = \frac{(vt-x) - \beta \sqrt{R^2(1-\beta^2) + (vt-x)^2}}{1-\beta^2} \quad (B-11)$$

Substituting Eqs (10) and (11) into Eq (9) yields

$$\frac{dF(z_0)}{dz} = \frac{2\beta(vt-x) - (1-\beta^2)\sqrt{R^2(1-\beta^2) + (vt-x)^2}}{\beta(vt-x) - \sqrt{R^2(1-\beta^2) + (vt-x)^2}} \quad (B-12)$$

Combining Eqs (2) and (3) and noting that

$$\frac{-(z_0 - vt)}{\beta} = |\vec{r} - R|$$

$$\begin{aligned} \phi(R, t) &= \frac{-Q}{4\pi\epsilon_0} \int \frac{dR \delta(R) \beta}{(z_0 - vt) \left(1 + \frac{\beta(z_0 - x)}{z_0 - vt} \right)} \\ &= \frac{-Q\beta}{4\pi\epsilon_0} \int \frac{dR \delta(R)}{(z_0 - vt) + \beta^2(z_0 - x)} \quad (B-13) \end{aligned}$$

Since R is a point, Eq (13) becomes

$$\phi(R, t) = \frac{-Q(1 - \beta^2)}{4\pi\epsilon_0 (2\beta(vt - x) - (1 - \beta^2) \sqrt{R^2(1 - \beta^2) + (vt - x)^2}}.$$

After substituting Eqs (10) and (11) which reduces to

$$\phi(R, t) = \frac{-Q}{4\pi\epsilon_0} \frac{1}{\frac{2\beta}{(1 - \beta^2)} ((vt - x) - \sqrt{R^2(1 - \beta^2) + (vt - x)^2})}.$$

$$\text{Now, } E = -\nabla\phi, \quad E_R = -\frac{d\phi}{dR}, \quad E_z = -\frac{d\phi}{dz}$$

$$E_R = \frac{Q}{4\pi\epsilon_0} \frac{R(1 - \beta^2)}{\left[\frac{2\beta}{1 - \beta^2} (vt - x) - \sqrt{R^2(1 - \beta^2) + (vt - x)^2} \right]^2 \sqrt{R^2(1 - \beta^2) + (vt - x)^2}} \quad (B-14)$$

$$E_z = \frac{Q}{4\pi\epsilon_0} \frac{\left(\frac{2\beta}{1-\beta^2}\right) - \frac{vt-x}{\sqrt{R^2(1-\beta^2) + (vt-x)^2}}}{\left[\left(\frac{2\beta}{1-\beta^2}\right)(vt-x) - \sqrt{R^2(1-\beta^2) + (vt-x)^2}\right]^2} .$$

(B-15)

As expected, E_z reduces to the familiar form

$$E = \frac{Q}{4\pi\epsilon_0 R^2}$$

as $\beta \rightarrow 0$, and the area of the interaction goes to a point ($R \rightarrow 0$). In the one-dimensional model, the radius of interaction will be fixed at (.001) even though the r dimension is nonexistent, and in the 2-D model it will be allowed to vary.

Appendix C

Derivation of Constants

The One-dimensional Model

Because of the large number of parameters and scaling factors used in the analytic solution and the equations which are used in the computer model, this section will go through the rationale used in the selection and derivation of these values.

The following constants have been used in evaluating the one-dimensional Vlasov equation:

1) X_0 , the distance scale parameter where $x = X_0 \frac{u}{\sqrt{1-u^2}}$
Assume target to be 1 meter thick and extends symmetrically over 17 cells with values of $u = -8/9$ to $+8/9$ in steps of .111, thus $X_0 = .2766 \text{ m}$

2) ϕ , the number of electrons/ m^3 - momentum

where N = number of electrons/ m^3 in the plasma. Assume the plasma electrons are the 3 outer shell electrons of the aluminum atom then

$$N = 1.8 \times 10^{29} \text{ electrons}/\text{m}^3$$

It should be noted that if energy greater than a few hundred eV is deposited in the plasma per aluminum atom more than the three outer electrons will be in the conductance band. For the first estimate, only the outer three were chosen but additional analysis of future data may require this value to change.

P_0 is a free parameter and will be discussed later.

3) E_o , the electric field scale factor which will be discussed in Appendix D and serves to condense the computer operations, we'll note

$$\frac{T_o P_o}{M \lambda_o} = 1 \quad , \quad \frac{T_o e E_o}{P_o} = 1$$

and

$$\frac{T_o e P_o^2 \phi}{2 E_o M} = 1$$

Solving these equations for T_o , P_o and E_o yields

$$\begin{aligned} T_o &= 7.25 \times 10^{-17} \text{ s} \\ P_o &= 3.48 \times 10^{-15} \text{ kg} \cdot \text{m} \\ E_o &= 3.0 \times 10^{20} \text{ V/m} \end{aligned}$$

4) Q , the charge of the pulse. The beam consists of a 1K amp proton beam chopped in 10^{-9} sec. pulses. Thus each pulse has a charge of $Q = 1 \times 10^{-6}$ coul.

5) β , the relativistic constant. The protons are rated at 10 GeV or 10^{10} ev. From relativity theory we know

$$\frac{T}{M_o c^2} = (1 - \beta^2)^{-1/2} - 1$$

where T = kinetic energy of particle, M_o = rest mass of proton. Therefore $\beta = .995$ and the velocity of the beam equals

$$V = c \beta = 2.986 \times 10^8 \text{ m/s}$$

The two-dimensional solution

1) R_o , the radial distance scale parameter. If we assume that the diameter of the actual beam is 10^{-3} meters instead of a point charge, the area of the target which will be of greatest interest will be within a radius of 5×10^{-4} meters. If we have nine points of observation in the radial direction, then 8 of those should be in the 5×10^{-4} m radius. Therefore:

$$0.0005 = R_o \frac{w}{1-w}$$

Let $w = 2/9$ then $R_o = 6.25 \times 10^{-5}$

2) E_0 , T_0 , P_0 , B_0 , the electric field, time, momentum and magnetic field parameters respectively. As will be developed in the two-dimensional method section (Appendix F), the nine constants of the solving equations are:

$$\begin{aligned} C_1 &= \frac{P_0 T_0}{M R_0} & C_2 &= \frac{P_0 T_0}{M Z_0} & C_3 &= \frac{e E_0 T_0}{P_0} \\ C_4 &= \frac{e B_0 T_0}{M} & C_5 &= \frac{C^2 B_0 T_0}{E_0 R_0} & C_6 &= \frac{C^2 B_0 T_0}{E_0 Z_0} \\ C_7 &= \frac{e P_0 N_0 T_0}{M T_0 E_0} & C_8 &= \frac{E_0 T_0}{B_0 R_0} & C_9 &= \frac{E_0 T_0}{B_0 Z_0} \end{aligned}$$

By making the following assumptions:

$$C_1 = C_5 = C_7 = C_8 = 1$$

The nine coefficients reduce to

$$\begin{aligned} C_1 &= 1 & C_2 &= R_0/Z_0 & C_7 &= 1 \\ C_8 &= 1 & C_9 &= R_0/Z_0 \end{aligned}$$

The values of the scaling parameters thus lead to:

$$\begin{aligned} E_0 &= \frac{e N_0 R_0}{E_0} = 2.0 \times 10^{11} \text{ V/m} \\ B_0 &= E_0/c = 6.78 \times 10^8 \text{ V.m/s} \\ P_0 &= \frac{E_0 M}{B_0} = 2.73 \times 10^{-22} \text{ kg.m/s} \\ T_0 &= \frac{M R_0}{P_0} = 2.08 \times 10^{-13} \text{ s} \end{aligned}$$

3) All other parameters remained the same as the one-dimensional model.

Appendix D

Moments for the One-dimensional Model

The taking of moments involves the integration out of the momentum components (phase-space components) in the particle distribution function and is given by

$$\int p^m f(p) dp$$

where $m = 0, 1, 2, \dots$ corresponds to the 1st, 2nd, etc. moments.

The first three moments of the Vlasov equation

$$\frac{df(x,p)}{dt} + \frac{p}{M} \frac{df(x,p)}{dx} + f \frac{dF}{dp} = 0 \quad (D-1)$$

in one-dimension will be taken. As stated earlier, the force F , is the one-dimensional Lorentzian force

$$F = gE \quad (D-2)$$

where E is the total electric field due to external charges and currents and the internal field due to displacement of any charges in the plasma.

Once the moments have been taken, the electric field components of the force will be examined, and the scaling parameters discussed earlier, will be introduced into the equation.

The First Moment, $m = 0$

Multiplying through Eq (1) by dp and integrating over all momentum ($\pm \infty$) yields

$$\frac{df}{dt} \int f(x,p) dp = -\frac{1}{M} \left[\frac{d}{dx} \int f(x,p) p dp \right] - \int f \frac{dF}{dp} dp \quad (D-3)$$

where the derivatives with respect to time and space are independent of momentum and have been taken out of the integral. Let us now define

$$N = \int f(x, p) dp$$

where N is the particle density and is obtained by integrating the distribution function, $f(x, p)$, over all momentum

$$N\langle p \rangle = \int p f(x, p) dp$$

where p is the expected value of p and is defined as the average value, \bar{p} , plus any small perturbations, \tilde{p} .

$$p = \bar{p} + \tilde{p}$$

so that

$$\langle p \rangle = \langle \bar{p} + \tilde{p} \rangle = \langle \bar{p} \rangle + \langle \tilde{p} \rangle$$

but by definition $\langle p \rangle = \bar{p}$ thus $\langle \tilde{p} \rangle = 0$.

Eq (3) thus becomes

$$\frac{dN}{dt} = -\frac{1}{M} \left[\frac{d(N\bar{p})}{dx} \right] - \int \frac{df}{dp} dp. \quad (D-4)$$

The second term on the right-hand side is a perfect differential, and is set to zero, if we assume that there are no particles at $\pm\infty$. Eq (4) thus reduces to

$$\frac{dN}{dt} = -\frac{1}{M} \left[N \frac{d\bar{p}}{dx} + \bar{p} \frac{dN}{dx} \right] \quad (D-5)$$

which agrees with Seshadri's equation Eq 8.9 (Ref 14) for a one-dimensional model. Dividing through by N , we obtain the first moment

$$\frac{d \ln N}{dt} = -\frac{1}{M} \left[\frac{d\bar{p}}{dx} + \bar{p} \frac{d \ln N}{dx} \right]. \quad (D-6)$$

The Second Moment, $m = 1$

The second moment is obtained by multiplying Eq (1) by $p dp$ and integrating over all momentum to yields

$$\frac{d}{dt} \int p f dp = -\frac{1}{M} \frac{d}{dx} \int p^2 f dp - \int p \frac{df}{dp} dp. \quad (0-7)$$

Eq (7) reduces to

$$\frac{d}{dt} (N \bar{p}) = -\frac{1}{M} \frac{d}{dx} (N \langle p^2 \rangle) - \int p f \Big|_{-\infty}^{\infty} - \int f p dp. \quad (0-8)$$

By a similar analysis as in the first moment, $p f \Big|_{-\infty}^{\infty} = 0$ and

$$\langle p^2 \rangle = \langle \bar{p}^2 + 2 \bar{p} \tilde{p} + \tilde{p}^2 \rangle = \bar{p}^2 + \langle \tilde{p}^2 \rangle.$$

Thus, Eq (8) reduces to

$$\frac{d}{dt} (N \bar{p}) = \frac{1}{M} \frac{d}{dx} [N (\bar{p}^2 + \langle \tilde{p}^2 \rangle)] + F N. \quad (0-9)$$

Let us now define $\frac{N \bar{p}^2}{M}$ as the kinetic energy term of the plasma. Since $\bar{p} = M \bar{v}$ the term may be written as $\frac{N \bar{p}^2}{M} = N (M \bar{v}^2)$ which has units of kinetic energy per unit volume and $\frac{N \langle \tilde{p}^2 \rangle}{M}$ is a kinetic pressure term.

If $\langle \tilde{p}^2 \rangle$ is written in vector notation as $\langle \tilde{p}^2 \rangle = \langle \tilde{p}_i \tilde{p}_j \rangle$, it can be shown that only the following terms are nonzero in three dimensions

$$\langle \tilde{p}^2 \rangle = \langle \tilde{p}_x \tilde{p}_x \rangle + \langle \tilde{p}_y \tilde{p}_y \rangle + \langle \tilde{p}_z \tilde{p}_z \rangle$$

$$\frac{1}{3} \frac{\langle \tilde{p}^2 \rangle}{M} = \frac{K T}{M}$$

or $\frac{\langle \tilde{p}^2 \rangle}{M^2} = \frac{K T}{M} \quad \text{in 1-Dimension}$

where K is the Boltzmann constant and T is the uniform temperature. The static pressure is given by NKT thus

$$\frac{N \langle \tilde{p}^2 \rangle}{M} = NM \left(\frac{\langle \tilde{p}^2 \rangle}{M^2} \right) = NKT = P.$$

Thus Eq (9) may be written

$$\frac{d(N\bar{P})}{dt} = \frac{d}{dx} (N\bar{P}^2 + P) \quad (D-10)$$

which agrees with Eq (II-3) of La 4700. (Ref 17). For our purpose, however, let us keep the notation of \tilde{p}^2 and assume it to be a modified pressure. Thus, Eq (10) may be written

$$\frac{d(N\bar{P})}{dt} = -\frac{1}{M} \frac{d}{dx} [N\bar{P}^2 + N\tilde{p}^2] \quad (D-11)$$

expanding Eq (11) and substituting into the expansion of Eq (5)

$$\begin{aligned} N \frac{d\bar{P}}{dt} &= -\frac{1}{M} \left[\frac{d}{dx} (N\tilde{p}^2 + N\bar{P}^2) - \bar{P} \frac{d}{dx} (N\bar{P}) \right] + FN \\ &= -\frac{1}{M} \left[\tilde{p}^2 \frac{dN}{dx} + N \frac{d\tilde{p}^2}{dx} + \bar{P} N \frac{d\bar{P}}{dx} \right] + FN. \end{aligned} \quad (D-12)$$

Canceling out the N yields

$$\frac{d\bar{P}}{dt} = F - \frac{1}{M} \left[\tilde{p}^2 \frac{d \ln N}{dx} + \frac{d\tilde{p}^2}{dx} + \bar{P} \frac{d\bar{P}}{dx} \right] \quad (D-13)$$

the equation for the second moment.

The Third Moment

Similarly as in the first two moments, Eq (1) is multiplied through by $p^2 dp$ and integrated to yield

$$\frac{d}{dt} \int f p^2 dp = - \frac{1}{M} \left[\frac{d}{dx} \int p^3 f dp \right] - \int p^2 \frac{df}{dp} dp. \quad (D-14)$$

After integration we obtain

$$\frac{d}{dt} (N (\bar{p}^2 + \tilde{p}^2)) = - \frac{1}{M} \frac{d}{dx} [N \langle p^3 \rangle] + 2 \mathcal{F} N \bar{p}.$$

But $\langle p^3 \rangle = \langle \bar{p}^3 + 3\bar{p}\tilde{p} + \tilde{p}^3 \rangle$ when the $\langle \tilde{p} \rangle$ terms are set to zero. Eq (14) then becomes

$$\frac{d}{dt} (N (\langle \tilde{p}^2 \rangle + \bar{p}^2)) = - \frac{1}{M} \frac{d}{dx} [N (\bar{p}^3 + 3\bar{p}\langle \tilde{p}^2 \rangle + \langle \tilde{p}^3 \rangle)] + 2 \mathcal{F} N \bar{p}. \quad (D-15)$$

In order to close the set of equations, let us set all \tilde{p}^3 terms equal to zero. In actuality this term, $\frac{N \bar{p}^3}{M}$, is an energy-flux term. Eq (15) then becomes

$$\frac{d}{dt} [N (\bar{p}^2 + \langle \tilde{p}^2 \rangle)] = - \frac{1}{M} \frac{d}{dx} [N (\bar{p}^3 + 3\bar{p}\langle \tilde{p}^2 \rangle)] + 2 \mathcal{F} N \bar{p}. \quad (D-16)$$

Substituting Eq (11) and Eq (5) into Eq (16) and collecting terms yields

$$\frac{d \langle \tilde{p}^2 \rangle}{dt} = - \frac{1}{M} \left[2 \langle \tilde{p}^2 \rangle \frac{d \bar{p}}{dx} + \bar{p} \frac{d \langle \tilde{p}^2 \rangle}{dx} \right]. \quad (D-17)$$

The third moment, which agrees with Seshadri's equation (10.31) if written in Eulerian derivatives where

$$\frac{df}{dt} = \frac{df}{dt} + \frac{df}{dx} dx.$$

To quickly summarize, the first three moments

$$m = 0$$

$$\frac{d \ln N}{dt} = \frac{1}{M} \left[\frac{d \bar{P}}{dx} + \bar{P} \frac{d \ln N}{dx} \right] \quad (D-6)$$

$$m = 1$$

$$\frac{d \bar{P}}{dt} = J - \frac{1}{M} \left[\langle \tilde{P}^2 \rangle \frac{d \ln N}{dx} + \frac{d \langle \tilde{P}^2 \rangle}{dx} + \bar{P} \frac{d \bar{P}}{dx} \right] \quad (D-13)$$

$$m = 2$$

$$\frac{d \langle \tilde{P}^2 \rangle}{dt} = -\frac{1}{M} \left[2 \langle \tilde{P} \rangle^2 \frac{d \bar{P}}{dx} + \bar{P} \frac{d \langle \tilde{P}^2 \rangle}{dx} \right]. \quad (D-17)$$

Let us now look at the force term, F . In one dimension, term is given by

$$F = q(E_{int} + E_{ext}).$$

The external electric field is developed in Appendix B and will receive no further discussion at this point, except to note that it is independent of the plasma.

The internal electric field can be evaluated through Maxwell's equations

$$\mathcal{H}_0 (\nabla \times \bar{B}) = J + \epsilon_0 \frac{dE}{dt} \quad (D-18)$$

where \bar{J} is the current density and is given by

$$\bar{J} = \frac{q}{\epsilon_0 M} \int p f(x, p) dp. \quad (D-19)$$

Combining Eqs (18) and (19) and noting that $(\nabla \times B) = 0$ in one dimension

$$\frac{dE}{dt} = -\frac{q}{\epsilon_0 M} \int p f dp. \quad (D-20)$$

After integrating over all momentum Eq (20) becomes

$$\frac{dE}{dt} = \frac{q}{\epsilon_0 M} N \bar{p} \quad (D-21)$$

where $q = -e$ the charge of an electron.

The Lorentzian force may then be written as a sum of the two electric fields after a differential equation solving routine has been used to calculate E_{int} .

At this point, we have four linear differential equations, Eqs (6), (13), (17) and (21), which can be solved by a standard solving routine and thus stepped in time.

As was discussed in a previous section, it is necessary to scale the parameters of the four equations. The scaling factors are as follows:

$$X = X_0 \frac{u}{\sqrt{1-u^2}} \quad dX = X_0 \frac{1}{(1-u^2)^{3/2}} du \quad -1 < u < 1$$

$$T = T_0 \sinh(s) \quad dT = T_0 \cosh(s) ds$$

$$\tilde{p}^z = p_0^z \sinh(\tilde{V}^z) \quad d\tilde{p}^z = p_0^z \cosh(\tilde{V}^z) d\tilde{V}^z.$$

$$P = P_0 \sinh(v) \quad dP = P_0 \cosh(v)$$

$$f = f^* \phi \quad \phi = \text{Particles}/M^3\text{-MOMENTUM} = N_0/P_0$$

$$E = E_0 E^* \quad E = \left(\frac{E}{E_0} \right)$$

With these substitutions, our four equations change to

$$\frac{d \ln N}{ds} = - \frac{T_0 P_0}{M X_0} (1-u^2)^{3/2} \cosh(s) \left[\cosh(v) \frac{dV}{du} + \sinh(v) \frac{d \ln N}{du} \right] \quad (D-22)$$

$$\sinh(v) \frac{dV}{ds} = \frac{T_0 e E_0}{P_0} \cosh(s) E^* - \frac{T_0 P_0}{M X_0} \cosh(s) (1-u^2)^{3/2}$$

$$\left[\sinh(\tilde{v}^*) \frac{d \ln N}{du} + \cosh(\tilde{v}^*) \frac{d \tilde{v}^*}{du} + \sinh(v) \cosh(v) \frac{dV}{du} \right] \quad (D-23)$$

$$\sinh(\tilde{v}^*) \frac{d \tilde{v}^*}{ds} = \frac{T_0 P_0}{M X_0} \left[2 \sinh(\tilde{v}^*) \cosh(v) \frac{dV}{du} + \sinh(v) \cosh(\tilde{v}^*) \frac{d \tilde{v}^*}{du} \right] \quad (D-24)$$

$$\frac{dE}{ds} = \frac{T_0 e P_0 N_0}{2 E_0 M E_0} \int f^* \sinh(2v) dv \quad (D-25)$$

If we now let

$$\frac{T_o P_o}{M X_o} = 1, \quad \frac{T_o e E_o}{P_o} = 1, \quad \frac{T_o e P_o N_o}{2 \epsilon_o M E} = 1$$

these three equations can be solved in terms of one parameter, E_o

$$E_o = \frac{X_o e N_o}{2 \epsilon_o}.$$

Call

$$Y_1 = \ln N$$

$$Y_2 = \sinh(v)$$

$$Y_3 = \sinh(\tilde{v}^2)$$

$$Y_4 = E_{int}.$$

Then,

Eqs (22), (23), (24) and (25) reduce to

$$\frac{dY_1}{dS} = -R \left[\frac{dY_2}{dU} + Y_2 \frac{dY_1}{dU} \right] \quad (D-26)$$

$$\frac{dY_2}{dS} = -R \left[Y_3 \frac{dY_1}{dU} + \frac{dY_1}{dU} + Y_2 \frac{dY_2}{dU} \right] + \frac{\cosh(S)}{E_o} (Y_4 + E_{ext}) \quad (D-27)$$

$$\frac{dY_3}{dS} = -R \left\{ 2 Y_3 \frac{dY_2}{dU} + Y_2 \frac{dY_3}{dU} \right\} \quad (D-28)$$

$$\frac{dY_4}{ds} = -2 E_0 \cosh(s) Y_2 \exp(Y_1) \quad (D-29)$$

where $R = \cosh(s) (1-u^2)^{3/2}$.

These four equations are those used in the solving routine.

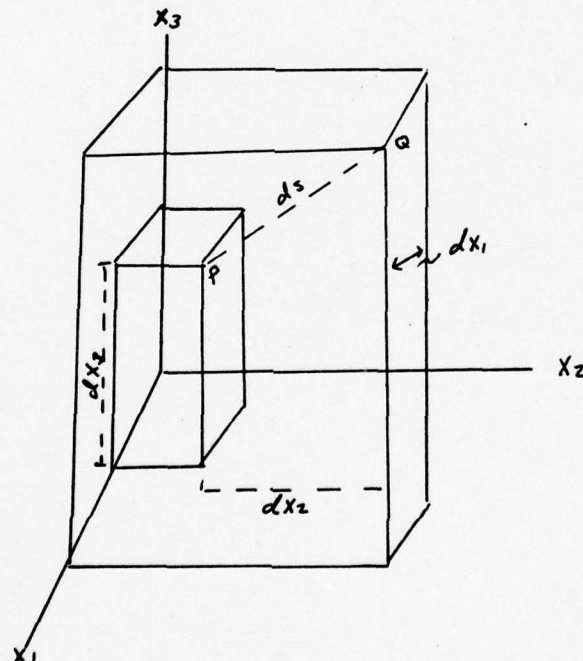
Appendix E

Derivation of Moment Equations

In Cylindrical Coordinates

In this section, a general discussion of the metric tensor and other properties of tensors necessary to find the moments of the Vlasov equation in 2-D cylindrical coordinates will be discussed. Once the basic groundwork has been established, the first three moments will be taken. Maxwell's equations will also be integrated into the equations as required by the Lorentzian force term. These equations will then be simplified to meet the assumptions of our model.

The Metric Tensor



The distance between points P and Q is ds . To evaluate this distance, we take the square root of the sum of the

squares of the three increments dx^1 , dx^2 and dx^3 ,

$$(ds)^2 = (dx^1)^2 + (dx^2)^2 + (dx^3)^2.$$

If X has the form

$$x^i = f^i(z^1, z^2, z^3) \quad i = 1, 2, 3$$

then

$$dx^r = \frac{df^r}{dz^s} dz^s$$

where summation notation has been used and s represents a sum $s = 1, 2, \dots$ etc. but

$$(ds)^2 = dx^r dx^r$$

so

$$(ds)^2 = \left(\frac{df^r}{dz^i} dz^i \right) \left(\frac{df^r}{dz^j} dz^j \right) = \left(\frac{df^r}{dz^i} \cdot \frac{df^r}{dz^j} \right) dz^i dz^j \quad (E-1)$$

where the dummy index s has been changed to avoid confusion. Eq (1) represents a homogeneous quadratic form in the variable dz^i . Let

$$b_{ij} = \left(\frac{df^r}{dz^i} \cdot \frac{df^r}{dz^j} \right) \quad \text{where} \quad \begin{matrix} i = 1, 2, 3 \\ j = 1, 2, 3 \end{matrix}$$

then $(ds)^2$ has the form

$$(ds)^2 = b_{ij} dz^i dz^j \quad (E-2)$$

where b_{ij} for a three-dimensional space is

$$b_{ij} = \begin{pmatrix} b_{11} & b_{12} & b_{13} \\ b_{21} & b_{22} & b_{23} \\ b_{31} & b_{32} & b_{33} \end{pmatrix}.$$

The expanded form of the quadratic equation, Eq (2), is

$$(ds)^2 = b_{11} dz^1 dz^1 + b_{12} dz^1 dz^2 + b_{13} dz^1 dz^3 \\ + b_{21} dz^2 dz^1 + \dots \dots \dots + b_{33} dz^3 dz^3.$$

Rearrangement yields

$$(ds)^2 = b_{11} (dz^1)^2 + b_{22} (dz^2)^2 + b_{33} (dz^3)^2 + (b_{12} + b_{21}) \\ dz^1 dz^2 + (b_{13} + b_{31}) dz^1 dz^3 + (b_{23} + b_{32}) dz^2 dz^3$$

or in a general form

$$(ds)^2 = \left(\frac{b_{iJ} + b_{Ji}}{2} \right) dz^i dz^J. \quad (E-3)$$

Let us define

$$g_{iJ} = \frac{(b_{iJ} + b_{Ji})}{2} \quad (E-4)$$

hence,

$$(ds)^2 = g_{iJ} dz^i dz^J$$

(Note: $g_{iJ} = g_{Ji}$).

g_{iJ} is a covariant second-order tensor and is called the metric tensor. A covariant tensor transforms a tensor in one system to a tensor in a second system via

$$A'_{rs} = \frac{dz^t}{dz'^r} \frac{dz^u}{dz'^s} A^{tu}.$$

The Metric Tensor In Cylindrical Coordinates

The Cartesian coordinates x^1, x^2, x^3 are related to the cylindrical coordinates r, ϕ, z by

$$x^1 = r \cos \theta = z^1 \cos z^2$$

$$x^2 = r \sin \theta = z^1 \sin z^2$$

$$x^3 = z = z^3.$$

Employing the general equation (Eq (4)) yields

$$g_{ij} = \frac{d(r \cos \theta)}{dz^i} \frac{d(r \cos \theta)}{dz^j} + \frac{d(r \sin \theta)}{dz^i} \frac{d(r \sin \theta)}{dz^j} + \frac{dz}{dz^i} \frac{dz}{dz^j}.$$

If $i = j = 1$

$$dz_i = dz_j = dr$$

then

$$g_{ij} = \cos^2 \theta + \sin^2 \theta = 1 = g_{11}.$$

If $i = j = 2$

$$g_{ij} = r^2 \cos^2 \theta + r^2 \sin^2 \theta = r^2 = g_{22}.$$

If $i = j = 3$

$$g_{ij} = 0 + 0 + 1 = 1 = g_{33}$$

all other possible combinations of i and j result in $g_{ij} = 0$.

Thus,

$$g_{ij} = \begin{pmatrix} 1 & 0 & 0 \\ 0 & r^2 & 0 \\ 0 & 0 & 1 \end{pmatrix}$$

$$g_{ij} = \begin{pmatrix} 1 & 0 & 0 \\ 0 & r^2 & 0 \\ 0 & 0 & 1 \end{pmatrix}. \quad (E-5)$$

This is the metric tensor in cylindrical coordinates. Thus, the distance between two points in cylindrical coordinates is given by $(ds)^2 = \sum_{ij} g_{ij} dz_i dz_j$ or

$$(ds)^2 = \begin{pmatrix} 1 & 0 & 0 \\ 0 & r^2 & 0 \\ 0 & 0 & 1 \end{pmatrix} dz_i dz_j.$$

Christoffel Symbols

The partial derivative of a vector \bar{A} with respect to x^j is given by

$$\frac{d\bar{A}}{dx^j} = \frac{dA^i}{dx^j} \hat{a}_i + \frac{d\hat{a}_i}{dx^j} A^i \quad (E-6)$$

where $\bar{A} = A \hat{a}_i$ and \hat{a}_i is a unit vector of the space to be used.

Let us define

$$\frac{d\hat{a}_i}{dx^j} = \{^A_{ij}\} a_A \quad (E-7)$$

where $\{^A_{ij}\}$ is called a Christoffel symbol of the second kind. Substituting Eq (7) back into Eq (6) yields

$$\frac{d\bar{A}}{dx^j} = - \frac{d\bar{A}^i}{dx^j} - \{^A_{ij}\} A_A.$$

In other words, the Christoffel symbol serves to take the derivative of the space in which the vector is defined. Thus, the covariant derivative of a covariant tensor is

defined as

$$A_{i,j} = \frac{dA_i}{dx^j} - \left\{ \begin{matrix} \alpha \\ i j \end{matrix} \right\} A_\alpha \quad (E-8)$$

where j means the covariant derivative with respect to j , and a covariant tensor is defined by

$$B_i = \frac{dX^\alpha}{dY^i} A_\alpha$$

where B_i is defined in the y -coordinate system and A in the X -coordinate system and the covariant derivative of a contravariant vector is given by

$$A_{,j}^i = \frac{dA^i}{dx^j} + \left\{ \begin{matrix} i \\ \alpha j \end{matrix} \right\} A^\alpha \quad (E-9)$$

where the superscript means contravariant, and subscript means covariant, and the contravariant vector is defined by

$$B^i = \frac{dY^i}{dX^\alpha} A^\alpha$$

If the tensor is of rank two (i, j) instead of rank one (a vector), Eq (9), expands to

$$A_{,k}^{ij} = \frac{dA^{ij}}{dY^k} + \left\{ \begin{matrix} i \\ \alpha k \end{matrix} \right\} A^{\alpha j} + \left\{ \begin{matrix} j \\ \alpha k \end{matrix} \right\} A^{i\alpha} \quad (E-10)$$

In Ref 18, the Christoffel symbols for cylindrical coordinates are derived and will be only stated here as

$$\begin{aligned} \left\{ \begin{matrix} 2 \\ 1 \end{matrix} \right\} &= \left\{ \begin{matrix} 1 \\ 2 \end{matrix} \right\} = 1/r \\ \left\{ \begin{matrix} 1 \\ 2 \end{matrix} \right\} &= -r \end{aligned} \quad (E-11)$$

Equipped with the Christoffel symbols and the definitions of the derivatives of tensors, Eqs (8), (9), and (10), we are ready to take the moments of the Vlasov equation.

The Moments to the Boltzmann-Vlasov Equation

The Vlasov equation is given by

$$\frac{df}{dt} = \frac{1}{M} p^\alpha \frac{df}{dx^\alpha} - F^\alpha \frac{df}{dp^\alpha} \quad (E-12)$$

where f = the distribution function

p^α = the momentum tensor in the α direction

M = the mass of the electron

F^α = the force tensor in the α direction.

If we define

$$\rho(x) = \int d\vec{p} f(x, p) \quad (E-13)$$

$$\rho_\alpha(x) = \int d\vec{p} p^\alpha f(x, p) \quad (E-14)$$

where $d\vec{p} = d^3p^\alpha$, $\alpha = 1, 2, 3$ and p^α is the value of the average momentum as was discussed in Appendix D.

Then after multiplying Eq (12) by and integrating over all momentum we obtain

$$\frac{d}{dt} \int f d\rho = \frac{1}{M} \frac{d}{dx^\alpha} \left[\int p^\alpha f d\vec{p} \right] - F^\alpha \int \frac{df}{dp^\alpha} d\vec{p} \quad (E-15)$$

where F^α is a function of x and t usually thought of as the Lorentzian force, $F = g(E + (V \times B))$ and is independent of the integration.

The last term on the right-hand side of Eq (15) vanishes since it is a perfect differential, and the value of f at the limits is assumed to be zero.

Substituting Eqs (13) and (14) into Eq (15)

$$\frac{d}{dt} \rho(x) = -\frac{1}{M} \left[\rho(x) \rho_i^i(x) \right]_{,a} = -\frac{1}{M} \left[\rho_{,a} \rho_i^i + \rho \rho_{i,a}^i \right] \quad (E-16)$$

which is in agreement with Eq (8.9), the equation of continuity, of Ref 14. Expanding the covariant derivatives via Eq (9) yields

$$\frac{d}{dt} \rho = -\frac{1}{M} \left[\frac{d\rho}{dx^a} \rho_i^i + \rho \left(\frac{d\rho_i^i}{dx^a} + \left\{ \begin{matrix} a \\ \alpha\beta \end{matrix} \right\} \rho_i^\beta \right) \right]$$

$\alpha = r, \phi, z = 1, 2, 3$ respectively or x, y, z if in Cartesian coordinate, only the values of the Christoffel symbols change. The assumption is now made that the momentum in the ϕ direction will always be nonexistent due to symmetrical modeling; thus

$$\rho_i^\phi = \rho_i^2 = 0$$

and Eq (16) becomes

$$\frac{d\rho}{dt} = -\frac{1}{M} \left[\frac{d\rho}{dr} \rho_i^r + \frac{d\rho}{dz} \rho_i^z + \rho \left[\frac{d\rho_i^r}{dr} + \frac{d\rho_i^z}{dz} + \frac{1}{r} \rho_i^r \right] \right] \quad (E-17)$$

where

$$\left\{ \begin{matrix} \phi \\ r \end{matrix} \right\} = \left\{ \begin{matrix} 2 \\ 1 \end{matrix} \right\} = 1/r$$

Define

$$\rho_0(x) \rho_2^{\alpha\beta}(x) = \int d\vec{p} (\mathcal{P}^\alpha - \rho_1^\alpha)(\mathcal{P}^\beta - \rho_1^\beta) f(x, p)$$

where $(\mathcal{P} - \rho)$ is a small perturbation term, $\mathcal{P} = (\rho - \tilde{\rho})$, and $\rho_2^{\alpha\beta}$ is the modified pressure term as described in Appendix D.

Upon expanding the integral, the equation reduces to

$$\rho_0 \rho_2^{\alpha\beta} = \int d\vec{p} f \mathcal{P}^\alpha \mathcal{P}^\beta - \rho_0 \rho_1^\alpha \rho_1^\beta$$

Multiplying Eq (12) by $\rho_1^\beta d\vec{p}$ and integrating yields

$$\frac{d}{dt} \int \rho_1^\beta f d\vec{p} = -\frac{1}{M} \frac{d}{dx^\alpha} \int \mathcal{P}^\alpha \mathcal{P}^\beta f d\vec{p} - \mathcal{F}^\alpha \int \rho^\beta \frac{df}{dx^\alpha} d\vec{p}$$

or after substituting

$$\begin{aligned} \frac{d}{dt} \rho_1^\beta(x) \rho_0(x) &= -\frac{1}{M} \left[\rho_0(x) \rho_2^{\alpha\beta}(x) + \rho_0(x) \rho_1^\alpha(x) \rho_1^\beta(x) \right],_\alpha \\ &+ \mathcal{F}^\alpha \int d\vec{p} \int_{\alpha}^{\beta} f \end{aligned}$$

$\int_{\alpha}^{\beta} =$ delta function = 1 if $\alpha = \beta$, 0, otherwise. Eq (II-3)

of Ref 17, if the force term is added, agrees with the above.

Expanding the differentiation and substituting Eq (16) yields

$$\begin{aligned} \frac{d\rho^\beta}{dt} &= \mathcal{F}^\beta - \frac{1}{M} \left\{ \rho_2^{\alpha\beta} \frac{d}{dx^\alpha} (\ln \rho_0) + \frac{d\rho_2^{\alpha\beta}}{dx^\alpha} + \left\{ \alpha^{\alpha} \right\} \rho_2^{\gamma\beta} \right. \\ &+ \left. \left\{ \alpha^{\beta} \right\} \rho_2^{\gamma\alpha} + \rho_1^\alpha \frac{d\rho^\beta}{dx^\alpha} + \rho_1^\alpha \rho_1^\gamma \left\{ \alpha^{\beta} \right\} \right\}. \quad (E-18) \end{aligned}$$

Thus, for $\beta = r$ $\alpha = (r, \phi, z)$

$$\frac{d\rho_1^r}{dt} = \mathcal{F}^r - \frac{1}{M} \left[\rho_2^{rr} \frac{d \ln \rho_0}{dr} + \rho_2^{zr} \frac{d \ln \rho_0}{dz} + \frac{d\rho_2^{rr}}{dr} \right. \\ \left. + \frac{d\rho_2^{zr}}{dz} - r \rho_2^{\phi\phi} + \rho_1^r \frac{d\rho_1^r}{dr} + \rho_1^z \frac{d\rho_1^r}{dz} \right] \quad (E-19)$$

$$\beta = \phi$$

$$\frac{d\rho_1^\phi}{dt} = \mathcal{F}^\phi - \frac{1}{M} \left[\rho_2^{r\phi} \frac{d \ln \rho_0}{dr} + \rho_2^{z\phi} \frac{d \ln \rho_0}{dz} + \frac{d\rho_2^{r\phi}}{dr} \right. \\ \left. + \frac{d\rho_2^{z\phi}}{dz} + \frac{1}{r} \rho_2^{r\phi} + \frac{z}{r} \rho_2^{\phi r} + \rho_1^r \frac{d\rho_1^\phi}{dr} + \rho_1^z \frac{d\rho_1^\phi}{dz} \right. \\ \left. + \frac{z}{r} \rho_1^\phi \rho_1^r \right] \quad (E-20)$$

$$\beta = z$$

$$\frac{d\rho_1^z}{dt} = \mathcal{F}^z - \frac{1}{M} \left[\rho_2^{rz} \frac{d \ln \rho_0}{dr} + \rho_2^{zz} \frac{d \ln \rho_0}{dz} + \frac{d\rho_2^{rz}}{dr} \right. \\ \left. + \frac{d\rho_2^{zz}}{dz} + \frac{1}{r} \rho_2^{rz} + \rho_1^r \frac{d\rho_1^z}{dr} + \rho_1^z \frac{d\rho_1^z}{dz} \right] \quad (E-21)$$

Let us now define

$$\begin{aligned}\rho_3^{\alpha\beta\gamma}(x) \rho_0(x) &= \int d\vec{p} f (p-\rho_1)^\alpha (p-\rho_1)^\beta (p-\rho_1)^\gamma \\ &= \int d\vec{p} f p^\alpha p^\beta p^\gamma - \rho_0 \rho_1^\alpha \rho_2^{\beta\gamma} - \rho_0 \rho_1^\beta \rho_2^{\alpha\gamma} \\ &\quad - \rho_0 \rho_2^{\alpha\beta} \rho_1^\gamma - 4 \rho_0 \rho_1^\alpha \rho_1^\beta \rho_1^\gamma\end{aligned}$$

OR

$$\int d\vec{p} p^\alpha p^\beta p^\gamma f = \rho_0 [\rho_3^{\alpha\beta\gamma} + \rho_1^\alpha \rho_2^{\beta\gamma} + \rho_1^\beta \rho_2^{\alpha\gamma} + \rho_2^{\alpha\beta} \rho_1^\gamma - 2 \rho_1^\alpha \rho_1^\beta \rho_1^\gamma].$$

The third moment is found by multiplying through Eq (12) by $p^\beta p^\gamma$ and integrating to yield

$$\begin{aligned}\frac{d}{dt} \int d\vec{p} p^\beta p^\gamma f &= -\frac{1}{M} \left[\frac{d}{dx^\alpha} \int p^\alpha p^\beta p^\gamma f d\vec{p} \right] + \mathcal{F}^\alpha \int d\vec{p} \\ &\quad (\delta_\alpha^\beta p^\gamma + \delta_\alpha^\gamma p^\beta) f.\end{aligned}$$

Substituting in definitions result in

$$\begin{aligned}\frac{d}{dt} [\rho_0 (\rho_2^{\beta\gamma} + \rho_1^\beta \rho_1^\gamma)] &= -\frac{1}{M} [\rho_0 (\rho_3^{\alpha\beta\gamma} + \rho_1^\alpha \rho_2^{\beta\gamma} + \rho_1^\beta \rho_2^{\alpha\gamma} \\ &\quad + \rho_2^{\alpha\beta} \rho_1^\gamma + 4 \rho_1^\alpha \rho_1^\beta \rho_1^\gamma)]_{,\alpha} + \mathcal{F}^\beta [\rho_0 \rho_1^\gamma] \\ &\quad + \mathcal{F}^\gamma [\rho_0 \rho_1^\beta].\end{aligned}\tag{E-22}$$

The left-hand side of Eq (22) changes to

$$\rho_0 \frac{d}{dt} \rho_2^{\gamma\beta} + \rho_2^{\gamma\beta} \frac{d}{dt} \rho_0 + \rho_1^\beta \rho_1^\gamma \frac{d}{dt} \rho_0 + \rho_1^\gamma \rho_0 \frac{d}{dt} \rho_1^\beta + \rho_1^\beta \rho_0 \frac{d}{dt} \rho_1^\gamma.$$

Solving for $\frac{d\rho_2^{\gamma\beta}}{dt}$ by substituting into Eq (22) the simplified values derived or defined above yields after much simplification

$$\begin{aligned} \frac{d}{dt} \rho_2^{\gamma\beta} = & -\frac{1}{M} \left[\frac{d \ln \rho_0}{dx^a} (\rho_3^{\alpha\beta\gamma} + \rho_1^\alpha \rho_1^\beta \rho_1^\gamma) + \frac{d \rho_3^{\alpha\beta\gamma}}{dt} + \{\alpha\delta\} \rho_3^{\delta\beta\gamma} \right. \\ & + \{\alpha\delta\} \rho_3^{\alpha\delta\gamma} + \{\alpha\delta\} \rho_3^{\alpha\beta\delta} + \rho_1^\beta \rho_1^\gamma \left[\frac{d \rho_1^\alpha}{dx^a} + \{\alpha\delta\} \rho_1^\delta \right] \\ & + (\rho_2^{\alpha\gamma} + \rho_1^\alpha \rho_1^\gamma) \left[\frac{d \rho_1^\beta}{dx^a} + \{\alpha\delta\} \rho_1^\delta \right] + (\rho_2^{\alpha\beta} + \rho_1^\alpha \rho_1^\beta) \\ & \left. \left[\frac{d \rho_1^\gamma}{dx^a} + \{\alpha\delta\} \rho_1^\delta \right] + \rho_1^\alpha \left[\frac{d \rho_3^{\beta\gamma}}{dx^a} + \{\alpha\delta\} \rho_2^{\delta\gamma} + \{\alpha\delta\} \rho_2^{\beta\delta} \right] \right]. \end{aligned}$$

(E-23)

Now if $\gamma = \beta = r$

$$\frac{d}{dt} \rho_2^{rr} = -\frac{1}{M} \left[\frac{d \ln \rho_0}{dx^r} (\rho_3^{rrr} + [\rho_1^r]^3) + \frac{d \rho_3^{rrr}}{dt} (\rho_3^{2rr} + \rho_1^2 [\rho_1^r]^2) \right]$$

$$+ \frac{d\rho_3^{rrr}}{dr} + \frac{d\rho_3^{zrr}}{dz} + \frac{1}{r} \rho_3^{rrr} - r \rho_3^{\phi\phi r} - r \rho_3^{\phi r \phi} + [\rho_1^r]^2$$

$$\left(\frac{d\rho_1^r}{dr} + \frac{d\rho_1^z}{dz} + \frac{1}{r} \rho_1^\phi \right) + (\rho_2^{rr} + \rho_2^{zr} + \rho_2^{\phi r} + [\rho_1^r]^2 + \rho_1^\phi \rho_1^r$$

$$+ \rho_1^z \rho_1^r) \left[\frac{d\rho_1^r}{dr} + \frac{d\rho_1^z}{dz} - r \rho_1^\phi \right] + (\rho_2^{rr} + \rho_2^{\phi r} + \rho_2^{rz}$$

$$+ [\rho_1^r]^2 + \rho_1^\phi \rho_1^r + \rho_1^z \rho_1^r) \left[\frac{d\rho_1^r}{dr} + \frac{d\rho_1^z}{dz} - r \rho_1^\phi \right]$$

$$+ \rho_1^r \left(\frac{d\rho_2^{rr}}{dr} \right) + \rho_1^\phi [-r \rho_2^{\phi r} - r \rho_2^{r \phi}] + \rho_1^z \left(\frac{d\rho_2^{rz}}{dz} \right)] .$$

(E-24)

In a similar manner, Eq (23) must be solved for $\gamma = \beta = z$,
 $\beta = \phi$ $\gamma = r$, $\beta = r$ $\gamma = z$, $\beta = \phi$ $\gamma = z$.

The total process results in ten equations, but in the model we have chosen, there is symmetry in the ϕ direction initially and remains throughout the problem; then ρ_1^ϕ , $\rho_2^{\phi\phi}$, $\rho_3^{\phi\phi}$ equal zero. The $\rho_3^{\phi\phi\phi}$, $\rho_2^{\phi\phi}$ terms, however, do not disappear.

With the above simplification and stopping with the

third movement, all $\rho_3^{\gamma\beta\alpha} = 0$, the equations reduce to the following:

$$\frac{d\rho_0}{dt} = -\frac{1}{M} \left[\frac{d\rho_0}{dr} \rho_1^r + \frac{d\rho_0}{dz} \rho_1^z + \rho_0 \left[\frac{d\rho_1^r}{dr} + \frac{d\rho_1^z}{dz} + \frac{1}{r} \rho_1^r \right] \right] \quad (\text{E-25})$$

$$\begin{aligned} \frac{d\rho_1^r}{dt} = & \mathcal{F}^r - \frac{1}{M} \left[\rho_2^{rr} \frac{d \ln \rho_0}{dr} + \rho_2^{zr} \frac{d \ln \rho_0}{dz} + \frac{d\rho_2^{rr}}{dr} + \frac{d\rho_2^{rz}}{dz} \right. \\ & \left. + \frac{1}{r} \rho_2^{rr} - r \rho_2^{\theta\theta} + \rho_1^r \frac{d\rho_1^r}{dr} + \rho_1^z \frac{d\rho_1^r}{dz} \right] \quad (\text{E-26}) \end{aligned}$$

$$\begin{aligned} \frac{d\rho_1^z}{dt} = & \mathcal{F}^z - \frac{1}{M} \left[\rho_2^{rz} \frac{d \ln \rho_0}{dr} + \rho_2^{zz} \frac{d \ln \rho_0}{dz} + \frac{d\rho_2^{rz}}{dr} + \frac{d\rho_2^{zz}}{dz} \right. \\ & \left. + \rho_1^r \frac{d\rho_1^z}{dr} + \rho_1^z \frac{d\rho_1^z}{dz} \right] \quad (\text{E-27}) \end{aligned}$$

$$\frac{d\rho_2^{rr}}{dt} = -\frac{1}{M} \left[\frac{d \ln \rho_0}{dr} (\rho_1^r)^3 + \frac{d \ln \rho_0}{dz} (\rho_1^z (\rho_1^r)^2) \right]$$

$$+ (\rho_1^r)^2 \left[\frac{d\rho_1^r}{dr} + \frac{d\rho_1^z}{dz} \right] + 2 (\rho_2^{rr} + \rho_2^{zz} + (\rho_1^r)^2 + \rho_2^z \rho_1^r)$$

$$\left[\frac{d\rho_1^r}{dr} + \frac{d\rho_1^z}{dz} \right] + \rho_1^r \left(\frac{d\rho_2^{rr}}{dr} \right) + \rho_1^z \left(\frac{d\rho_2^{rz}}{dz} \right) \quad (E-28)$$

$$\frac{d\rho_2^{\phi\phi}}{dt} = -\frac{1}{M} \left[\rho_2^{\phi\phi} (\rho_1^r) + 4 \rho_2^{\phi\phi} \frac{\rho_1^r}{r} + \rho_1^z \frac{d\rho_2^{\phi\phi}}{dz} \right] \quad (E-29)$$

$$\frac{d\rho_2^{zz}}{dt} = -\frac{1}{M} \left[\frac{d \ln \rho_0}{dr} (\rho_1^r (\rho_1^z)^2) + \frac{d \ln \rho_0}{dz} (\rho_1^z)^3 \right.$$

$$+ (\rho_1^z)^2 \left(\frac{d\rho_1^r}{dr} + \frac{d\rho_1^z}{dz} + \frac{1}{r} \rho_1^r \right) + 2 [\rho_2^{rz}$$

$$+ \rho_2^{zz} + \rho_1^r \rho_2^z + (\rho_1^z)^2] \left(\frac{d\rho_1^z}{dr} + \frac{d\rho_1^z}{dz} \right)$$

$$+ \rho_1^r \left(\frac{d\rho_2^{zz}}{dr} \right) + \rho_1^z \left(\frac{d\rho_2^{zz}}{dz} \right) \quad (E-30)$$

$$\begin{aligned}
\frac{d}{dt} \rho_2^{r^2} = & -\frac{1}{M} \left[\frac{d \ln \rho_2}{d r} (\rho_1^r)^2 (\rho_1^z) + \frac{d \ln \rho_2}{d z} (\rho_1^z)^2 (\rho_1^r) \right. \\
& + \rho_1^r \rho_1^z \left(\frac{d \rho_1^r}{d r} + \frac{d \rho_1^z}{d z} + \frac{1}{r} \rho_1^r \right) + (\rho_2^{r^2} + \rho_2^{z^2} + \rho_1^r \rho_1^z \\
& + (\rho_1^z)^2) \left[\frac{d \rho_1^r}{d r} + \frac{d \rho_1^z}{d z} \right] + (\rho_2^{rr} + \rho_2^{zz} + (\rho_1^r)^2 + \rho_1^z \rho_1^r) \\
& \left. \left[\frac{d \rho_1^z}{d r} + \frac{d \rho_1^r}{d z} \right] + \rho_1^r \frac{d \rho_2^{r^2}}{d r} + \rho_1^z \frac{d \rho_2^{r^2}}{d z} \right]. \quad (E-31)
\end{aligned}$$

The only terms yet to be defined are the force terms \mathcal{F}^r and \mathcal{F}^z . The forces exerted on the electrons will come from both external and internal electric and magnetic fields. For this model, we have chosen the external magnetic field to be zero because of the large difference in the magnitude of electric and magnetic fields of a common point charge.

The force on an electron is given by

$$\bar{F} = g(\bar{E} + \bar{V} \times \bar{B}) \quad (E-32)$$

Where $\bar{E} = E_{ext} + E_{int}$

E external is evaluated in Appendix B. The internal electric and magnetic fields can be obtained from Maxwell's equations

$$\frac{d\bar{B}}{dt} = -\bar{\nabla} \times \bar{E} \quad (E-33)$$

$$\frac{d\bar{E}}{dt} = \frac{1}{\mu_0 \epsilon_0} \bar{\nabla} \times \bar{B} - \frac{\bar{J}}{\epsilon_0} \quad (E-34)$$

Since, as we have stated earlier, only the ϕ component of B is nonzero and only the r and z components of E are non-vanishing, then

$$\frac{dB_\phi}{dt} = -\left[\frac{dE_r}{dz} - \frac{dE_z}{dr}\right] \phi \quad (E-35)$$

where $\nabla \times B$ in cylindrical coordinates is given as

$$\bar{\nabla} \times \bar{B} = \left(\frac{1}{r} \frac{dB_z}{d\phi} - \frac{dB_\phi}{dz}\right) \hat{r} + \left(\frac{dB_r}{dz} - \frac{dB_z}{dr}\right) \hat{\phi} + \frac{1}{r} \left(\frac{d}{dr}(rB_\phi) - \frac{dB_r}{d\phi}\right) \hat{z} \quad (E-36)$$

The time derivatives of the electric fields are

$$\frac{dE_r}{dt} = -\frac{J_r}{\epsilon_0} - \frac{1}{\mu_0 \epsilon_0} \frac{dB_\phi}{dz}$$

$$J_r = \frac{q}{\epsilon_0 M} \int \rho^r f d\rho = \frac{-e}{\epsilon_0 M} \rho_i^r \rho_o$$

thus,

$$\frac{dE_r}{dt} = \frac{e}{\epsilon_0 M} (\rho_o \rho_i^r) - c^2 \frac{dB_\phi}{dz} \quad (E-37)$$

where C = speed of light

$$\begin{aligned} \frac{d E_z}{d t} &= -\frac{J_z}{\epsilon_0} + \frac{1}{\mu_0 \epsilon_0} \left(\frac{1}{r} \frac{d}{d r} (r B_\phi) \right) \\ &= \frac{e}{\epsilon_0 M} \rho_i^z \rho_o + c^2 \left(\frac{d B_\phi}{d r} + \frac{B_\phi}{r} \right). \quad (E-38) \end{aligned}$$

The differential equation solving routine used to solve for the moments can be used to obtain solutions for E_r , E_z and B_ϕ . Equipped with these solutions, the forces on the electrons can be evaluated. The forces in the radial direction are given by

$$\begin{aligned} f_r &= -e \left(E_r + \frac{\rho_i^z B_\phi}{M} \hat{r} \cdot (\hat{z} \times \hat{\phi}) \right) \\ &= -e \left(E_r - \frac{\rho_i^z B_\phi}{M} \right) \end{aligned}$$

where $E_r = E_r^{ext} + E_r^{int}$.

The forces in the z direction are given by

$$f_z = -e \left(E_z + \frac{\rho_i^r B_\phi}{M} \hat{z} \cdot (\hat{r} \times \hat{\phi}) \right) = -e \left(E_z + \frac{\rho_i^r}{M} B_\phi \right)$$

In summary, we have ten partial differential equations with respect to time which when given initial conditions can be stepped in time to yield solutions at later times. The ten equations are Eqs (25-31) and Eqs (35), (37) and (38).

Scaling the Equations

As in the one-dimensional model, it becomes necessary to scale the various parameters in order to reduce the large magnitude of the numerical values. As in the one-dimensional case,

$$T = T_0 \tau$$

$$\rho = \rho_0 v$$

$$X = X_0 x^* \quad \text{or} \quad r = R_0 \omega, \quad z = z_0 u$$

$$E = E_0 M$$

$$B = B_0 \beta$$

$$f = \phi f^* \quad \text{where} \quad \phi = \frac{N_0}{R_0^2}$$

Thus, Eq (12) may be written

$$\frac{df^*}{d\tau} = - \frac{\rho_0 T_0}{M X_0} V^* \frac{df^*}{dx^*} + \left(\frac{e E_0 T_0}{P_0} \eta^* + \frac{e B_0 T_0}{M} (v \times B) \right) \frac{df^*}{dV}. \quad (E-39)$$

In a similar manner, the equations for the time derivatives at the electric and magnetic fields are given by

$$\frac{d\eta^*}{d\tau} = \frac{c^2 B_0 T_0}{X_0 E_0} (\nabla \times \beta) + \frac{e P_0^2 N_0 T_0}{M E_0 E_0} \int dV V^* f^* \quad (E-40)$$

$$\frac{d\beta^*}{d\tau} = - \frac{E_0 T_0}{X_0 B_0} (\nabla \times \eta^*). \quad (E-41)$$

Since we may not wish to work with the same scale parameter in the r and z direction, we can expand the above equations to have the same form except the $\frac{d}{dx^*}$ terms will have two components, $\frac{d}{dx^*}$ and $\frac{d}{dz^*}$ and corresponding values of R_0 and z_0 .

Let us define

$$C_1 = \frac{P_o T_o}{M R_o}$$

$$C_2 = \frac{P_o T_o}{M Z_o}$$

$$C_3 = \frac{e E_o T_o}{P_o}$$

$$C_4 = \frac{e B_o T_o}{M}$$

$$C_5 = \frac{c^2 B_o T_o}{E_o R_o}$$

$$C_6 = \frac{c^2 B_o T_o}{E_o Z_o}$$

$$C_7 = \frac{e P_o N_o T_o}{M E_o E_o}$$

$$C_8 = \frac{E_o T_o}{B_o R_o}$$

$$C_9 = \frac{E_o T_o}{B_o Z_o}$$

These nine equations have only four unknowns if we pick R_o , Z_o to be related to the target dimensions and can thus be solved to yield the values given in Appendix C.

Eq (39) thus reduces to

$$\frac{df^*}{d\tau} + V^x \frac{df^*}{dX^x} - C_2 (\gamma^x + E^{x\beta\gamma} V^\beta B^\gamma) \frac{d\phi}{dV^x} = 0 \quad (E-42)$$

and the electric and magnetic fields to

$$\frac{d\eta^x}{d\tau} = E^{x\beta\gamma} \frac{d\beta^\gamma}{dX^x} + \int dV V^x f^* \quad (E-43)$$

$$\frac{d\beta^x}{d\tau} = -E^{x\beta\gamma} \frac{d\eta^\gamma}{dX^x} \quad (E-44)$$

Eqs (42), (43) and (44) have the same form as their unscaled equations used in previous sections of this appendix, except for the constant which can be carried through without modifying previous work.

As was the case for the one-dimensional model, the true form of γ , v , x , γ is given by

$$p = p_0 \sinh(v)$$

$$T = T_0 \sinh(s)$$

$$u = x_0 \frac{u}{\sqrt{1-u^2}}$$

$$R = R_0 \omega / (1-\omega)$$

These factors will not change the form of any of the ten partial differential equations and will only come into consideration when the analysis of the data is required.

Appendix F

The Computer Programs

The One-dimensional Computer Program

The listing for the one-dimensional model consists of a main or calling program and four major subroutines. The calling program serves to input the initial conditions to the solving routine, to input step sizes and accuracies to the solving routine, and to output the new values at the time step established.

The variables used in the calling routine are as follows:

- AL - Array containing relative error tolerances
- AW - Scratch array
- DS - Size of time step
- DU - Size of spatial step
- EO - Constant E_0
- F - Array of time derivatives
- H - Step size estimate
- IB - Negative number means no size estimate given;
zero minus size estimate given
- N - Number of spatial points
- NA - Total number of time steps to be taken
- ND - Total number of equations
- P - Array to output E_{int} at each spatial point
- PO - Momentum scale factor
- RT - Tolerance for solving routine

RT - Tolerance for solving routine
 S - Time at calculation
 SI = Time into solving routine, initial time
 SO - Time out of routine, time you desire answer
 SZ - Array containing guesses for size of solutions
 U - Location of spatial points (scales)
 Y - Array containing current solutions
 YS - Initial input and final output array listing

```

PROGRAM QUICK(INPUT,OUTPUT)
DIMENSION YS(17,4),Y(17,4,12),F(17,4,12),S(12),AL(68),AW(68)
1,SZ(63),P(17)
COMMON EQ,DU
EXTERNAL FCN
DU=.1111111
READ99,NA,EQ,DS,RT,P0
SO=-20.7N=17SN0=597IB=-1
CALL ZERO(YS,1,ND)
PRINT*, "STARTING TIME=",SO, "INTERVAL=",DS
H=.11*DS
001I=1,ND
1 AL(I)=RT
002I=1,N
U=(I-9.)*2/81.
YS(I,1)=-32.*(U**3)+12.*(U*U)-1.125*U+.015625
2 CONTINUE
PRINT98,IB,SO,((YS(I,J),J=1,4),I=1,N)
003IA=1,NA
SI=SO7SO=SO+DS
CALL BLOCK0(FCN,ND,ND,SI,SO,YS,S,Y,F,AL,AW,H,SZ,IB)
PRINT98,IB,SO,((YS(I,J),J=1,4),I=1,N)
DO 5 I=1,17
5 P(I)=EXT(I,SO)
PRINT95,(P(I),I=1,17)
3 CONTINUE
99 FORMAT(I5,6E12.4)
99 FORMAT(//I5,1PE13.4/(2X,1P4F13.4))
95 FORMAT(2X,1PE13.4)
STOP
END
  
```


The differential equation solving routine was an eight-point Newton-Raphsen method routine and will not be discussed in any detail, because any standard differential equation solving routine could be adapted to the program.

The second major subroutine consists of the moment equations derived in previous sections. This subroutine, when called on by the differential equation solving routine, and given values of the function at an initial time, will return values of the time derivative.

The following is a list of additional variables used in this subroutine:

CS - Hyperbolic cosine of the time

DYI - $i = 1, 2, 3$ derivatives of the function Y_1, Y_2, Y_3 respectively

RU - A portion of the scaling parameter

YI - $i = 1, 2, 3$ and 4 values of $N, \bar{p}, P^{\sim 2}$ Eint respectively.

```

SUBROUTINE FCN(S,Y,F)
DIMENSION Y(17,4),F(17,4)
COMMON E0,DU
CS=-COSH(S)
CALL ZERO(F,17,4) $CALL ZERO(F(17,1),17,4)
DO1I=1,17
U=(I-9.)**2/81.
RU=SQRT((1.-J)**3)
R=CS*RJ
Y1=Y(I,1)$Y2=Y(I,2)$Y3=Y(I,3)$Y4=Y(I,4)
DY1=DBDU(Y,I,17)$DY2=DBDU(Y(1,2),I,17)$DY3=DBDU(Y(1,3),I,17)
F(I,1)=R*(Y2*DY1+DY2)
F(I,2)=R*(Y3*DY1+DY3+Y2*DY2)+CS*(Y4+EEXT(I,S))/E0
F(I,3)=R*(2.*Y3*DY2+Y2*DY3)
1 F(I,4)=-2.*E0*CS*EXP(Y1)*Y2
RETURN
END

```

The third subroutine calculates the derivative of a function by an eight-order numerical routine. The numerical differentiation, as described in Milne, (Ref 20), calculates the derivatives at eight equally spaced points. The accuracy of the numerical solutions is much better for points in the center; thus, in the subroutine the coefficients for the fifth point are used for positions 5 through 13 in our 17 position scheme. A typical derivative at the first point is given by

$$Y_1' = \frac{1}{15444h} \left(-19210 Y_0 + 13358 Y_1 + 12839 Y_2 + 1206 Y_3 - 7616 Y_4 - 6750 Y_5 + 1633 Y_6 + 8314 Y_7 - 3974 Y_8 \right)$$

where h is the value of the constant interval.

The coefficients to the numerical solutions are stored in the array RP(9,10), with the last member of each array row going to the factor which multiplies the constant interval size. The actual calculation of the derivative is done by matrix multiplication of the proper rows of Y, with the proper rows of RP, and then divided by RP(I,10) another constant interval distance.

The following new variables appear in DBDU:

RP - the coefficients as discussed above

DBDU - the value of the derivative at the point of interest

```

FUNCTION DBDU(Y,I,N)
DIMENSION Y(1),RP(9,10)
COMMON E0,DU
DATA ((RP(I,J),J=1,10),I=1,9)/
1 -19210.,13358.,12839.,1206.,-7416.,-6750.,1633.,8314.,-3974.,1544
2 4.,-7198.,800.,3323.,2844.,1242.,-198.,-785.,-422.,394.,15444.,-8
3 14.,-4408.,-1615.,2268.,4068.,2736.,-653.,-2900.,1318.,15444.,145
4 4.,-4534.,-3163.,450.,3006.,3024.,841.,-1389.,310.,15444.,85.,-14
5 2.,-193.,-126.,0.,126.,193.,142.,-86.,1188.,-310.,1388.,-841.,-30
6 24.,-3006.,-450.,3163.,4534.,-1454.,15444.,-1318.,2900.,653.,-273
7 5.,-4058.,-2268.,1615.,4408.,814.,15444.,-394.,422.,785.,198.,-12
8 42.,-2844.,-3323.,-800.,7198.,15444.,3974.,-8314.,-1633.,6750.,74
9 16.,-1206.,-12839.,-13358.,19210.,15444./
IF(I-5) 1,2,5
5 IF(N-I-4) 3,2,2
1 DBDJ=VPROD(RP(I,1),9,Y(1),1,9,XX)/(DU*RP(I,10))
GO TO 4
2 DBDJ=VPROD(RP(5,1),9,Y(I-4),1,9,XX)/(DU*RP(5,10))
GO TO 4
3 DBDJ=VPROD(RP(I-8,1),9,Y(N-8),1,9,XX)/(DJ*RP(I-8,10))
4 RETURN
END

```

The last subroutine calculates the value of the electric field due to the beam at a specific point within the material. Eq (B-15) is the source for values returned.

The following variables are found in EEXT:

β = the relativistic constant

C = the speed of light

E = the value of the electric field

EPS0 = ϵ_0 ; the permittivity of free space

PI = 3.14159

Q = the charge in one pulse of the beam

R = radius of interaction - a constant in 1-D

To = time scale parameter

V = velocity of beam

X_1 = distance scale parameter

```
FUNCTION EEXT(I,X)
PI=3.1416
Q=1.E-05
C=3.0E9
V=2.999E8
EPSO=8.854E-12
TO=7.25E-17
XO=.274
R=.001
B=V/C
U=(I-Q)/9.
D=Q/(4*PI*EPSO)
A=V*TO*SINH(X)-XO*U/SQRT(1-U*U)
E=D*((2*B/(1-B*B))-A/SQRT(R*R*(1-B*B)+A*A))
+/( ((2*B/(1-B*B))*A-SQRT(R*R*(1-B*B)+A*A))**2)
EEXT=E
RETURN
END
```

The Two-dimensional Computer Program

The components of the 2-D program are identical to the 1-D model except for the extension in the radial direction of the spatial nodes and the electric and magnetic fields. The extensions require additional storage space and sub-routines for taking derivatives and calculating the radial component of the external electric field.

The main program serves the same functions as described for the 1-D program. The following is a listing of additional variables used in the 2-D main program.

DW - The step size in the radial direction
EE - The charge on an electron
EO - ϵ_0 , permittivity of free space
FF - Common storage array

RO - The radial distance parameter
 TO - Time parameter
 YY - Common storage array
 ZO - Axial distance parameter
 Z5 - The unscaled time of solution
 EM - The electron mass

```

PROGRAM THESIS (INPUT,OUTPUT)
DIMENSION YS(17,9,10),S(12),AL(1530),AW(1530),SZ(1530)
COMMON// FF(1530,12),YY(1530,12)
COMMON/ONE/ RP(9,10),EO,OU,OW,RO,ZO,EM,EE,TO
EXTERNAL FCN
OU=OW=.11111
N=17
ND=1530
IB=-1
EE=1.6E-19
RO=5.25E-5
ZO=.2765
TO=7.25E-17
EM=9.11E-31
READ 99,NA,EO,DS,RT,PO
SO=1
CALL ZERO(YS,1,ND)
H=.01*DS
DO 1 I=1,ND
1  AL(I)=RT
  READ 10,((RP(I,J),J=1,10),I=1,9)
10  FORMAT(10F8.3)
  DO 2 I=1,17
  DO 2 J=1,8
    U=(I-9)**2/81.
2  YS(I,J,1)=-32.*(U**3)+12.*(U*U)-1.125*U+.015625
    PRINT 98,(((YS(I,J,K),K=1,10),J=1,9),I=1,17)
  DO 3 I=1,NA
    SI=SO
    SO=SO+DS
    CALL BLOCKD(FCN,ND,ND,SI,SO,YS,S,YY,FF,AL,AW,H,SZ,IB)
    PRINT*,IB,SO
    Z5=TO*SINH(SO)
    PRINT*, "TIME = ",Z5
    PRINT 98,(((YS(I,J,K),K=1,10),J=1,9),L=1,17)
3  CONTINUE
98  FORMAT(2X,1P10E13.4)
99  FORMAT(I5,6E12.4)
    STOP
  END
  
```

The differential equation solving routine, and the derivative subroutine in the axial direction remain the same as in the 1-D program.

The third subroutine which calculates the values of the time derivatives serves the same function as in the 1-D program.

The following variables have a different meaning or are absent in the 1-D model:

B_2 - B_3 - Hyperbolic cosine of P_1^R and P_1^Z , respectively

CON - The constant C_2 described in Appendix F

EN - Initial number of electrons in the plasma

R - Value of the radius (scales)

RW - A portion of the derivative with respect to R

W - Location of nodes in the scales R direction

X - Time (scaled)

```

SUBROUTINE FCN (X,Y,F)
  DIMENSION Y (17,9,10), F(17,9,10), FORCE (17,9,2), DBDW(8,10)
  +, DBDU(17,10)
  COMMON/ONE/ RP(9,10), FO, DU, DW, RO, ZO, EM, EE, TO
  NW=3
  NU=17
  CON=2.480E7
  C=3. E8
  EN=1.8E+28
  DO 1 J=2,9
  DO 1 I=1,17
  U=(I-9.)/9.
  W=(J-1.)/9.
  R=RO*W/(1.-W)
  RU=SQRT((1-U*U)**3)/ZO
  RW=(1-W)**2/RO
  A=COSH(X)
  Y1=Y (I, J, 1)
  Y2=Y (I, J, 2)
  Y3=Y (I, J, 3)
  Y4=Y (I, J, 4)
  Y5=Y (I, J, 5)
  Y6=Y (I, J, 6)
  Y7=Y (I, J, 7)

```

```

Y8=Y(I,J,8)
Y9=Y(I,J,9)
Y10=Y(I,J,10)
R2=COSH(Y(I,J,2))
R3=COSH(Y(I,J,3))
DBDW(J,1)=DERW(Y(I,1,1),J,NW)*RW
DBDW(J,2)=DERW(Y(I,1,2),J,NW)*RW/R2
DBDW(J,3)=DERW(Y(I,1,3),J,NW)*RW/R3
DBDU(I,1)=DERU(Y(I,J,1),I,NU)*RU*RO/ZO
DBDU(I,2)=DERU(Y(I,J,2),I,NU)*RU*RO/(ZO*R2)
DBDU(I,3)=DERU(Y(I,J,3),I,NU)*RU*RO/(R3*ZO)
DO 2 K=4,10
2 DBDW(J,K)=DERW(Y(I,1,K),J,NW)*RW
  DBDU(I,K)=DERU(Y(I,J,K),I,NU)*RU*RO/ZO
  FORCE(I,J,1)=-CON*(Y8-Y3*Y10)*CON
  FORCE(I,J,2)=-CON*(Y9+Y2*Y10)
  T=Y2*DBDW(J,1)+Y3*DBDU(I,1)+DBDW(J,2)+DBDU(I,3)+Y2/R
  F(I,J,1)=A*(DBDW(J,1)*Y2/Y1+DBDU(I,1)*Y3/Y1+Y1*(DBDW(J,2)+DBDU(I,3)
  +Y2/R))
  F(I,J,2)=A*FORCE(I,J,1)-A*(Y4*DBDW(J,1)+Y5*DBDU(I,1)+DBDW(J,4)
  +DBDU(I,5)+Y4/R-R*Y6+Y2*DBDW(J,2)+Y3*DBDU(I,2))
  F(I,J,3)=A*FORCE(I,J,2)-A*(Y5*DBDW(J,1)+Y7*DBDU(I,1)+DBDW(J,5)
  +DBDU(I,7)+Y2*DBDW(J,3)+Y3*DBDU(I,3))
  F(I,J,4)=-A*(T*Y2*Y2+2*(DBDW(J,2)+DBDU(I,3))*(Y4+Y5+
  +Y2*Y2+Y4*Y2)+Y2*DBDW(J,4)+Y3*DBDU(I,5))
  F(I,J,5)=-A*(T*Y2*Y3+(Y5+Y7+Y2*Y3+Y3*Y3)*(DBDW(J,2)+
  +DBDU(I,2))+(Y4+Y5+Y2*Y2+Y2*Y3)*(DBDW(J,3)+DBDU(I,3))+Y2*DBDW(J,5)
  +Y3*DBDU(I,5))
  F(I,J,6)=-A*(Y6+Y2/R+Y2*(DBDW(J,6)+4.*Y6/R)+Y3*DBDU(I,6))
  F(I,J,7)=-A*(T*Y3*Y3+2*(Y5+Y7+Y2*Y3+Y3*Y3)*(DBDW(J,3)
  +DBDU(I,3))+Y2*DBDW(J,7)+Y3*DBDU(I,7))
  F(I,J,8)=A*(-DBDU(I,10)+Y2*EXP(Y1))
  F(I,J,9)=A*(DBDW(J,10)+Y10/R+Y3*EXP(Y1))
FCN      74/74      OPT=1                      FTN 4.5+414          09/

1  F(I,J,10)=A*(DBDW(J,9)-DBDU(I,8))
   CONTINUE
   RETURN
   END

```

The subroutine DERW takes the derivative of the function in the radial direction. This numerical derivative is taken in exactly the same manner as was the radial component, except the matrix multiplication is done along the radial direction of the Y matrix.


```

FUNCTION DERW(Y,J,N)
DIMENSION Y(N)
COMMON/ONE/ RP(9,10),EO,DU,DA,RD,ZD,EM,EE,TO
DERW=VPROD(RP(J,1),9,Y(1),144,9,XX)/(DW*RP(J,10))
RETURN
END

```

The external electric field in the axial direction is calculated in a similar manner as was done in the 1-D program except the radius of the point is allowed to vary.

The external electric field in the radial direction is obtained through the use of Eq(8-14). The variables in EEXTR are consistent with the rest of the program.

```

FUNCTION EEXTR(I,J,X)
COMMON/ONE/ RP(9,10),EO,DU,DA,RD,ZD,EM,EE,TO
DATA PI,Q,C,V,EPS0/3.14159,1.0E-6,3.0E8,2.989E8,8.854E-12/
B=V/C
W=(J-1.)/9.
R=RD*W/(1.-W)
U=(I-9.)/9.
Z=ZD*U/SQRT(1.-U*U)
D=Q/(4*PI*EPS0)
A=V*TD*SINH(X)-ZD*U/SQRT(1.-U*U)
F=SQRT(R*R*(1.-B*B)+A*A)
G=2.*B/(1.-B*B)
E=D*R**((1.-B*B)/(((G*A-F)**2)*F))
EEXTR=E
RETURN
END

```


Appendix G

Derivation of Plasma Frequency From The Moments of the Vlasov Equation

Because we have chosen to use the plasma oscillation as a standard for validation of the technique and models, it becomes necessary to justify that ω_p (the plasma frequency) is a valid solution.

If we linearize the first three moments of the Vlasov equation, Eqs (D-6), (D-13) and D-17),

$$\begin{aligned} N &= N_0 + N_1 \\ \bar{P} &= \bar{P}_0 + \bar{P}_1 \\ F &= F_0 = F_1 \\ \tilde{P}^2 &= \tilde{P}_0 + \tilde{P}_1 \\ \tilde{P}^3 &= 0 \end{aligned}$$

where N_0 , \bar{P}_0 , \tilde{P}_0 , F_0 are constants and N_1 , \bar{P}_1 , \tilde{P}_1 , F_1 are small perturbations to the initial values, and if we assume the plasma to initially be cold ($\bar{P}_0 = 0$, $\tilde{P}_0 = 0$ and $F_1 = 0$; no initial momentum or temperature) the first three moments become

First Moment

$$\frac{dN_1}{dt} = -\frac{1}{M} \left(\bar{P}_1 \frac{dN_1}{dx} + N_0 \frac{d\bar{P}_1}{dx} + N_1 \frac{d\bar{P}_0}{dx} \right) \quad (E-1)$$

Second Moment

$$N_0 + N_1 \frac{d\bar{P}_1}{dt} = F_0 (N_0 + N_1) - \frac{1}{M} \left((N_0 + N_1) \frac{d\tilde{P}_1^2}{dx} + \tilde{P}_1^2 \frac{dN_1}{dx} \right)$$

$$+ (N_0 + N_1) \bar{P}_1 \frac{d}{dx} \bar{P}_1 \quad (E-2)$$

Third Moment

$$(N_0 + N_1) \frac{d\tilde{P}^2}{dx} = - \frac{1}{M} \left(\bar{P}_1 (N_0 + N_1) \frac{d\tilde{P}^2}{dx} + 2 \tilde{P}^2 (N_0 + N_1) \frac{d\bar{P}_1}{dx} \right). \quad (E-3)$$

If we now keep only the first-order perturbation terms and assume that a small perturbation times a small perturbation is negligible, Eqs (1), (2) and (3) become

$$\frac{dN_1}{dt} = - \frac{1}{M} N_0 \frac{d\bar{P}_1}{dx} \quad (E-4)$$

$$N_0 \frac{d\bar{P}_1}{dt} = F_1 N_0 - \frac{1}{M} \left(N_0 \frac{d\tilde{P}_1^2}{dx} \right) \quad (E-5)$$

$$N_0 \frac{d\tilde{P}_1^2}{dt} = 0. \quad (E-6)$$

From Eq (6), we know that $N_0 \neq 0$ thus, $\frac{d}{dt} \tilde{P}_1^2 = 0$ or perturbations of temperature in a plasma are not a function of time. Eq (5) then reduces to

$$N_0 \frac{d\bar{P}_1}{dt} = F_1 N_0. \quad (E-7)$$

Let us now look at the force term. If we assume N_1, P_1, F_1 have the form

$$A_1 = A_1 e^{-i(kx - \omega t)}$$

then

$$F = e(E^x + E^i)$$

where

E^x = the external electric field

E^i = the internal electric field.

But we know

$$\frac{dE^i}{dt} = \frac{J}{\epsilon_0} = \frac{e}{Mc\epsilon_0} \int \rho f d\rho = \frac{e}{Mc\epsilon_0} \bar{P}_1 N_0$$

and that

$$\frac{dE^i}{dt} = -i\omega E^i = \frac{e}{Mc\epsilon_0} \bar{P}_1 N_0 \quad (G-8)$$

Substituting this result into Eq (7) yields

$$N_0 \frac{d\bar{P}_1}{dt} = \frac{e^2 N_0^2 \bar{P}_1}{Mc\epsilon_0 i\omega} + e E^x N_0 \quad (G-9)$$

Taking the partial derivative of Eq (9) and canceling like terms yields

$$\bar{P}_1 = \frac{e E^x}{\left(\omega i - \frac{e^2 N_0}{i\omega Mc\epsilon_0}\right)}$$

Substituting this equation into Eq (4) and reducing, defines N_1 as

$$N_1 = \frac{N_0 K e E^x \epsilon_0}{(-\omega^2 Mc\epsilon_0 - N_0 e^2)}$$

Thus, if there are no density perturbations involved in simple harmonic motion $N_1 = 0$ and $E_x = 0$

$$\omega = \frac{N_0 e^2}{M \epsilon_0} = \omega_p^2$$

where ω_p = the plasma frequency. Ref. 15 demonstrated the fact that as the plasma becomes finite radially, instead of the infinite model chosen in the deviation, the frequency of the plasma approaches

$$\omega = \frac{\omega_p}{\sqrt{2}} .$$

VITA

Gene Paul Bender was born 28 October 1946 in Tell City, Indiana. He graduated from Tell City High School in 1964 and attended the University of Kentucky from which he earned a Bachelor of Science degree in December 1968. Upon graduation, he enlisted in the U. S. Navy and was sent to the Naval Training Center in San Diego, California where he attended Basic Electronics School. In October 1969, he applied for and was selected for an assignment to the Naval Air Station, Pensacola, Florida as an Aviation Officer Candidate. He completed helicopter pilot training and received his "Wings of Gold" in March 1971, after which he served as a SH-3G aircraft commander at HC-1, Naval Air Station, Imperial Beach, California from October 1971 to August 1974. During this time, he was attached to the aircraft carriers U. S. S. Kitty Hawk and U. S. S. Oriskany where he helped to provide logistics and sea-air rescue support during the Vietnam Conflict. He entered the School of Engineering, Air Force Institute of Technology, in August 1974.

Permanent address: 1326 - 11th Street
Tell City, Indiana 47586

UNCLASSIFIED

SECURITY CLASSIFICATION OF THIS PAGE (When Data Entered)

REPORT DOCUMENTATION PAGE		READ INSTRUCTIONS BEFORE COMPLETING FORM
1. REPORT NUMBER GNE/PH/76D-1	2. GOVT ACCESSION NO.	3. RECIPIENT'S CATALOG NUMBER
4. TITLE (and Subtitle) INTERACTION OF RELATIVISTIC PROTONS WITH MATTER		5. TYPE OF REPORT & PERIOD COVERED MS Thesis
7. AUTHOR(s) Gene P. Bender Lt. USN		6. PERFORMING ORG. REPORT NUMBER
9. PERFORMING ORGANIZATION NAME AND ADDRESS Air Force Institute of Technology Wright-Patterson AFB, Ohio 45433		10. PROGRAM ELEMENT, PROJECT, TASK AREA & WORK UNIT NUMBERS
11. CONTROLLING OFFICE NAME AND ADDRESS Air Force Weapons Laboratory AFWL/DYT Kirtland Air Force Base, New Mexico 87117		12. REPORT DATE December, 1976
14. MONITORING AGENCY NAME & ADDRESS (if different from Controlling Office)		13. NUMBER OF PAGES
		15. SECURITY CLASS. (of this report) UNCLASSIFIED
16. DISTRIBUTION STATEMENT (of this Report) Approved for public release; distribution unlimited		15a. DECLASSIFICATION/DOWNGRADING SCHEDULE
17. DISTRIBUTION STATEMENT (of the abstract entered in Block 20, if different from Report)		
18. SUPPLEMENTARY NOTES Approved for public release; IAW AFR 190-17 JERRAL F. GUESS, Captain, USAF Director of Information		
19. KEY WORDS (Continue on reverse side if necessary and identify by block number) Relativistic Proton Beams Collective and Collisional Interactions		
20. ABSTRACT (Continue on reverse side if necessary and identify by block number) The mechanisms associated with the interaction of a relativistic proton beam with a target material are summarized, and a simple analytic calculation for each mechanism relates its importance in the deposition of energy. Because it was found that possible significant contributions could be related to collective effects, the first three moments of the Boltzmann-Vlasov equation and the equations (over)		

DD FORM 1 JAN 73 1473

EDITION OF 1 NOV 65 IS OBSOLETE


UNCLASSIFIED

SECURITY CLASSIFICATION OF THIS PAGE (When Data Entered)

UNCLASSIFIED

SECURITY CLASSIFICATION OF THIS PAGE(When Data Entered)

→ necessary to describe the internal and external electromagnetic fields associated with the target are developed. These equations are then formulated into a computer program to describe the collective interaction process. Sample runs demonstrate the ability of the computer model to predict plasma oscillations at the proper frequency. Although an instability developed in the runs with the beam approaching the target, the preliminary analysis was accomplished, and the need for future detailed analysis of this process was established.



UNCLASSIFIED

SECURITY CLASSIFICATION OF THIS PAGE(When Data Entered)